

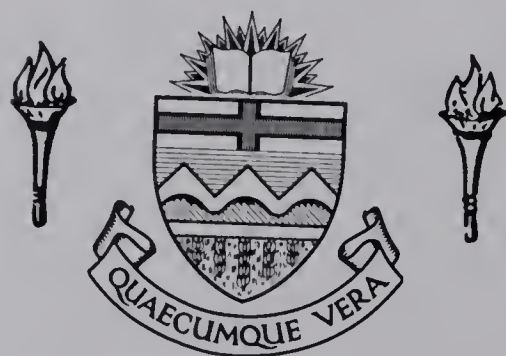
For Reference

NOT TO BE TAKEN FROM THIS ROOM

For Reference

NOT TO BE TAKEN FROM THIS ROOM

Ex libris
UNIVERSITATIS
ALBERTAENSIS



THE UNIVERSITY OF ALBERTA

A MODEL STUDY OF ISOLATED WELL PATTERNS

by



S. K. BHATIA

A THESIS

SUBMITTED TO THE FACULTY OF GRADUATE STUDIES
IN PARTIAL FULFILMENT OF THE REQUIREMENTS FOR THE
DEGREE OF MASTER OF SCIENCE

IN

PETROLEUM ENGINEERING

FACULTY OF ENGINEERING

DEPARTMENT OF CHEMICAL AND PETROLEUM ENGINEERING

EDMONTON, ALBERTA

APRIL, 1967

UNIVERSITY OF ALBERTA
FACULTY OF GRADUATE STUDIES

The undersigned certify that they have read, and recommend to the Faculty of Graduate Studies for acceptance a thesis entitled A MODEL STUDY OF ISOLATED WELL PATTERNS submitted by S. K. Bhatia in partial fulfilment of the requirements for the degree of Master of Science in Petroleum Engineering.

ABSTRACT

The performance of a water-flood has been investigated by many workers using various types of models. In the present study, a physical model made of lucite and packed with fine uniform-size glass beads was used. Only two phases: water and oil were present. Two different patterns: isolated normal five-spot (4 injectors and 1 producer) and four inverted five-spot (4 injectors and 9 producers) were studied.

The fluids used (distilled water and kerosene) were immiscible. Relative permeability curves were determined using a linear lucite tube packed with same glass beads as in the actual model. To trace the flood front, injection water was colored with a fluorescent dye, insoluble in oil phase. Flood front was traced from time to time during a run using a polaroid camera, thus enabling the calculation of areal sweep efficiency at any stage.

The results show that in case of an isolated normal five-spot, a large quantity of oil lying outside the flood pattern is swept into the producing well,

giving a far too optimistic recovery. Four inverted five-spot pattern gives a performance closer to the confined case. A significant change in oil recovery and areal sweep efficiency is noticed with a change in mobility ratio from 0.32 to 0.98, for the case of an isolated normal five-spot. The behavior of the model in giving different recoveries on varying the back pressure in case of an isolated normal five-spot is explained and the shortcomings of the model are discussed.

ACKNOWLEDGEMENTS

The author wishes to express his appreciation for the cooperation and assistance he received from the Department of Chemical and Petroleum Engineering, University of Alberta. He is particularly grateful to Dr. D. L. Flock, Professor of Petroleum Engineering, under whose guidance this project was carried out.

In addition, the author expresses thanks to the technical staff of the Chemical and Petroleum Engineering shop and store for their cooperation and assistance. The author also thanks his friends and colleagues for their helpful suggestions and assistance in conducting the tests.

Acknowledgement is made to the National Research Council for their financial assistance, which made this work possible.

TABLE OF CONTENTS

	<u>Page</u>
LIST OF FIGURES	iii
INTRODUCTION	1
LITERATURE SURVEY	4
DESCRIPTION OF THE MODEL	33
PACKING OF THE MODEL	38
MODEL PROPERTIES	39
FLUID PROPERTIES	45
SCALING	47
EXPERIMENTAL PROCEDURE	50
RESULTS AND DISCUSSION	53
CONCLUSIONS	101
REFERENCES	104

APPENDICES:

- I. Calculation of the Porosity of the Glass-Bead Pack in the Model
- II. Calculation of the Absolute Permeability of the Model
- III. Determination of Relative Permeability Curves
- IV. Calculation of Mobility Ratio
- V. Measurement of Contact Angle by Capillary Rise Method

TABLE OF CONTENTS
(cont'd)

VI.	Calculation of Critical Rate of Injection	
VII(a).	Calculation of Displacement Efficiency for Isolated Normal Five-Spot	
VII(b).	Calculation of Displacement Efficiency for Four Inverted Five-Spot	
VIII.	Experimental Data and Calculations	

LIST OF FIGURES

<u>Figure No.</u>		<u>Page</u>
1	Plan of the Model	34
2	Schematic Diagram of the Model	36
3	Well Detail	37
4	Relative Permeability Curves	44
5	Isolated Normal Five-Spot: Photographs of Area Swept by Flooding Water at Different Throughputs	57
6	Four Inverted Five-Spot: Photographs of Area Swept by Flooding Water at Different Throughputs	58
7	Isolated Normal Five-Spot: Throughput in Network Pore Volume vs. Oil Recovery in Network Pore Volume	62
8	Isolated Normal Five-Spot: Throughput in Network Pore Volume vs. Oil Recovery in Network Hydrocarbon Pore Volume	63
9	Isolated Normal Five-Spot: Throughput in Network Hydrocarbon Pore Volume vs. Oil Recovery in Network Hydrocarbon Pore Volume	64
10	Isolated Normal Five-Spot: Throughput in Network Pore Volume vs. Areal Sweep Efficiency	66
11	Isolated Normal Five-Spot: Throughput in Network Displaceable Pore Volume vs. Oil Recovery in Network Displaceable Pore Volume	68

<u>Figure No.</u>		<u>Page</u>
12	Isolated Normal Five-Spot: Throughput in Network Displaceable Pore Volume vs. Areal Sweep Efficiency	69
13	Isolated Normal Five-Spot: Throughput in Network Pore Volume vs. Instantaneous Water-Oil Ratio	70
14	Isolated Normal Five-Spot: Effect of Mobility Ratio on Oil Recovery	73
15	Isolated Normal Five-Spot: Effect of Mobility Ratio on Areal Sweep Efficiency	75
16	Four Inverted Five-Spot: Throughput in Network Pore Volume vs. Oil Recovery in Network Pore Volume	80
17	Four Inverted Five-Spot: Throughput in Network Pore Volume vs. Oil Recovery in Network Hydrocarbon Pore Volume	81
18	Four Inverted Five-Spot: Throughput in Network Hydrocarbon Pore Volume vs. Oil Recovery in Network Hydrocarbon Pore Volume	82
19	Four Inverted Five-Spot: Throughput in Network Pore Volume vs. Areal Sweep Efficiency	84
20	Four Inverted Five-Spot: Throughput in Network Displaceable Pore Volume vs. Oil Recovery in Network Displaceable Pore Volume	85
21	Four Inverted Five-Spot: Throughput in Network Displaceable Pore Volume vs. Areal Sweep Efficiency	86

<u>Figure No.</u>		<u>Page</u>
22	Four Inverted Five-Spot: Throughput in Network Pore Volume vs. Instantaneous Water-Oil Ratio	88
23	Effect of Well-Pattern on Oil Recovery	90
24	Effect of Well-Pattern on Areal Sweep Efficiency	93
25	Performance of Inner Normal Five-Spot of Four Inverted Five-Spot Pattern	97

APPENDICES

26	Average Thickness vs. Diameter in the Center of the Model
27	Linear Test: Throughput in Pore Volume vs. Average Water Saturation
28	Linear Test: $1/W_i$ vs. $1/W_i I_r$
29	Linear Test: Water Saturation vs. Fractional Flow of Water

INTRODUCTION

Oil recovery by water flooding is still one of the most important secondary recovery processes employed in Petroleum Industry. One method commonly used to study the field performance of a water flood is the pilot flood. The pilot water flood generally involves a small number of reservoir wells in an isolated area within the field. The results of the performance of the pilot are, in some way, related to the performance of a field-wide water flood. One of the major well patterns utilized for water flooding is a five-spot pattern. In the literature, most of the workers, who have studied the five-spot pattern in the laboratory have used a quarter of a five-spot in which there is an injection well and a producing well at diagonally opposite corners. Such an arrangement is valid for both normal and inverted five-spot patterns in a fully-developed field. They have assumed that being fully symmetrical there is no flow of fluids across the boundary of a five-spot or in other words the pattern is confined. This assumption is true only in case of a completely developed field. In general practice, while investigating the performance of a pilot flood to test the economic feasibility of water flooding in a

particular field, this assumption does not hold. Pilot floods contain only one or a few five-spot unit patterns which are unconfined. It has been noticed that if a single five-spot unit is employed for testing the economic feasibility of a water flood and if the oil recovery is assumed to be coming from within the network area, the results might be too optimistic. The major reason for this behavior is the migration of fluids into or out of the network area as these unconfined patterns are not balanced by other similar units. If a number of five-spot units in the pilot are tested, a better estimate of the performance expected from a fully-developed field may be made. However, there is a practical limit to the number of wells placed in the pilot. A compromise has to be sought between the accuracy of results and number of injection wells employed. Bernard and Caudle [4] have suggested a grouping of four inverted five-spot as the most desirable pattern.

In the present study, two different patterns - an isolated normal five-spot (4 injectors, 1 producer)

and a four inverted five-spot (4 injectors, 9 producers), illustrated in Figure 1 were studied for oil recovery and areal sweep efficiency at a mobility ratio of 0.98. It was the purpose of this study to examine the influence of well pattern on oil recovery and areal sweep efficiency. The performance of the four inverted five-spot was compared with that of an isolated normal five-spot pattern. The influence of mobility ratio on the performance of an isolated normal five-spot was also studied. Finally, the reasons for the change in oil recovery and areal sweep efficiency with a variation in back pressure on the model, as reported by Serra [43] were investigated.

LITERATURE SURVEY

If, in a water flood, it is assumed that the reservoir fluids are incompressible and immiscible, the recovery of oil will be directly proportional to that portion of the reservoir contacted by the injection water. The area contacted by the flooding water as a fraction or percent of the total network area is defined as the "areal sweep efficiency".

The recovery of oil by water flooding is a function of several factors:

- 1) The amount of oil originally present in the reservoir.
- 2) The rate of water injection.
- 3) The viscosity of oil, injection water, and connate water.
- 4) The mobility ratio ($M = \lambda_{\text{displacing}} / \lambda_{\text{displaced}} = \lambda_w / \lambda_o$, where $\lambda = \text{Mobility}$)*
- 5) The amount of original free gas saturation.
- 6) Interfacial tension between oil and water.
- 7) Pore size distribution which together with interfacial tension affects the capillary pressure characteristics of the rock.

* Defined in a later section

- 8) Wettability of the rock.
- 9) Gravity effects.
- 10) The well configuration.

A number of workers [5, 18, 22, 23, 24, 25, 26, 27, 28, 38, 46] have investigated the influence of these various factors on waterflood recovery using short or long linear, consolidated or unconsolidated, cores. Other workers [2, 4, 11, 13, 14, 15, 22, 34, 44, 45, 47, 48] have used various model techniques to study the areal sweep efficiency and oil recovery performance of waterfloods. The major modelling techniques which have been considered are analytical [31, 20], potentiometric [32, 2], electrolytic [48], resistance network [34], gelatin model [14], "fluid mapper" [11], and the X-ray shadow-graph [44].

Cheek and Menzie [11] have described a "fluid mapper" model to study the influence of mobility ratio on sweep efficiency. The model consists of a base slab of dental stone shaped to represent the prototype. A plate glass slightly larger than the slab is placed above and parallel to the slab by means of thin uniform spacers.

Dye was used to trace the flow patterns. The main difficulty with this method was the determination of the time of breakthrough.

Slobad and Caudle [44] have described an "X-ray Shadowgraph" technique which utilizes the principles of radiography to study the effect of factors which influence the areal sweep efficiency in secondary recovery operations. The advantage of this method was that any type of porous system may be studied. Either the displacing or the displaced fluid contains an X-ray absorbing chemical to trace the flood front by focussing a beam of X-ray from below the model and photographing it from the top. The extension of this technique to include the determination of the fluid saturation by means of optical density of the radiographic plate allows the quantitative study of displacement efficiencies within the swept area.

Van Meurs [45] has described a technique which permits visual observation of oil displacement throughout the interior of a porous structure as thick as two inches. A model having glass walls is filled with

finely powdered glass. Such a model becomes completely transparent if the powdered glass pack is saturated with an oil having the same refractive index as the glass. When water or gas, with a refractive index different from that of the oil (glass) is injected, the model becomes opaque in the space occupied by the water (gas). Visual observation and photographs of these displacement processes are thus rendered possible. The main disadvantage with this technique is that the wettability of dry glass beads, which are first saturated with oil, may not represent the wettability of any practical system. Secondly, one cannot simulate the conditions of initial connate water, as the model has to be first saturated with oil.

The effect of injection rate on oil recovery has always been a controversial issue. Many engineers have long held that slower velocities of water encroachment through a sand will yield the greatest ultimate oil recovery [7], while others maintain that the highest possible velocities will yield by far the greatest oil recovery. Earlougher [18] has shown, from tests of

several hundred core samples, that for any given oil saturation, there is a critical maximum velocity above which the recovery efficiency falls off rapidly and the water-oil ratio rises extremely fast. He also found that the critical velocity in a sand varies with the initial oil saturation and is higher for higher oil saturation. Various other workers have studied the effect of injection rate on oil recovery [5, 19, 39, 40]. Beston and Hughes [5], using two long consolidated cores and live natural crude and natural brine, have found (with a few exceptions) that higher flooding pressure gradients and hence higher flooding rates results in higher recoveries. Very low pressure gradients and flooding velocities result in markedly lower recoveries. Engelberts and Klinkenberg [19], using packs of granular material, have found that the higher the viscosity of the oil, the lower is the rate of displacement, resulting in a reduction of the water-oil ratio. They noticed that the rate of displacement, resulting in a reduction of the water-oil ratio. They noticed that the rate of displacement will probably not affect the ultimate recovery for the case of oils of viscosities less than 30 cp. Richardson and Perkins [40]

concluded from their tests that under a wide variety of conditions, oil recovery by water flooding clean water-wet sands is independent of the rate of displacement. Similarly the authors found that the recovery was independent of the pressure level at which the water flood is performed. This gives strong support to the theory that the microscopic distribution of water, oil and gas is controlled at all practical rates by the capillary forces. Rappoport, Carpenter and Leas [39], using a flow model of a quarter of a five-spot, have found that with increasing injection rates the recovery of oil continues to increase. Later on the difference diminishes and after a certain limit there was no appreciable change. At this stage the flood was said to have stabilized. This indicates that every sand which can be water flooded will not produce the maximum yield of oil at high pressure gradients and hence at high injection rates. There may well be an optimum pressure for many sands depending upon their physical and chemical characteristics and upon the ratio and mode of distribution of their water and hydrocarbon content.

Dalton, Rappoport and Carpenter [15] have studied the behavior of an unconfined pilot water flood using potentiometric and flow models. They have shown that the significant feature of an unconfined pilot flood lies in the competition between the producers of the pilot and the surrounding reservoir for the flow of oil and water. For a given static reservoir pressure, p_s , the total flow from the pilot area toward the surrounding reservoir tends to increase as the sand-face injection pressure, p_{wi} , increases. Conversely, the lower the flowing bottom-hole pressure, p_{wp} , at the producing wells, the more effectively they can compete with the surrounding reservoir in capturing the fluids. It has been shown that for a given porous medium and fluid system, the behavior of an unconfined pilot water flood is governed by the dimensionless pressure parameter, defined as the " π -ratio".

$$\pi = \frac{p_s - p_{wp}}{p_{wi} - p_s} = \frac{\Delta p_p}{\Delta p_u} \quad (1)$$

It was found that the oil recovery of an unconfined pilot increases with an increasing π -ratio. This occurs because the area supplying oil to the pilot producers actually extends beyond the perimeter of the pilot area. The oil recovery of the center well is practically independent of π -ratio, while that of the corner and side producers is greatly influenced by it. Also, the center well receives considerably more oil than each of the corner producers. This results because the center well receives essentially all of the oil moving in its direction, while a portion of the oil moving toward the side and corner producers can escape into the surrounding reservoir, particularly when the pilot is operating at a low π -ratio.

The influence of mobility ratio and viscosity ratio on flooding efficiencies has been investigated by many researchers. Muskat [31] was probably the first to point out that the fluid mobilities (k/μ) in the oil and water regions would affect the performance of the water-flood, and he estimated the general effect of these variables. Since then, studies of the influence

of mobility ratio on secondary recovery have been reported where mathematical [20], potentiometric [2], and scaled flow models [44] have been utilized. Aronofsky [2] used a potentiometric analyzer and numerical computations and studied mobility ratios of 10, 1, and 0.1. He found that the sweep efficiency was very much dependent upon the mobility ratio, and so should be considered in practical field problems. He also found that the "fingering" or "cusping" near the producing well was more pronounced for a mobility ratio of 10 than that for 1 and the flooded area was also smaller in the former case. On the other hand the flooded area is greater for a mobility ratio of 0.1 as compared to that of 1.0. Slobod and Caudle [44] have shown that the use of miscible phases instead of immiscible phases to determine the influence of mobility ratio on area sweepout efficiencies is justified. Dyes, Caudle and Erickson [16] have studied the influence of mobility ratio on the oil production after breakthrough. It was noted that high mobility ratios led to early declines in the fraction of total flow from the unswept region and therefore result in a less

favorable rate of oil recovery. Though the ultimate oil recovery was nearly the same, there was a vast difference in operating life for different mobility ratios. At higher mobility ratios, nearly one-half of the recoverable oil may be produced after breakthrough. Cheek and Menzie [11] used a "fluid mapper" model to study the influence of mobility ratio on areal sweep efficiency and found identical results for lower values of mobility ratio but noted a wide discrepancy at higher values. Aronofsky and Ramey [3] studied the influence of mobility ratio on production and injection histories using potentiometric model. The range of mobility ratios investigated was 0.1 to infinity. They found wide disagreement in the results obtained for areal sweep efficiency by this method and those obtained by other workers using different types of models. As the degree of reproducibility reported by other workers was much higher than the difference in the results, it was inferred that there are fundamental differences between the models which become important at high and low mobility ratios. Van Meurs [45] used a transparent three-dimensional model and found that at high oil-to-

water viscosity ratios the recovery of oil is adversely affected as a consequence of the phenomenon of viscous fingering. Rappoport, Carpenter and Leas [39] have found that the water-invaded zone is radial during the initial flooding stages, following which it then stretches into a squared-off pattern, and finally developing a cusp toward the producing wells. With increasing oil-to-water viscosity ratios this cusp becomes more pronounced and begins to form at an earlier flooding stage, resulting in an overall decrease of areal coverage at water breakthrough. Caudle and Witte [9] have studied the influence of mobility ratio on the rate of oil recovery in a five-spot. The results show a change in fluid conductivity (total flow rate/pressure drop) as the sweepout pattern increases for mobility ratios between 0.1 and 10. If the mobility ratio is favorable (<1), the conductance will drop continuously whereas if the mobility ratio is unfavorable, the conductance ratio will increase continuously. Studies reported by Pye [37] and Sandiford [41] have indicated that chemicals to increase injection water viscosity are now available and can be used to reduce the overall mobility ratio

of a waterflood. Where mobility ratios are controlled by the injection of viscous fluids, the connate water of the reservoir may play an important part in the displacement of the reservoir oil. Kelley and Caudle [22] have investigated the role of connate water in high-viscosity crude oil reservoirs. They have found that the connate water is mobile and was banked ahead of the viscous injection water. Early water breakthrough should be expected even though overall mobility ratios are reduced by the injection of viscous water. Although the connate water adversely affects the oil recoveries, sizeable additional oil recoveries are still obtained by the injection of viscous water. In all of these studies the basic assumption was that the displacing fluid swept the displaced fluid down to a residual value, so that there was no saturation gradient present either in the swept or the unswept region. In each region it was assumed there was only one mobil fluid and its mobility was constant throughout the region. Most of the workers used miscible fluids. The use of immiscible fluids leads to difficulty in assigning a mobility ratio to the system since a small gradient in saturation

represents a large gradient in mobility. It is also difficult to define accurately the field relative permeability relationships from results on small laboratory samples.

The effect of the presence of a free gas saturation on water-flooding efficiencies has also been investigated. Richardson and Perkins [40] have shown that the presence of free gas lowers, by a very small amount, the residual oil saturation remaining after water flooding unconsolidated sands. The presence of a free gas saturation in a thick homogeneous reservoir sand causes an early water breakthrough. The presence of a free gas saturation in a stratified reservoir increases the tendency for water to channel through the more permeable sand. The total oil recovered for a given amount of water injected is always slightly greater when gas is present. Kennedy and Guerrero [23] have noted that the presence of gas, regardless of the surface and interfacial tensions, exerts a substantial beneficial effect on the recovery. No additional oil can be obtained by waterflooding a core which has been

previously waterflooded above the bubble point and pressure depleted. Neilson and Flock [33] have concluded that the ultimate recovery from an isolated inverted five-spot may be increased by establishing a gas saturation prior to flooding as long as "fill-up" is obtained prior to water breakthrough. Craig [13] has found that in a normal five-spot pattern, the oil migration outside the pilot area occurs only after there is liquid fill-up within the pilot area. As the initial gas saturation is increased, there is less time for migration to occur between fill-up and flood-out of the pilot area. It is possible for the initial gas saturation to be sufficiently large so that when waterflood fronts from each of the four injection wells meet, liquid fill-up occurs within the pilot area. This value of initial gas saturation is termed as the maximum effective gas saturation, S_g^* , given by,

$$S_g^* = \pi/4 (1.0 - S_{wc} - S_{or}) \quad (2)$$

where

S_{wc} = Connate water saturation

S_{or} = Residual oil saturation

Interfacial tension and wettability play an important part in oil recovery by water flooding. Wettability, qualitatively speaking, denotes the ease with which a fluid can displace other fluids or spread over a solid surface in the presence of other fluids [42]. A quantitative definition of wettability has not been given so far and is difficult to state. Hence, relative wettability is used. In the case of a porous medium, one fluid will preferentially wet the porous surface compared to the other. The adhesion tension, which is a function of the interfacial tension and the contact angle, determines which fluid will preferentially wet the solid. A positive adhesion tension, or in other words, contact angles less than 90° , indicates that the water phase preferentially wets the solid.

The capillary pressure is defined as the interface pressure drop between a continuous oil phase

and a continuous water phase in a porous material. The magnitude of this pressure difference depends on the interfacial curvature and the interfacial tension. The former is determined by the geometry of the pore spaces, the wettability of the rock surfaces, and the quantity of each phase present. Mathematically, for a capillary of space between particles that has a shape other than cylindrical, the capillary pressure, P_c , is related to the curvature of the meniscus by the equation,

$$P_c = \sigma \left(\frac{1}{R_1} + \frac{1}{R_2} \right) \quad (3)$$

where R_1 and R_2 are principal radii of curvature of the meniscus.

σ is the interfacial tension.

If $R_1 = R_2 = R$,

$$P_c = \sigma (2/R)$$

For cylindrical shape of the pore space,

$$R = r / \cos \theta$$

where r is the radius of capillary

θ is the contact angle measured through the denser liquid phase when both the fluids are in contact with the solid surface.

With these substitutions, equation (3) becomes,

$$P_c = \frac{2 \sigma \cos \theta}{r} \quad (3a)$$

On the microscopic scale the capillary forces, which act over a distance of one or two sand grain diameters, control the distribution of oil and water under static equilibrium conditions. When an external force is applied, as in the case of water injection, the applied forces tend to distort the oil-water interfaces. However, in most fine-grained, water-wet sands the applied pressure difference across one or two grain diameters is usually several orders of magnitude less than the capillary pressure difference. These considerations lead to the theory that even during flow the capillary forces continue to control the microscopic distribution of oil and water within the pores of a porous material for all practical reservoir and laboratory flow rates.

Based on the Buckley-Leverett [7] concept, the fractional flow of displacing fluid in the total flowing stream, f_d , is given by,

$$f_d = \frac{1 - \frac{k_o}{\mu_o q_t} \left(\frac{\partial P_c}{\partial x} + g \Delta \rho \sin \theta \right)}{1 + \frac{k_o}{k_d} \cdot \frac{\mu_d}{\mu_o}} \quad (4)$$

where $P_c = P_d - P_o$

$\Delta \rho = \rho_d - \rho_o$

k_d, k_o = effective permeability to displacing phase and oil, respectively

μ_d, μ_o = viscosity of displacing phase and oil, respectively

q_t = total flow rate

θ = positive updip

As the experimental values of $\partial P_c / \partial x$ are always negative, according to the definition of capillary pressure, the net effect of including the capillary term

is to increase the value of the calculated fraction of displacing fluid in the flow stream at any saturation and to decrease the recovery of displaced fluid [25]. Perkins [35] has shown that the influence of capillary pressure gradients on the macroscopic flow behavior increases as the flow rate decreases.

Kinney and Neilson [24] have found that the percentage of recoverable oil produced before water breakthrough is greater in a preferentially oil-wet porous medium. They have also shown that wettabilities are affected by the order or sequence in which two liquids are allowed to enter the solid. Engelberts and Klinkenberg [19] have stated that it is not to be expected that changes in the capillary forces will substantially affect water-drive processes under field conditions. Kennedy and Guerrero [23] have found that the reduction in the interfacial tension between oil and brine reduces slightly the recovery of oil by water flooding above the bubble point. Below the bubble point, in the presence of gas, a reduction of interfacial and surface tensions of the liquids has a small or negligible

effect on recovery. Their results are in contradiction with theoretical predictions that if the oil phase is distributed as droplets in the porous medium, the recovery of oil should be increased by decreasing the interfacial tensions between the liquids. From this they have concluded that the oil does not occur as segregated droplets, as commonly assumed.

Moore and Slobod [26] have proposed a theory based on several thousand flooding experiments on a variety of porous media, known as the "Viscap Theory". According to this theory, interplay of capillary and viscous forces determines the efficiency of oil displacement and the production history after breakthrough. They have also shown that the wettability of the rock is of key importance in explaining or predicting the performance of water floods, either in the laboratory or in the field. They have classified the cores as strongly water-wet, strongly oil-wet or of intermediate wettability. For water-wet cores, the displacement of oil by water is almost always controlled by imbibition. The tests on oil-wet cores are affected

by end effects which result in a high oil saturation at the exit end, and hence this core data is not applicable to the reservoir unless run under conditions which suppress this end effect to an insignificant portion of the core length. A similar effect was noticed by Perkins [35] in water-wet cores in which water (wetting phase) accumulates at the outflow face and would not produce until there was a residual oil saturation. He termed it the "boundary effect" and noted that this effect would be minimized by using longer columns and/or higher injection rates. The ultimate residual oil saturation is independent of rate or column length. This indicates that the microscopic fluid distribution is controlled by capillary forces and is not rate sensitive.

Bobek and Mattax [6], and Mungan [27], have found that oil recoveries by water-flooding water-wet rocks are higher than from oil-wet rocks. Mungan [27] has also noted that a reduction in interfacial tension results in increased recovery. This increase in recovery is greater if the displaced phase is the wetting phase.

Mungan [28] has also found that the breakthrough of a non-wetting displacing liquid always occurs earlier than that of a wetting displacing liquid. It has been noted that the smaller the viscosity ratio, the closer are the final recoveries for the two cases. This suggests that for oil-wet rocks, as an alternative to decreasing the interfacial tension, one may increase the viscosity of the injected fluid to increase the final recovery. Also, when the displaced phase wets the core, a considerable amount of the production is obtained after breakthrough, even for a viscosity ratio of 1.0. Similarly, while investigating the influence of interfacial tension, he found that lowering the interfacial tension increases the recovery but not to a great extent if the displacing liquid is the wetting liquid. In the case of displaced phase being the wetting phase, a lowering of interfacial tension significantly increases the breakthrough recovery as well as the final recovery. Similar results were observed by Wagner and Leach [46].

In most of the laboratory investigation,

the gravity effects were neglected. This is justified if the thickness of the packing is small. Wyckoff, Botset and Muskat [48] have discussed the effect of gravity on the shape of encroaching front. According to them there are two types of distortion possible due to gravity: 1) a tendency for the assumed vertical wall of water to flatten out into a level surface causing earlier water breakthrough, and 2) in an inclined producing horizon there will be a tendency towards the suppression of the "fingering". The steeper the inclination of the stratum the greater will be the suppressing tendency.

Well configuration has a significant influence on areal sweep efficiency and hence on oil recovery by water flooding. Researchers have worked with different well patterns - line drive, staggered line drive, isolated normal and inverted five-spot pattern, and combinations of a series of five-spots, seven-spots, and nine-spots. Most of the workers, while investigating a five-spot pattern in the laboratory, have used a quarter of a five-spot because of symmetry. They have

assumed that the boundaries of a five-spot act as impermeable barriers. In an actual pilot flood in the field this assumption is not valid. The pilots generally consist of one or a few five-spot patterns, which may not behave as confined systems because there may be flow of fluids from and to the reservoir lying outside the pilot area. This point should be considered before one should attempt to extrapolate the results of a pilot flood, especially of a single normal five-spot (four injectors and one producer), to the full-scale operation.

Caudle and Loncaric [10] have pointed out that the amount and rate of oil recovery from an unconfined pilot area is not usually the same as from an equal area in a large-scale flood. This is true because the fluids are free to move across the boundary of a pilot area. From the data obtained, the authors have pointed out that the pilot flood oil recoveries may be wrong by as much as a factor of four if the recovery is supposed to be coming from the area within the four injection wells. They have suggested correction factors to take

this effect into account. These correction factors are the ratios of fully developed five-spot performance to five-spot pilot performance, which can be applied to pilot data to predict the reservoir performance. Similar results have been pointed out by Dalton, Rappoport and Carpenter [15]. They have shown that the recovery behavior of confined and unconfined floods differ in that only a certain fraction of the injection water actually sweeps oil towards the pilot producing wells because fluids can escape from the pilot pattern, while all the injection water sweeps oil toward confined producing wells. Also the reservoir area supplying oil to pilot producing wells is different from that supplying oil to confined producing wells. Neilson and Flock [33] have found that the rapid "water-out" characteristic common to linear floods and floods conducted in developed well patterns is not prevalent in the case of an isolated inverted five-spot. Instead, the producing water-oil ratio increases very slowly after breakthrough such that ultimate areal sweep efficiencies six times that at breakthrough were possible.

Craig [13] has pointed out that a single normal five-spot flood can yield a direct estimate of ultimate recovery and production performance possible by full-scale operations if the advance of the injected water is uniform and the condition ratio of pilot producer is at least 2.2. (The condition ratio has been defined as the ratio of a well's actual productivity to the productivity of an undamaged and non-stimulated, normal sized well in the same formation). Similarly, a single inverted five-spot pilot flood with no initial gas saturation can provide quantitative estimates of full-scale waterflood recovery, if the offset producing wells have condition ratios of 1.4 or above.

Bernard and Caudle [4] have shown that pilot water floods can adequately predict the performance to be expected from fully developed water floods if the proper pilot pattern and operating conditions are used. The type of pattern and the number of wells to be placed in the pattern depend on the oil-water mobility ratio and the expected oil-bank size. Pilot patterns

in reservoirs containing a dispersed, flowable free gas saturation will require fewer wells as compared to gas-free reservoirs. Unfavorable mobility ratios will, in general, require more wells in the pilot pattern than favorable mobility ratios. It was found that the most desirable pattern, with regard to accuracy of results and number of injection wells, was the grouping of four inverted five-spot (four injectors, nine producers).

Prats [36] has discussed the effect of off-pattern wells on the performance of a five-spot waterflood. He noted that the oil recovery at water breakthrough is always lower than that for regular five-spots. There was a loss in oil recovery, more or less depending upon the well's displacement, whether the off-pattern well is a production or injection well, or whether the off-pattern wells are separated by a regular five-spot, etc. Although the loss in oil recovery due to pattern irregularity often may be low, the off-pattern case will always require

injection of more water to reach the same final water-cut.

Dyes, Kemp and Caudle [17] have studied the effect of fractures on sweepout pattern and found that short fractures, either horizontal or vertical, could be used in flooding operations to gain an increase in injectivity or productivity without any serious harm to sweepout pattern. A long fracture does not harm the sweep if it is directed between producers. If it is directed towards a producer, the throughput volume necessary to attain a given recovery is increased. The ultimate recovery does not significantly reduce until the fracture length exceeds three-fourths of the distance between the well and the element boundary.

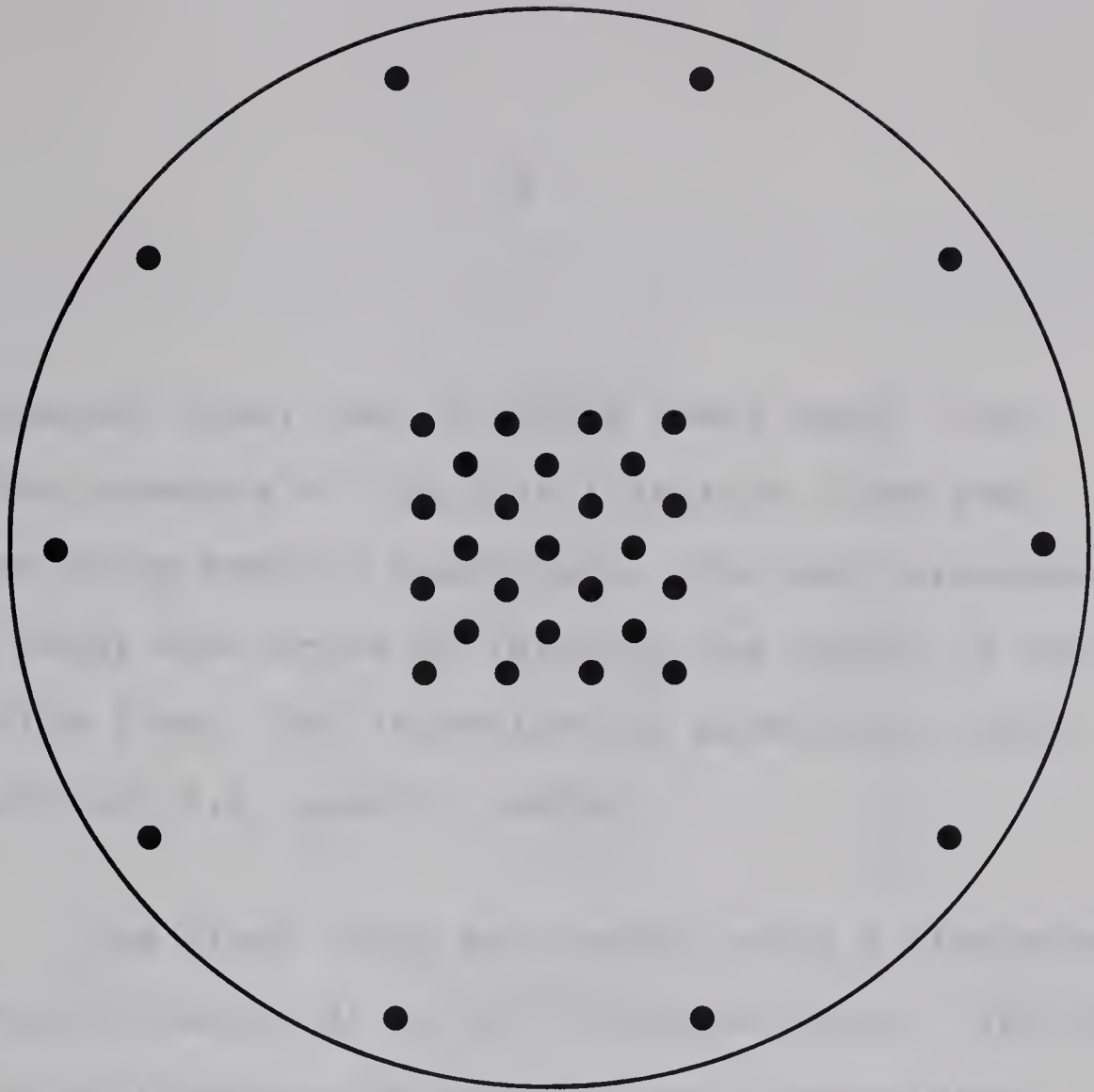
Caudle and Loncaric [10], Dalton, Rappoport and Carpenter [15], Neilson and Flock [33], Craig [13], and Bernard and Caudle [4] have studied the influence of fluid-flow beyond the network area on oil recovery and areal sweep efficiency in case of an isolated

pattern. These workers have pointed out the significant difference between the performance of an isolated pattern and a similar pattern in a fully developed field. They have suggested various ways, like correction factors [10], condition ratio of the pilot producer having a minimum value [13], selection of proper pilot pattern and operating conditions [4], etc., to enable the extrapolation of isolated pattern performance to the performance of a completely developed field. The present work was undertaken to further study the extent of fluid flow beyond the pattern area in case of an isolated normal five-spot and a grouping of four inverted five-spots.

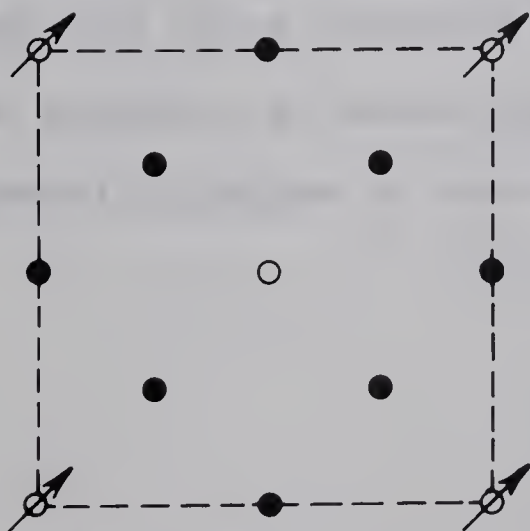
DESCRIPTION OF THE MODEL

The model consists of two circular transparent lucite plates about three feet in diameter and two inches thick. They are bolted around the periphery and sealed by two neoprene O-ring seals and separated by a quarter inch thick spacer. There are ten wells equally spaced around the periphery and twenty-five wells in the center in the form of a square pattern (Figure 1). The periphery wells were used to clean the model and to bring it to an irreducible water saturation condition. Various patterns were studied using the center wells. A scale drawing of the well is shown in Figure 3, and consists of a brass stem of 1/16-inch internal diameter, open at the bottom and reaches halfway through the packing when in position. The wells were opened or closed by means of a valve.

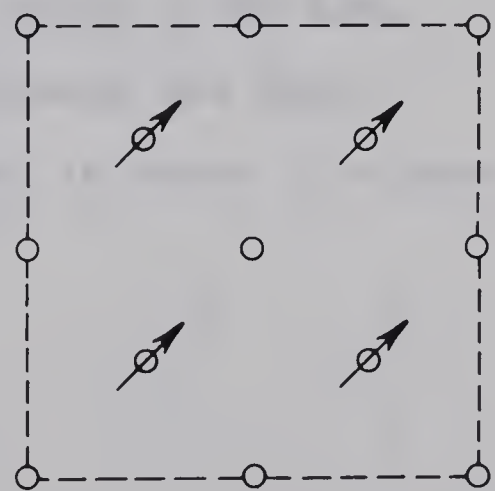
The injection system consists of four pistons mounted so a fifth double acting piston could drive them backward or forward at the same constant rate. The double acting piston was operated hydraulically



PLAN OF THE MODEL



ISOLATED NORMAL FIVE-SPOT



FOUR INVERTED FIVE-SPOT

- SHUT-IN WELL
- PRODUCTION WELL
- ⊙ INJECTION WELL

PATTERNS STUDIED

FIG. 1

by a constant rate, dual cylinder Ruska pump. The injection pressure of the four injection lines was measured using mercury manometers. The back pressure on the model was varied by latering the height of the production line. The injection and production lines were 1/8-inch I.D. plastic tubing.

The flood front was traced using a fluorescent dye (Dupont Uranine B) in the injection water. The dye was made to fluoresce by means of two ultra-violet tubes mounted below the model. A polaroid camera was mounted about five feet above the model to photograph the position of the flood front from time to time. A black and white polaroid film of speed 3,000 ASA, and an exposure of about fifteen seconds was used. A schematic diagram of the equipment is shown in Figure 2.

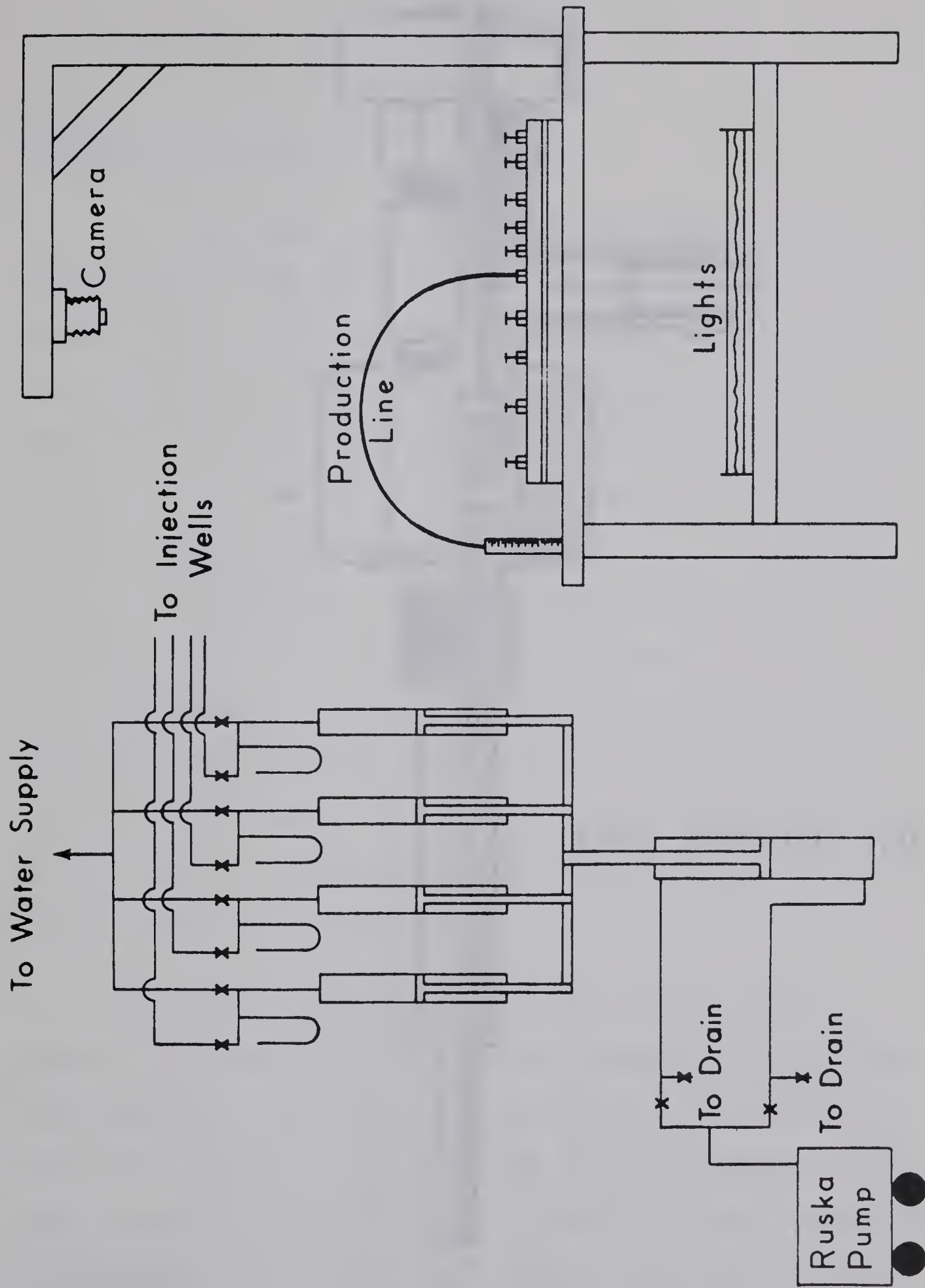
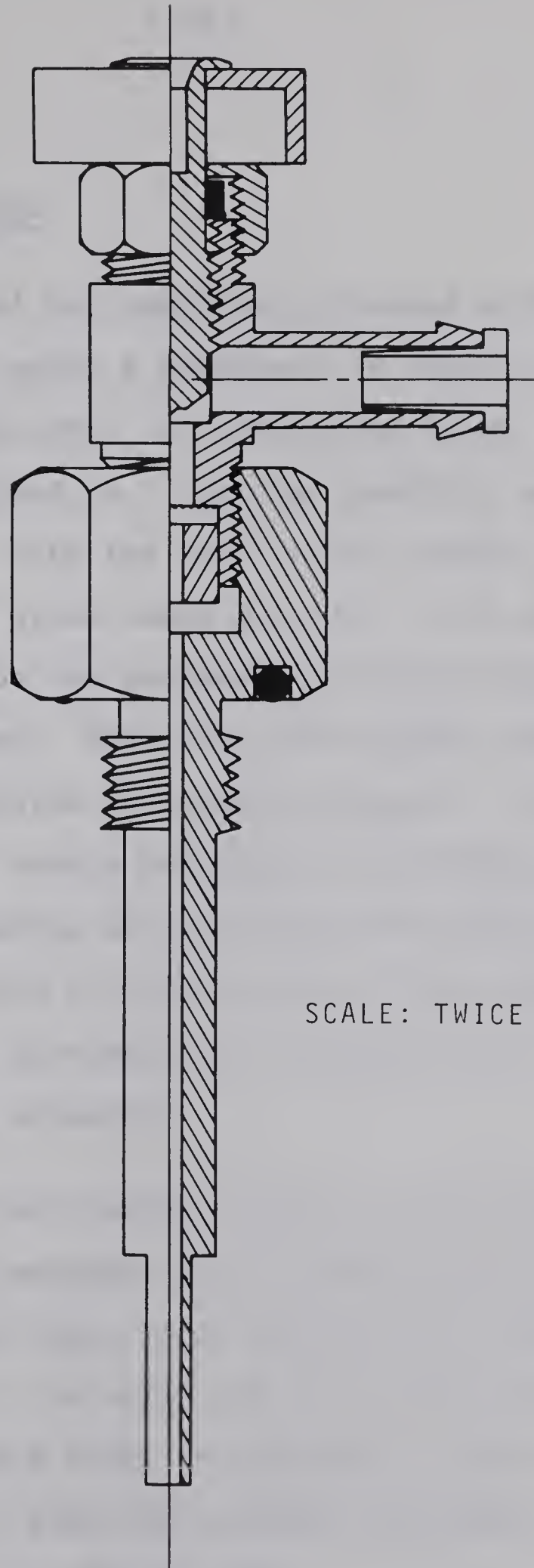


FIGURE 2

WELL DETAIL



SCALE: TWICE FULL SIZE

FIGURE 3

PACKING OF THE MODEL

The model was completely cleaned and the inside walls were washed using a detergent to remove any greasy or oily film. The model was completely dried, bolted and was made to stand in a vertical position on an electric vibrator with the hole in the upright position through which the glass beads were fed. The unconsolidated porous medium was prepared of uniform glass beads of 0.6 mm. diameter. They were fed through the hole as the model was vibrated and lightly tapped. To discharge the electrostatic charge developed in the beads due to vibration, the packing was saturated with distilled water and then dried by flowing air at low pressure for a long time. The procedure was repeated until a uniform tight packing was obtained.

Due to the flexible nature of the lucite plates, the model expanded in the middle during packing. This expansion was taken into account while calculating the bulk volume of the model and the network pore volume. The calculations are shown in Appendix I, and a correlation was established to find the average thickness of the packing for any area (Figure 26).

MODEL PROPERTIES

Porosity, absolute permeability, relative permeability, mobility ratio and the wettability of the model were established for the model and the detailed calculations are shown in Appendices I, II, III, and IV.

For this model, the bulk volume was determined from the physical dimensions of the model, taking into account any expansion during packing. The pore volume was determined by a simple material balance. The model was evacuated and saturated with distilled water. The volume of distilled water remaining inside the model gave the pore volume. The porosity of the pack was found to be 32.9%. The porosity of a pack of spherical particles of uniform size depends on a stacking arrangement and varies from 47.6% for cubic stacking to 25.9% for Rhombohedral stacking. An average for six different stacking arrangements is 34.8%.

The permeability of a porous medium may be defined as its fluid conductivity, or ability to let

fluid flow within its interconnected pore network.

According to Darcy's Law,

$$Q = - \frac{kA}{\mu} \cdot \frac{dp}{ds} \quad (5)$$

where Q = Rate of flow of the fluid, cc/sec

A = Cross-sectional area perpendicular to
fluid flow, sq. cm

μ = Fluid viscosity, cp

dp/ds = Pressure gradient, atm/cm

k = Permeability of the rock, Darcy

Except for gases at low pressures, the permeability of a porous medium is a property of the medium and not of the fluid flowing, provided that the fluid 100% saturates the pore space of the medium. This permeability at 100% saturation of a single fluid is called the absolute permeability of the medium. The absolute permeability of the model was calculated before the injection of an oil phase using Muskat's five-spot formula and was found to be equal to 1542 md.

In the case where the porous medium contains more than one fluid phase, the permeability is no longer constant, but varies for the different phases present and is dependent on their respective saturations in the medium. This is known as effective permeability and is the permeability of the porous medium to a particular fluid when that fluid has a pore saturation of less than 100%. Where two fluids are present, such as oil and water, their relative rates of flow are determined by their relative viscosities and their relative permeabilities. Relative permeability is the ratio of effective permeability to the absolute permeability.

Mobility of a fluid is defined as the effective permeability of the porous medium to the fluid divided by the fluid viscosity. The relative rates of flow of oil and water depend on the mobility ratio, M , which is defined as the ratio of the mobility of the region behind the flood front to the mobility of the region ahead of the flood front. Mathematically,

$$M = \frac{\lambda_w}{\lambda_o} = \frac{k_w/\mu_w}{k_o/\mu_o} \quad (6)$$

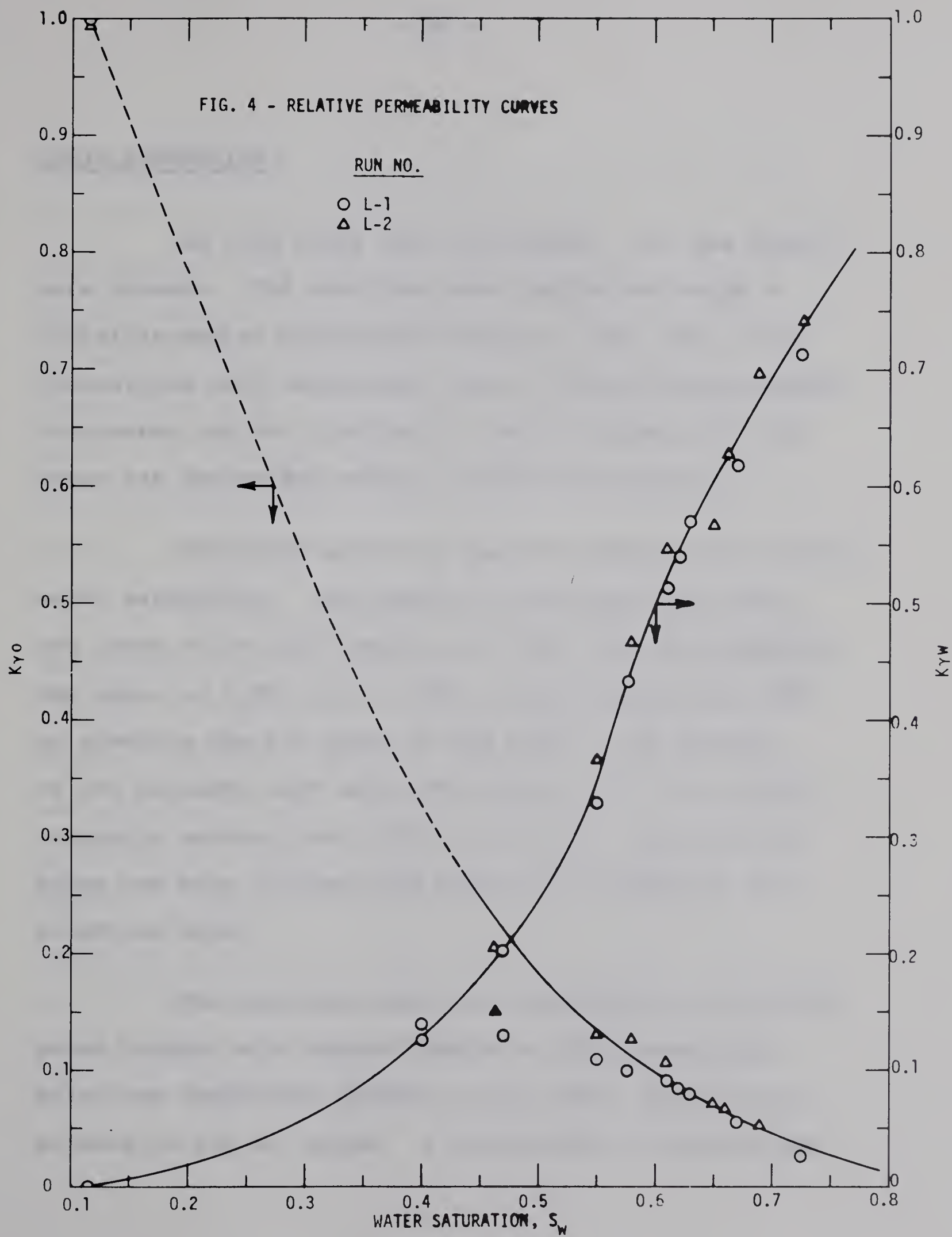
where λ_w , λ_o are the mobilities of the region behind the flood front and ahead of the flood front respectively.

In the laboratory experiments, it was noticed that the displacing water did not displace oil to its irreducible saturation and therefore there was two phase flow behind the flood front. In other words the saturation of oil and water was constantly changing behind the flood front and hence the relative permeability of the two fluids was changing. This in turn caused a constant change in the mobility of the region behind the flood front, resulting in a steadily varying mobility ratio. For this reason, the relative permeability curves for oil and water were determined using a linear pack of the glass beads. A lucite tube, 28.5 cm. in length, packed with glass beads was evacuated and saturated completely with distilled water. Oil was injected until an irreducible water saturation condition was established. Finally oil was displaced by water at a constant rate, the injection pressure was recorded and the corresponding recovery of oil and water was noted. From this data, relative

permeability for oil and water versus water saturation were obtained using the method suggested by Johnson, Bossler and Naumann [21]. These results are shown in Figure 4.

In the case of immiscible fluids, it is difficult to assign a mobility ratio to the system, since a small gradient in saturation represents a large gradient in mobility. Besides, the mobility in the swept region is not constant and is changing as more and more oil is produced. Using the relative permeability curves (Figure 4) and the method suggested by Craig, Geffen and Morse [12], the useful value of mobility ratio was calculated as 0.98, but could vary from 0.59 to 1.15.

FIG. 4 - RELATIVE PERMEABILITY CURVES



FLUID PROPERTIES

In this study only two phases - oil and water - were present. The densities were determined using a Christian-Becker Chainomatic Balance, Model SG-1; the viscosities were determined using a Cannon-Fenske-Ostwald viscometer and the interfacial tension between oil and water was determined using a Du-Nuoy Tensiometer.

Distilled water was used to simulate the connate water saturation. The density of the distilled water was found to be 0.997 gms/cc. at 75°F. and the viscosity was equal to 0.892 cp. at 78°F. Esso kerosene was used to simulate the oil phase in the model. The density of the kerosene used was 0.794 gms/cc. at 75°F. and the viscosity measure was 1.265 cp. at 78°F. Thus the oil phase was more viscous than either the connate or the injection water.

The injection water was simulated by distilled water colored with Dupont Uranine B fluorescent dye, which was completely soluble in the water phase but insoluble in the oil phase. A concentrate of the dye was

made with 5 gms of dye per 500 cc. of distilled water and 250 cc. of such concentrate was mixed in 8.25 litres of distilled water for the injection water. The coloring made it possible to photograph the flood position at any instant by using ultra-violet fluorescent lights at the base of the model. The density of this water was 0.996 gms/cc. at 78°F. and viscosity was 0.927 cp. at 78°F. The interfacial tension between the injection water and kerosene was 30.75 dynes/cm. at 75°F.

The contact angle, θ , was needed to calculate the injection rate above which the flood was stabilized and not rate sensitive. An approximate value of the contact angle was required. The capillary-rise method as described by Amyx, Bass and Whiting [1], was used to calculate the contact angle. The only assumption was that the wetting characteristics of the glass of capillary tube were the same as that of glass beads, and on this basis the contact angle was found to be equal to 14°. The calculations are given in Appendix V.

SCALING

The model was scaled such that the performance was not rate sensitive. In other words the assumption that the capillary pressure effects may be neglected was justified. For this purpose, the criterion of critical scaling coefficient, as suggested by Rappoport, Carpenter and Leas [39] was utilized. The displacement of oil by water in an immiscible and incompressible flow system with no gas liberation can be described by a differential equation combining the continuity equation, equation of state and Darcy's Law. This equation accounts explicitly for the frictional, gravitational, and capillary forces in the case of displacement of oil by water. It was noted from this equation that a dimensionless group of parameters, C_2 , given by*

$$C_2 = \frac{q \mu_w}{\sigma \cos \theta \sqrt{k\phi}} \quad (7)$$

characterizes the relative importance of the capillary forces in the displacement of oil by water. This group, C_2 , may be designated as the "Capillary Pressure Scaling

* The group C_2 as defined here is a more "general" form of that given in reference [39].

Coefficient". For a given value of C_2 , all porous flow systems of given geometry, operated under similar conditions would yield the same flooding behavior. Thus, group C_2 represents a scaling factor which may be used to relate the results of flow model experiments to field performance.

Rappoport, Carpenter and Leas [39] noted that "with increasing values of the scaling factor, C_2 , the relative importance of the capillary forces decreases and may eventually become negligible for a certain "critical" value of C_2 . At this stage, the system is said to have "stabilized" and is no longer influenced by capillary effects and becomes independent of the injection rate." They experimentally found that the value of critical scaling coefficient for a five-spot flood is of the order of 3.5×10^{-3} for an oil-water viscosity ratio of 1. This value is still less for higher oil-water viscosity ratios (3.2×10^{-3} for 40:1). (In calculating critical scaling coefficient, q was expressed in bbl/day/ft., μ_w in cp., σ in dyne/cm., k in md.). In other words, stabilized

flooding is insured for rates which give a value of critical scaling coefficient greater than above mentioned values.

The critical injection rate was calculated and all the rates employed in different runs were kept above this critical value. The calculation for the critical injection rate is given in Appendix VI.

EXPERIMENTAL PROCEDURE

The experiments were performed with the model in the horizontal position. It was completely evacuated and saturated with distilled water and the water injected and water produced were recorded. The pore volume of the model was established by material balance. The injection water was injected at a constant rate in an isolated normal five-spot pattern recording the history of injection pressure. The absolute permeability of the porous medium was calculated using these data. The flooding procedure used was as follows:

- 1) The dye was washed out by injecting distilled water in the periphery wells, one at a time, and producing from the center well.
- 2) Kerosene was injected through the center well and the fluids produced from the surrounding wells were collected and respective amounts of oil and water were noted. The oil-injection was continued until no more water was produced. From the material balance, and knowing the pore volume of the model,

the initial oil saturation and irreducible water or connate water saturation was calculated.

3) The flood pattern was selected, the four injection lines from the injection system were connected to injection wells and the producing line was led to a graduated test tube of 25 ml. capacity with graduations of 0.5 ml. apart. In the case of four inverted five-spot pattern, all the nine producing lines were taken to different test tubes. The initial manometer reading of the injection lines were recorded.

4) The pump was started which actuated the double acting cylinder, which in turn actuated the four single-acting cylinders causing all of them to inject at a constant rate.

5) The producing stream was collected in a graduated tube and recorded along with a record of injection pressure.

6) The flood front was traced from time to time by photographing the model. It showed the extent to which the injection water had

swept the model. A note was made of the volume of fluids produced at the time the photograph was taken, which also represented the cumulative throughput at that stage. Four photographs per run were taken to show the flood position at four different stages.

7) A run was terminated after about 8 to 8.5 network pore volumes of water had been injected.

8) The steps 1 through 7 were repeated for the next run. It was noticed that after step 2, the model returned to the original conditions of oil and irreducible water saturation and it therefore was not necessary to evacuate the model after every run.

The photographs were planimetered to find the area of the porous medium contacted by the flooding water at any stage. This allowed the calculation of the areal sweep efficiencies as a function of total throughput volume.

RESULTS AND DISCUSSION

Definition of Terms Used in Calculations and Plots

1. Network Pore Volume (P.V.) = Area of network x
Average thickness (h) x Porosity (ϕ)

2. Network Hydrocarbon Pore Volume (HCPV) = Network
Pore Volume x Initial Oil Saturation (S_{oi})

3. Displacement Efficiency (E_d)

$$= \frac{\text{Initial Oil Saturation}(S_{oi}) - \text{Residual Oil Saturation}(S_{or})}{\text{Initial Oil Saturation } (S_{oi})}$$
$$= \frac{\text{Oil Recovered at any Stage}}{\text{Area constacted by flooding water at this stage} \times h \times \phi \times S_{oi}}$$

4. Areal Sweep Efficiency (E_{as}) = $\frac{\text{Area contacted by flooding water}}{\text{Network Area}}$

$$= \frac{\text{Area contacted} \times h \times \phi \times (S_{oi} - S_{or}) \times S_{oi}}{\text{Network Area} \times h \times \phi \times (S_{oi} - S_{or}) \times S_{oi}}$$

$$= \frac{\text{Oil Recovery (cc.)}}{\text{Network Pore Volume} \times E_d \times S_{oi}}$$

$$= \frac{\text{Oil Recovery (cc.)}}{\text{Network Hydrocarbon Pore Volume (cc)} \times E_d}$$

$$= \frac{\text{Oil Recovery (Network HCPV)}}{E_d}$$

$$\begin{aligned} 5. \quad \text{Displaceable Pore Volume} &= \text{Network Pore Volume} \times (S_{oi} - S_{or}) \\ &= \text{Network HCPV} \times E_d \end{aligned}$$

$$6. \quad \text{Instantaneous Water-Oil Ratio (WOR)}$$

$$= \frac{\text{Water produced during any interval}}{\text{Oil produced during the same interval}}$$

Two different patterns - an isolated normal five-spot and four inverted five-spot - were studied. A total of 16 different runs were made but only 8 good runs, 5 for isolated normal five-spot and 3 for four inverted five-spot, are reported and analyzed. All the runs in the case of isolated normal five-spot were conducted at a constant injection rate of 400 cc/hr/well or 1600 cc/hr., which was well above the value calculated from Rappoport's scaling coefficient to make the flood independent of rate. Also a constant d/r_w ratio of approximately 181 was used, where d is the distance between the production and injection

well and r_w the radius of the well-bore. Tests were conducted at different back pressures to analyse the recovery and areal sweep efficiency as affected by the back pressure.

In the case of the four inverted five-spot, 3 runs were conducted. They were all at the same back pressure of 21.5 cm. of water. It was established from the isolated normal five-spot pattern study that back pressure did not affect the recovery or areal sweep efficiency as long as it was kept below a certain limit. This was attributed to a lack of expansion of the model at low back pressures and hence, no by-passing of fluids. In this case the d/r_w ratio was kept constant for all the three different runs, although it was exactly one-half of that employed in normal isolated five-spot case (approximately equal to 90.5). The injection rate of flooding water was varied for the three different runs to examine the dependency of rate on the flood performance.

An example of the photographs taken during a run showing the area contacted by flooding water for the cases of an isolated normal five-spot and four inverted

five-spot is shown in Figures 5 and 6 respectively. The white portion is the area contacted by flooding water. This area was planimetered and was expressed as a fraction of the total network area to give the areal sweep efficiency at any instant of time.

The mobility ratio for all the 8 runs was kept constant and was equal to 0.98 (the useful value of mobility ratio as calculated by Craig, Geffen and Morse [12] method). In all the runs, the injection was stopped corresponding to approximately 8 to 8.5 network pore volumes of fluid throughput. The network area was the same for both the isolated normal five-spot and the four inverted five-spot. As the fluids were incompressible and immiscible, the throughput was equal to the total amount of oil and water produced.

Before reviewing the actual results, it should be pointed out that for an isolated normal five-spot study on the present model, Serra [43] found a change in oil recovery and in areal sweep efficiency with a change in the back pressure on the model.

Area Swept as a Function of Cumulative Throughput

ISOLATED NORMAL FIVE-SPOT

RUN NO. 1

Injection Rate = 400 cc./hr./well = 1600 cc./hr.
Back Pressure = 0

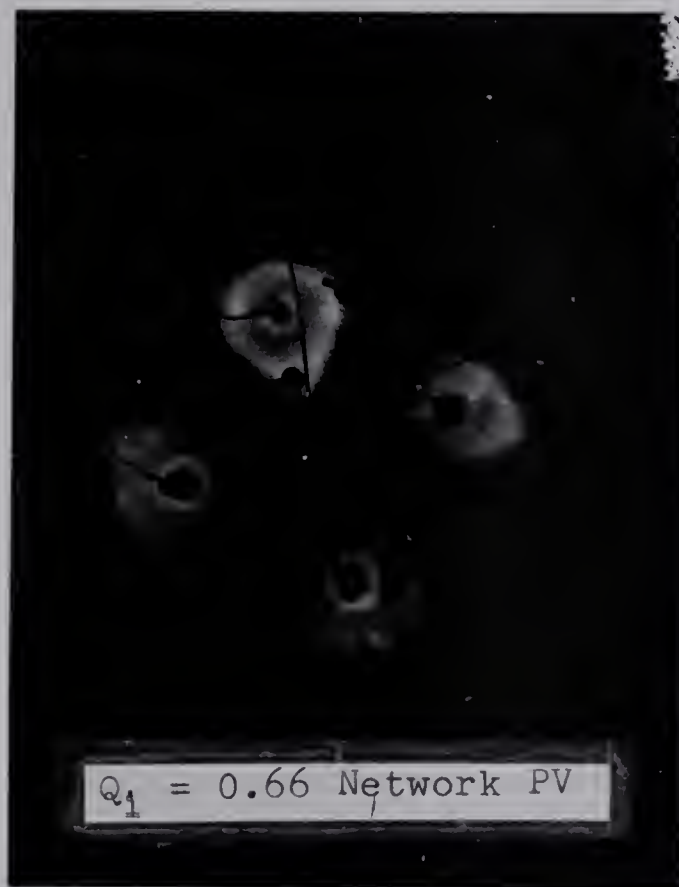


Fig. 5

Area Swept as a Function of Cumulative Throughput

FOUR INVERTED FIVE-SPOTS

RUN NO. 7

Injection Rate = 480 cc./hr./well = 1920 cc./hr.
Back Pressure = 21.5 cm. of water.



Fig. 6

There is no theoretical explanation for this behavior. According to Wyckoff, Botset and Muskat [48], there should not be any change in the distribution of equipressure lines and streamlines with a change in pressure at the input and output wells. The same phenomenon, though to a lesser extent, was also observed in the present study on the isolated normal five-spot pattern. On examining the data, it may be observed that there seems to be a trend in the recovery performance with the back pressure. The first three back pressures studied show a scattering of data with no particular trend. It is believed that this data is within experimental error of the equipment. To investigate the reason for this behavior, a record of injection pressures was made for all the runs. Since the injection rate for any particular run was constant, the injection pressure changed with the advance of flood front. It was noticed that the higher the back pressure used, the higher the injection pressure reached. The model was made of lucite plates which were held together only at the periphery. It was reasonable to expect a small amount of expansion in the model above

a certain limit of the injection pressure. This limit was found to be about 40 cms. of mercury (gauge). This expansion may result in by-passing of the fluids and hence account for the variation of results at different back pressures. It was also noticed that if the back pressure was held within a certain limit, so that the injection pressure did not cross the limit of 40 cm. of mercury (gauge) until the run was terminated, the recoveries and areal sweep efficiencies obtained were essentially independent of back pressure, within experimental error. This indicated that the performance of the floods was probably independent of back pressure below a certain level and the variations noticed were a result of the limitations of the model.

Isolated Normal Five-Spot

The performance of the isolated normal five-spot pattern is graphically shown in Figures 7 through 13. In all cases the data for run numbers 1, 2, and 3 (with constant injection rate and varying back pressures) have been curve fitted to a polynomial of the type

$$a_0 + a_1x + a_2x^2 + a_3x^3 + \dots \quad (8)$$

It has previously been shown that there was no effect of back pressure on the performance of the flood and the observed small variations were due to the experimental error. Run numbers 4 and 5 which were taken at a considerably higher back pressure (104.4 cm of water) are also shown but were not included in the curve-fit. These results show that at high back pressures, bypassing of the fluids occurred, resulting in higher areal sweep efficiencies and lower oil recoveries. Two runs at the same back pressure (104.4 cm. of water) were conducted to check the reproducibility of the results.

Figure 7 shows the cumulative throughput expressed in network pore volumes as a function of oil recovery in network pore volumes. Figure 8 shows the relationship of throughput versus oil recovery in network hydrocarbon pore volumes. Figure 9 shows the throughput in network hydrocarbon pore volumes versus oil recovery in network hydrocarbon pore volumes.

FIG. 7 - THROUGHPUT IN NETWORK PORE VOLUME Vs.
OIL RECOVERY IN NETWORK PORE VOLUME

ISOLATED NORMAL FIVE-SPOT

$Q = 400$ cc/hr/well

$\frac{d}{\gamma_w} = 181$

OIL RECOVERY IN NETWORK PORE VOLUME

P_b (CM. OF WATER)

RUN NO.

○	1	0
△	2	15.6
□	3	67.7
▲	4	104.4
●	5	104.4

— CURVE-FIT LINE THROUGH DATA OF RUN NOS. 1, 2 & 3.

THROUGHPUT IN NETWORK PORE VOLUME

FIG. 8 - THROUGHPUT IN NETWORK PORE VOLUME Vs.
OIL RECOVERY IN NETWORK HYDROCARBON PORE VOLUME

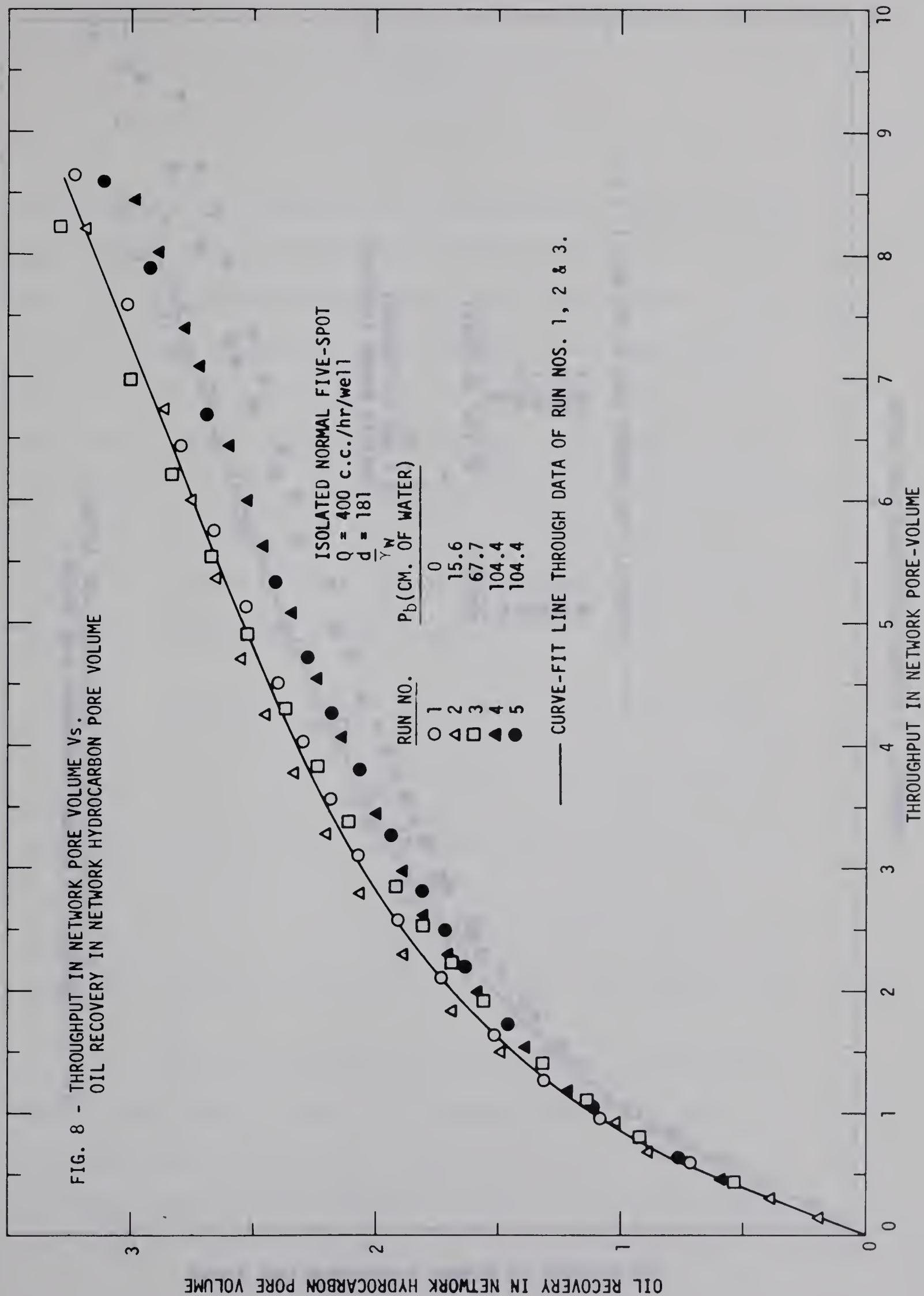
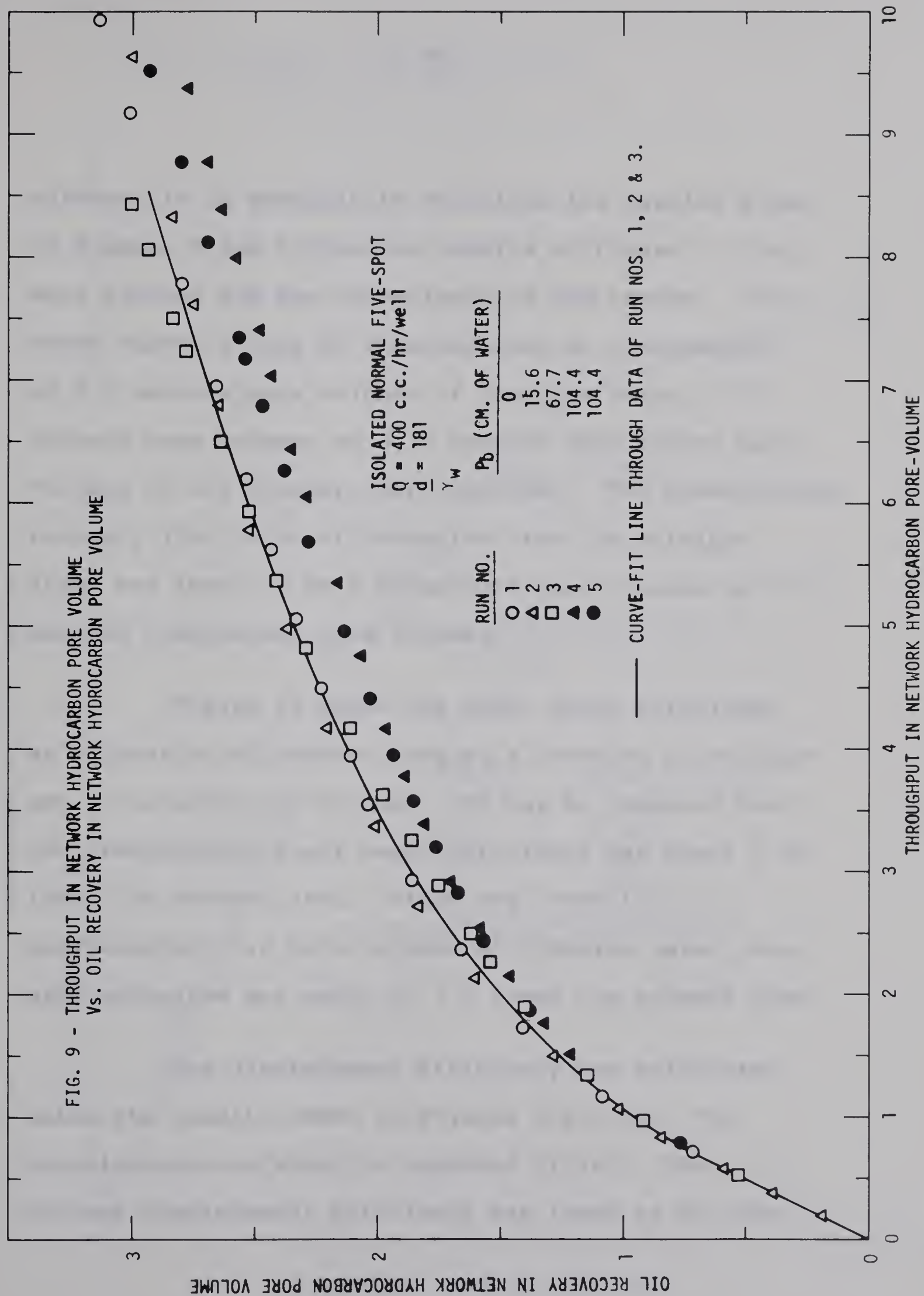




Fig. 1. Relationship between M_n and DP for various polymers.

Polystyrene (O), Polyisobutylene (●), Polypropylene (□), Polyethylene (■).

FIG. 9 - THROUGHPUT IN NETWORK HYDROCARBON PORE VOLUME
Vs. OIL RECOVERY IN NETWORK HYDROCARBON PORE VOLUME

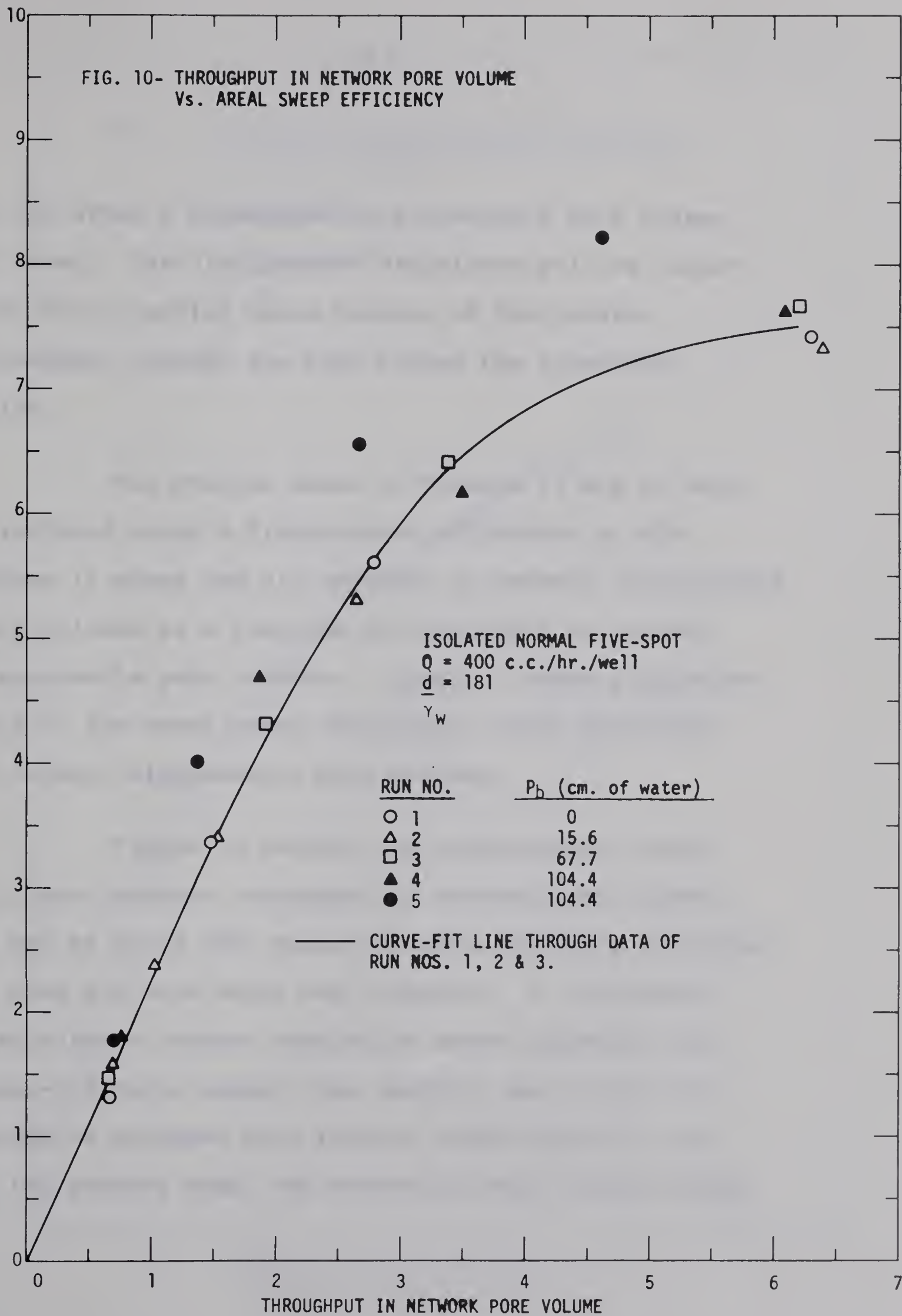


Although it is possible to calculate the results shown on Figures 8 and 9 from the results of Figure 7, they were plotted for the convenience of the reader. From these curves it may be observed that at a throughput of 8.0 network pore volumes of flooding water, 2.55 network pore volumes or 3.15 network hydrocarbon pore volumes of oil recovery were obtained. The breakthrough recovery (the point of deviation from the straight line) was found to be 0.65 network pore volumes or 0.75 network hydrocarbon pore volumes.

Figure 10 shows the areal sweep efficiency as a fraction of network area as a function of throughput in network pore volumes. It may be observed that the breakthrough areal sweep efficiency was about 3.35 times the network area. After the injection of approximately 6.0 pore volumes of flooding water, the area contacted was equal to 7.5 times the network area.

The displacement efficiency was calculated using the results shown in Figures 8 and 10. The calculations are shown in Appendix VII(a). The average displacement efficiency was found to be equal

AREAL SWEEP EFFICIENCY, FRACTION

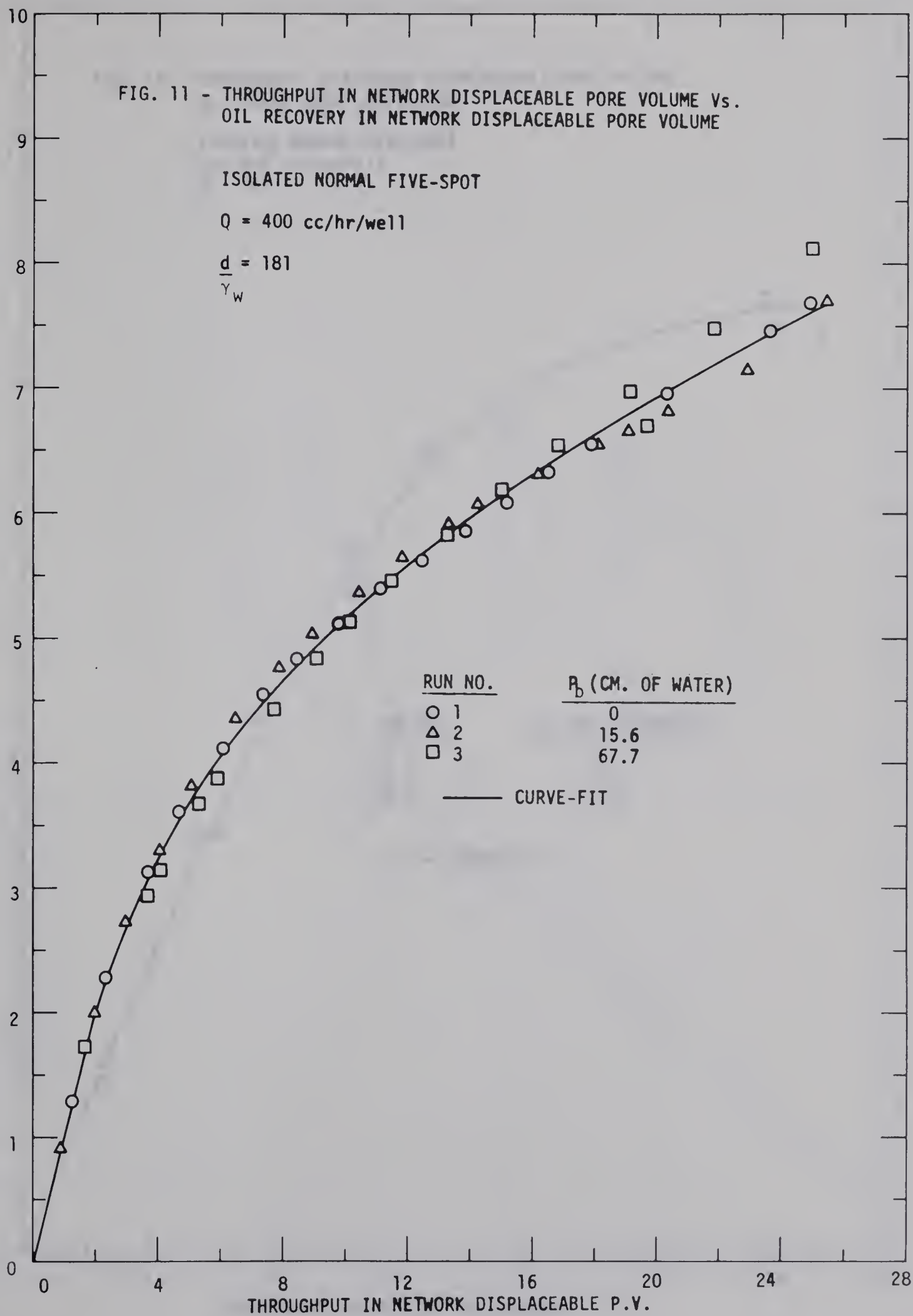


to 43% after a throughput of 6.0 network pore volume of water. The displacement efficiency will be higher near the injection wells because of the greater throughput through the area around the injection wells.

The results shown in Figures 11 and 12 were calculated using a displacement efficiency of 43%. Figure 11 shows the oil recovery in network displaceable pore volumes as a function of throughput in network displaceable pore volumes. Figure 12 shows a relationship of the areal sweep efficiency versus throughput in network displaceable pore volumes.

Figure 13 relates the instantaneous water-oil ratio against throughput in network pore volumes. It may be noted that water-oil ratio steadily increased as more and more water was injected. It is expected that after a certain cumulative water injection, the water-oil ratio should rise sharply, and no more oil should be produced with further water-injection, but in the present case, the water-oil ratio became steady

OIL RECOVERY IN NETWORK DISPLACEABLE P.V.



AREAL SWEEP EFFICIENCY, FRACTION

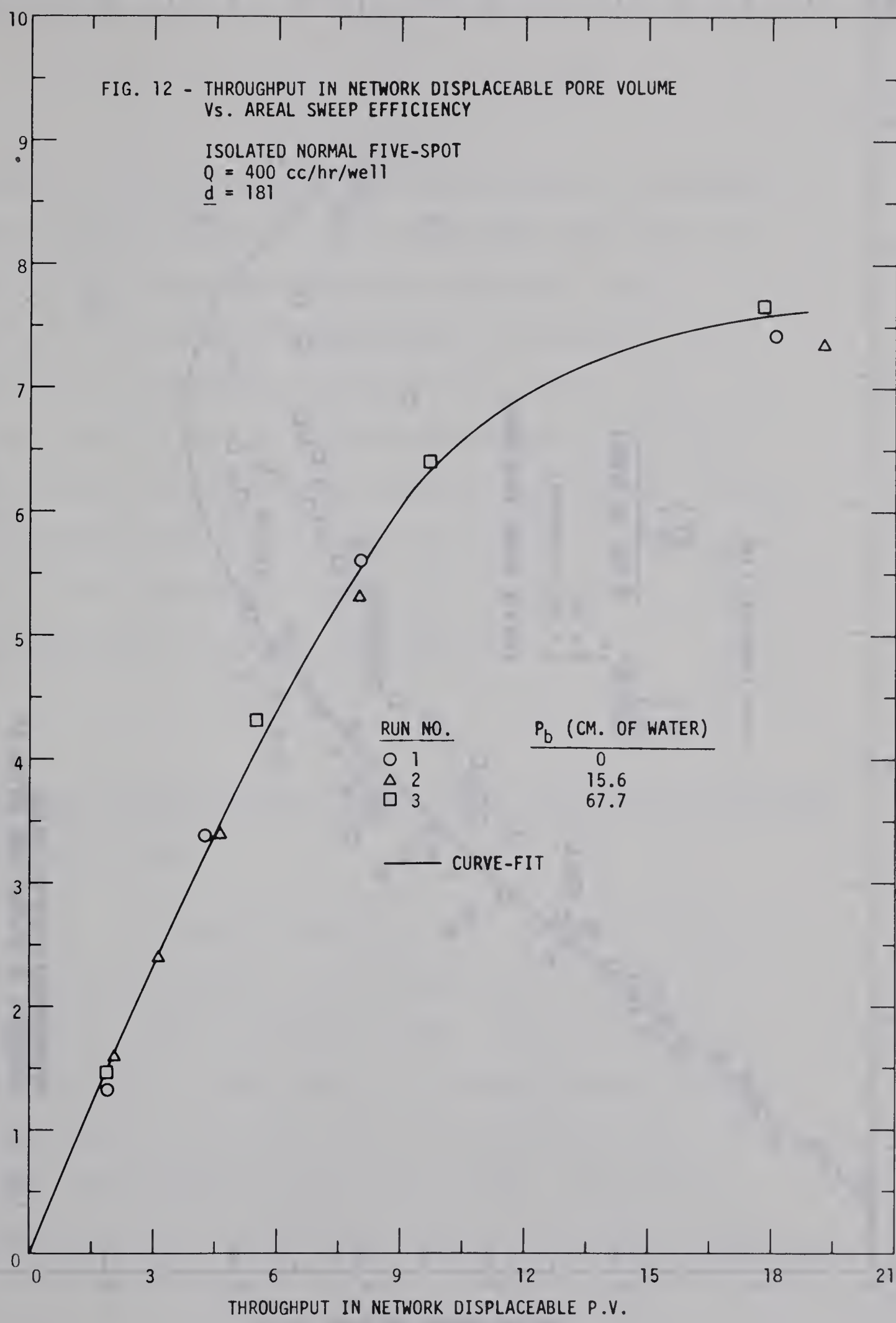


FIG. 13 - THROUGHPUT IN NETWORK PORE VOLUME Vs.
INSTANTANEOUS WATER-OIL RATIO

INSTANTANEOUS WATER-OIL RATIO

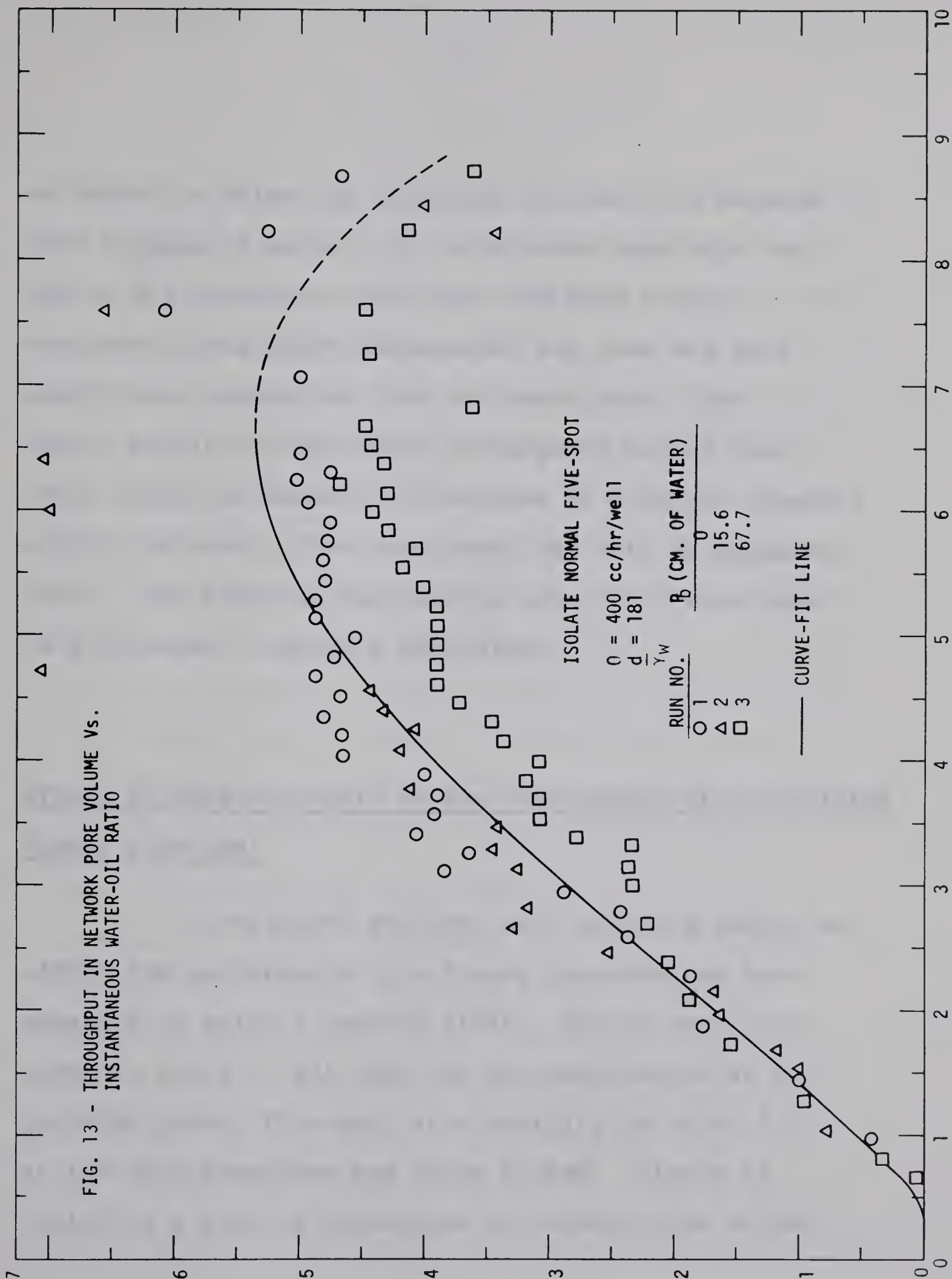
THROUGHPUT IN NETWORK PORE-VOLUME

ISOLATE NORMAL FIVE-SPOT

$Q = 400$ cc/hr/well
 $\bar{d} = 181$

RUN NO.	R_p (CM. OF WATER)
○ 1	0
△ 2	15.6
□ 3	67.7

— CURVE-FIT LINE



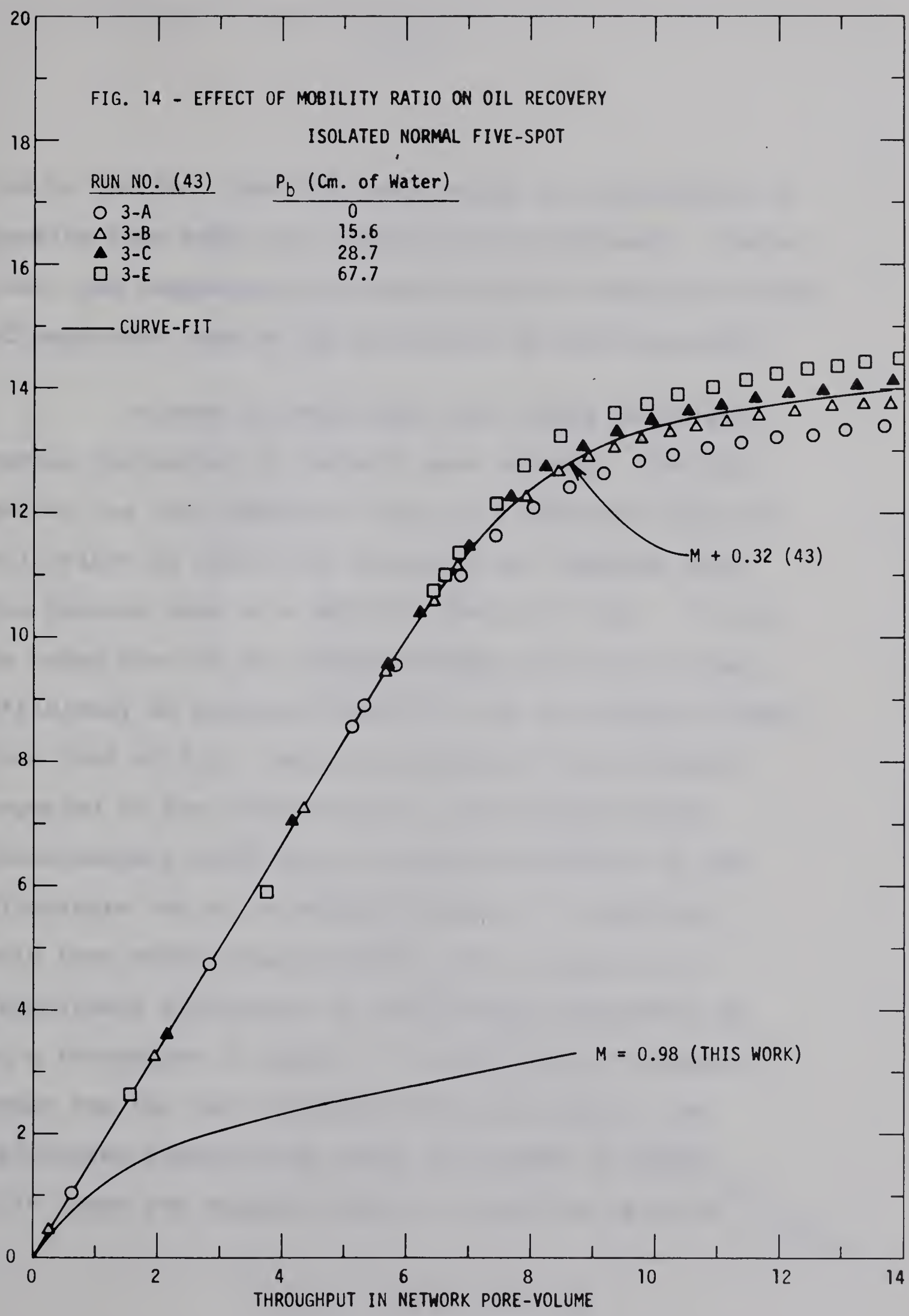
at about 5.4 after the injection of about 6.5 network pore volumes of water. It is believed that this was due to oil production from more and more freshly contacted areas which compensated for less and less subordinate production from the swept area. The latter portion of the curve corresponds to the time after injection ceased, but because of internal pressure within the model, flow continued (See data in Appendix VIII). The observed decrease in water-oil ratio might be attributed to gravity separation.

Effect of Mobility Ratio on the Performance of an Isolated Normal Five-Spot

As explained earlier, back pressure should not effect the performance of a flood, provided the back pressure is below a certain limit. Taking this into account, Serra's [43] data for the performance of an isolated normal five-spot at a mobility ratio of 0.32 at low back pressures was curve fitted. Figure 14 (which is a plot of throughput in network pore volumes

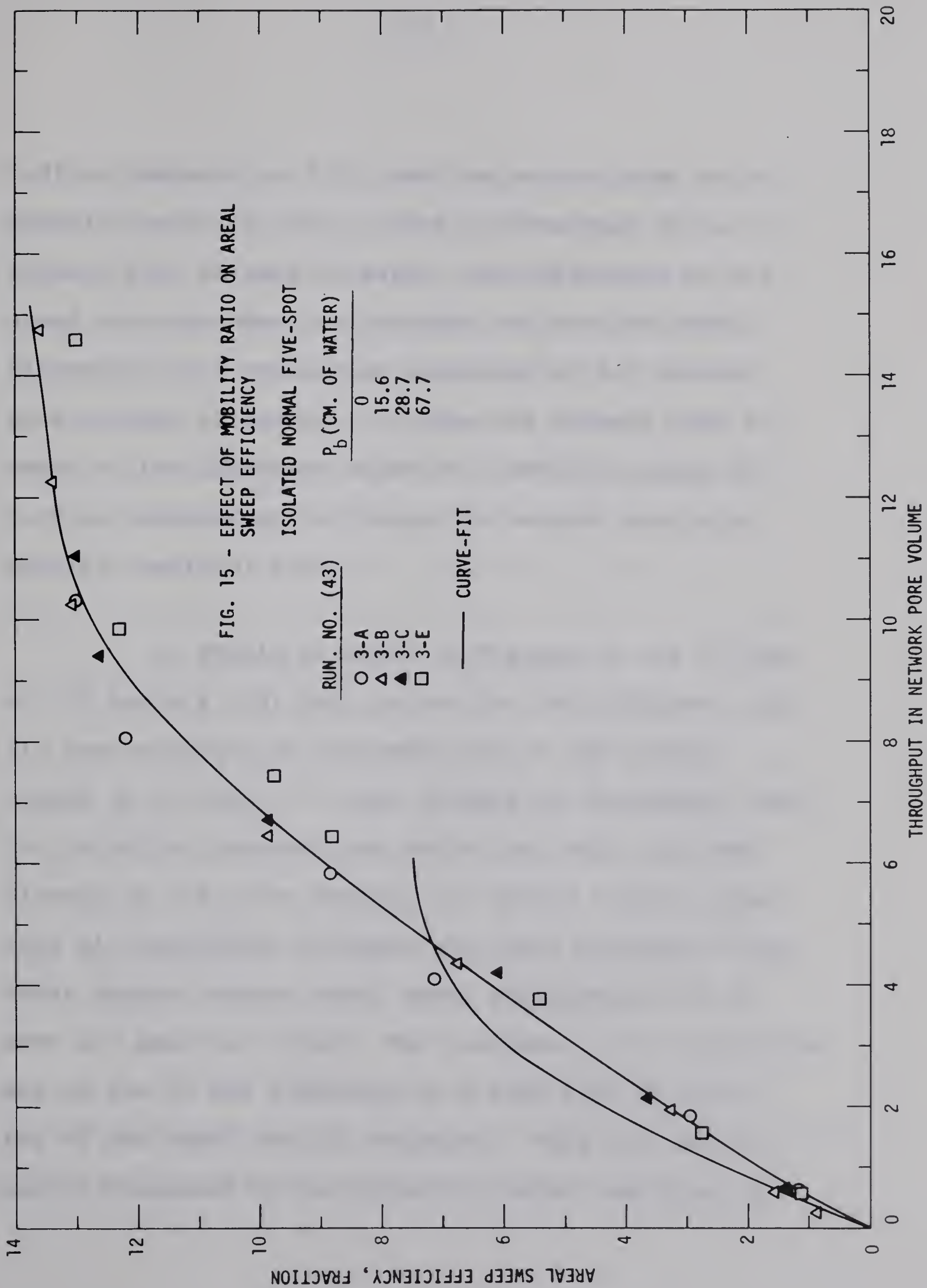
versus oil recovery in network hydrocarbon pore volumes) shows the experimental points for four different runs taken by Serra at a mobility ratio of 0.32, an injection rate of 480 cc/hr/well and a d/r_w ratio of 181. It also shows the curve-fit line for these experimental points and also the curve-fit line for the same pattern from the present study at a mobility ratio of 0.98. It may be observed that there is a significant difference in the recovery of oil at the two different mobility ratios. From the very beginning, the oil recovery at a mobility ratio 0.32 is higher. The oil recovery at breakthrough in the former case is about 9.6 network hydrocarbon pore volumes as compared to 0.75 network hydrocarbon pore volumes in the latter case. The difference goes on increasing as more and more water is injected and ultimately at a total throughput of about 8.0 network pore volumes of water, there was only 3.1 network hydrocarbon pore volumes of oil recovery at a mobility ratio of 0.98 as compared to 12.4 network hydrocarbon pore volumes of oil recovery at a mobility ratio of 0.32. It should be emphasized that the comparison of Serra's data and the present data is somewhat questionable

OIL RECOVERY IN NETWORK HYDROCARBON PORE-VOLUME



due to the fact that the basic model and the method of packing this model are significantly different. Therefore, the comparisons were made only to varify the order of magnitude results as influenced by mobility ratio.

Figure 15 shows the areal sweep efficiency versus throughput in network pore volumes. The data points for four different runs at a mobility ratio of 0.32 taken by Serra and curve-fit are compared with the present work at a mobility ratio of 0.98. It may be noted that in the initial stages, the areal sweep efficiency at mobility ratio of 0.98 is slightly higher than that at 0.32, which is contrary to the results reported in the literature for the confined case. Unfortunately there are no results available in the literature for an unconfined system. It might be said that within experimental error, there is no significant difference in areal sweep efficiency up to a throughput of about 4.7 network pore volumes of water for the two different mobility ratios. The calculated breakthrough sweep efficiency is about 3.35 times the network area at a mobility ratio of



0.98 as compared to 7.0 times the network area at a mobility ratio of 0.32. After a throughput of 4.7 network pore volumes of water, the difference in the areal coverage seems to increase for the two cases. Ultimately at a cumulative injection of 6.4 network pore volumes of water, 7.5 times the network area is swept by the injection water at a mobility ratio of 0.98 as compared to 9.4 times the network area at a mobility ratio of 0.32.

It should be noted in Figures 14 and 15 that all of Serra's [43] data points for the different runs lie approximately on the same line in the initial stages up to about 7.0 pore volumes of throughput, when the injection pressure was below the limit, but they diverge in the later stages. It should also be noted that oil recoveries increase with back pressure in the later stages whereas areal sweep efficiencies do not show any specific trend. The increase in oil recoveries may be due to the formation of a thin film of oil on top of the model when it expanded. This film may be easily displaced by the injection water resulting in

an increase in recovery. In the present work, the oil recoveries were essentially the same except for a very high back pressure, in which case they were lower (Figure 7). Similarly the areal sweep efficiencies were also essentially the same except for very high back pressure, when they were higher (Figure 10). The reason for the reversal of recovery at very high back pressure (hence very high injection pressure) from Serra's work may be due to fingering of injection water through the oil which is more viscous than water in the present study. This phenomenon did not occur in Serra's work because of his use of iso-octane as the non-wetting phase which was much less viscous than the injection water. This also explains the higher areal sweep at very high back pressures obtained in the present case. This reversal in oil recovery at high back pressure may also be due to non-linear flow as a result of the distortion in the model.

The main reason for believing that there is no effect of back pressure on oil recovery and areal sweep efficiency is that for low throughput volumes all the

data points for the two cases lie on the same line in both the present work as well as in Serra's work. One more point to be observed is the greater divergence of the data points in the later stages of Serra's work as compared to that of present work. This may be a result of the pressure at which the model was packed. It is believed that the model in the present case was packed at a higher pressure and thus there was less expansion as compared to that in Serra's case.

Four Inverted Five-Spot

The performance of the four inverted five-spot pattern is graphically shown in Figures 16 through 22. In all cases, run numbers 6, 7, and 8, have been plotted and curve fitted to give the best representative line for the performance of the flood. All the runs were taken at different injection rates, but at a constant back pressure. The d/r_w ratio in this case was 90.5. According to the theory, d/r_w ratio does not have any significant influence on areal sweep efficiency. The experimental points are not scattered and thus clearly shows that the floods were "stabilized" and hence, the

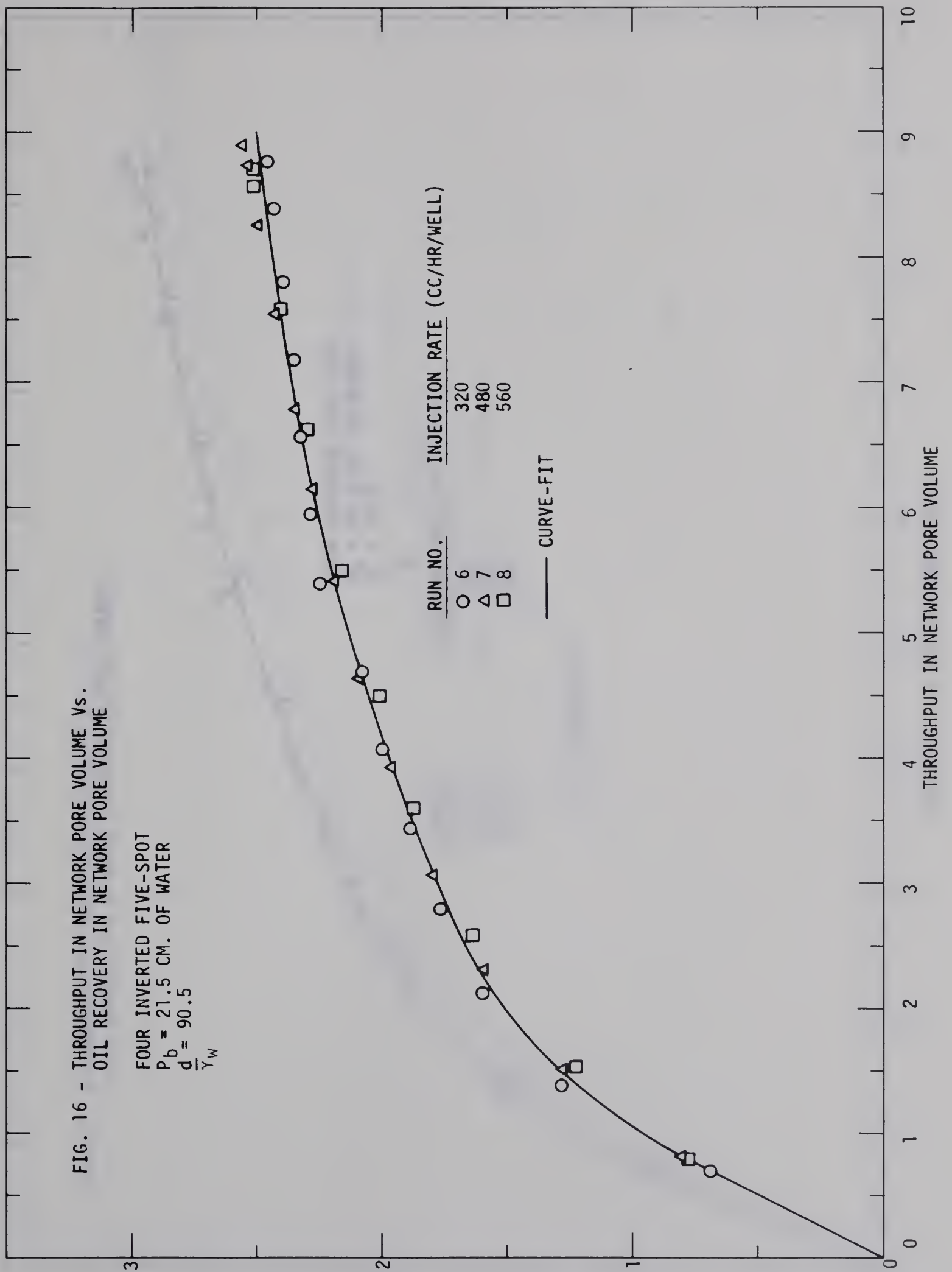
injection rates employed were above the critical rate. This supports the theory of Rappoport's critical scaling coefficient [39]. The back pressure employed was of a low magnitude (21.5 cm. of water). There were nine producers for four injectors as compared to one producer for four injectors in the isolated normal five-spot case. This resulted in very small injection pressures in the order of 6 to 8 cm. of mercury (gauge), which eliminated any possibility of the expansion of the model and hence by-passing of the fluids.

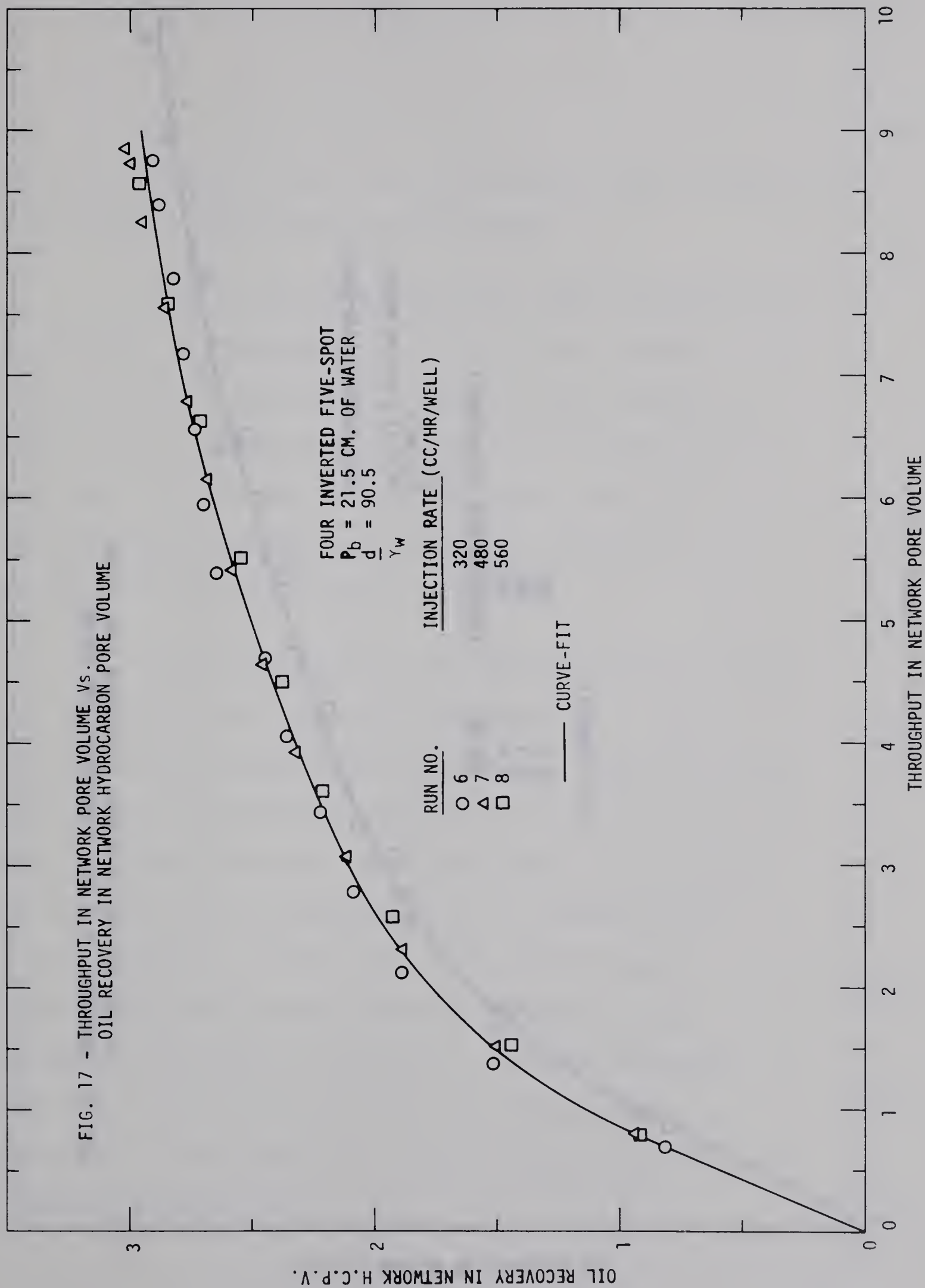
Figure 16 shows the relationship of throughput in network pore volumes against oil recovery in network pore volumes. Figure 17 illustrates the oil recovery in network hydrocarbon pore volumes versus throughput in network pore volumes. Figure 18 shows oil recovery in network hydrocarbon pore volumes versus throughput in network hydrocarbon pore volumes. From these curves, it may be noted that after an injection of 8.0 network pore volumes of water, 2.42 network pore volumes or 2.87 network hydrocarbon pore volumes of oil were produced. The breakthrough recovery, where the curve deviates

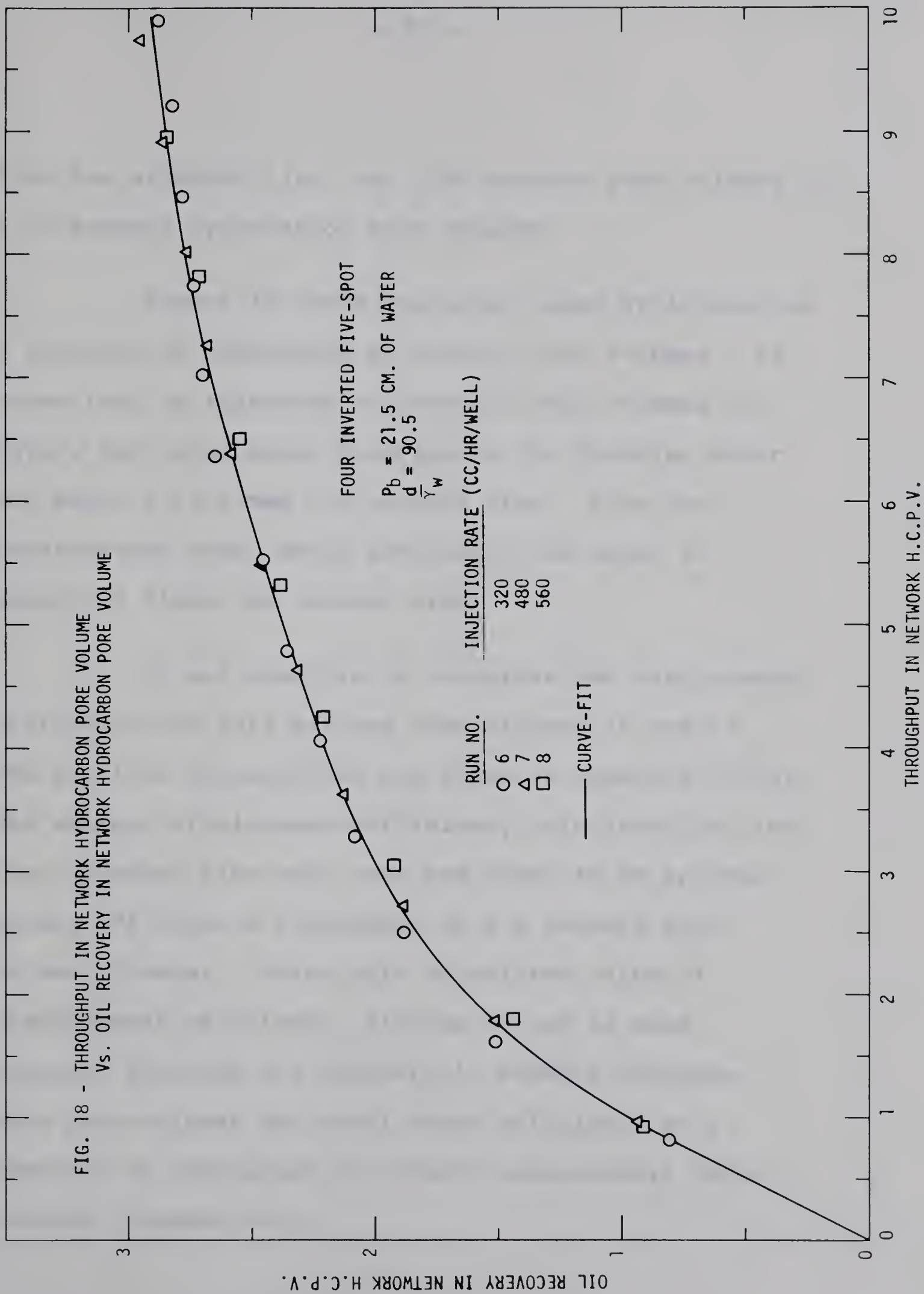
FIG. 16 - THROUGHPUT IN NETWORK PORE VOLUME Vs.
OIL RECOVERY IN NETWORK PORE VOLUME

FOUR INVERTED FIVE-SPOT
 $P_b = 21.5$ CM. OF WATER
 $\frac{d}{\bar{Y}_W} = 90.5$

OIL RECOVERY IN NETWORK PORE VOLUME



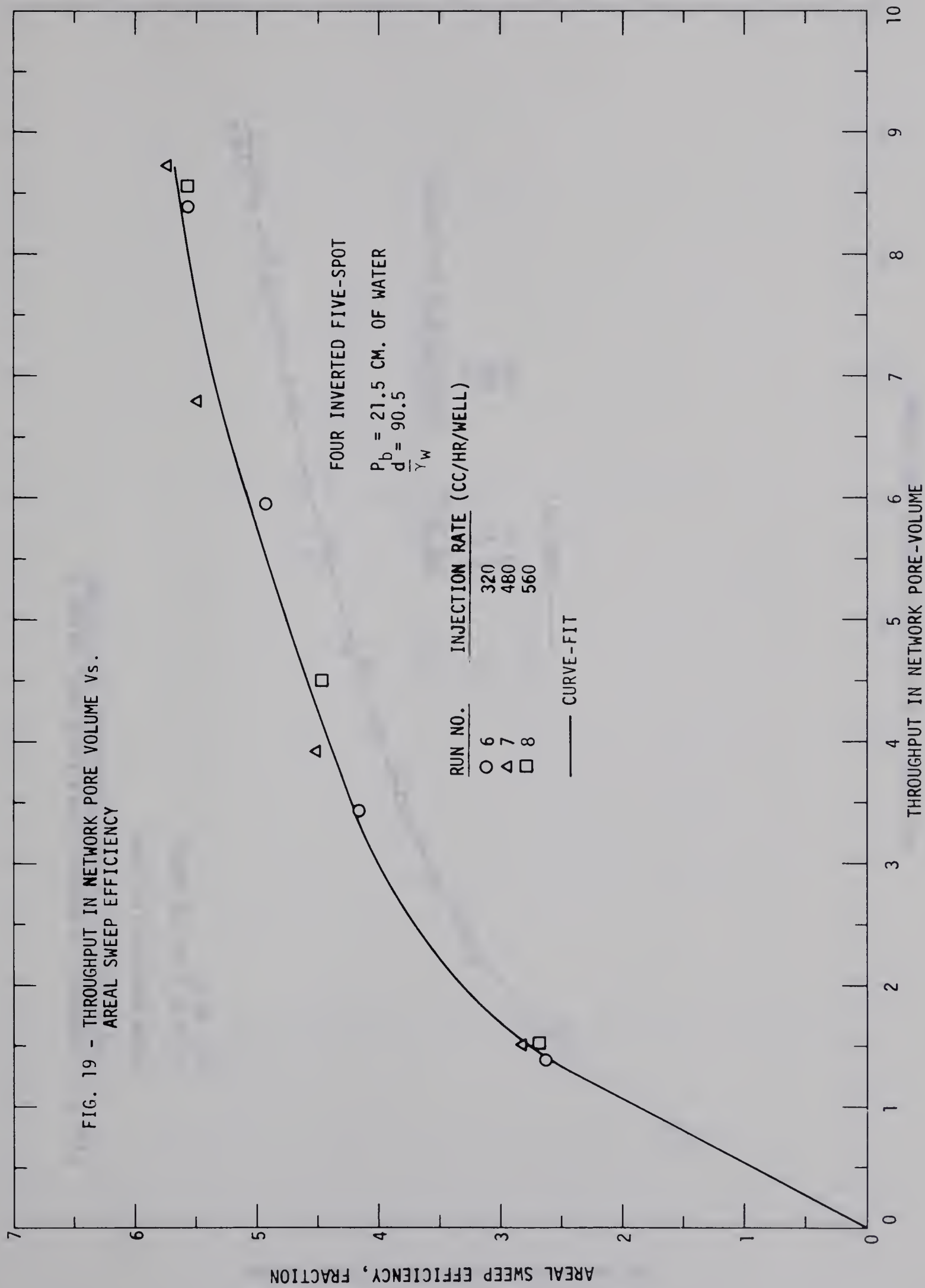


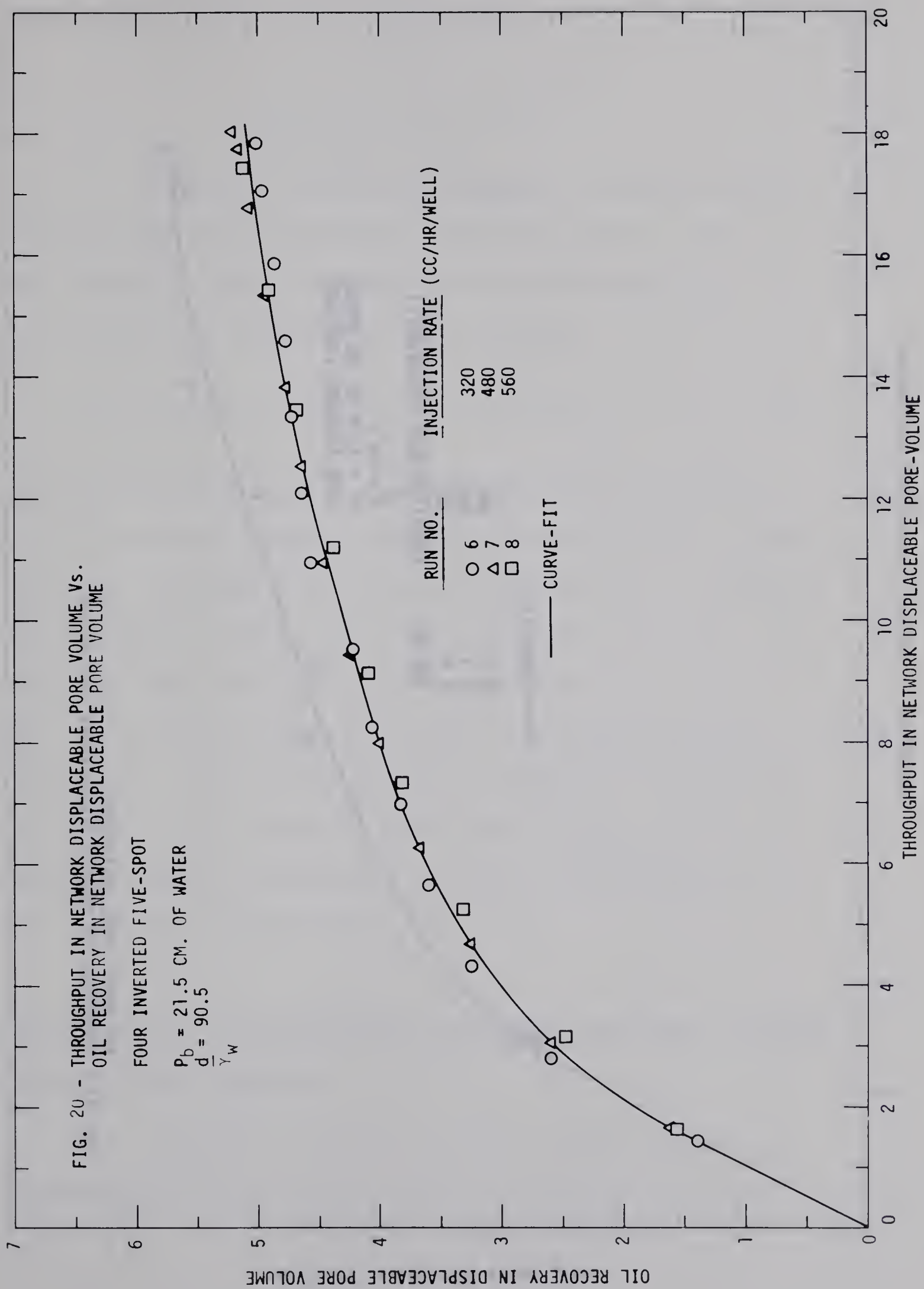


from the straight line, was 0.80 network pore volumes or 1.10 network hydrocarbon pore volumes.

Figure 19 shows the areal sweep efficiency as a function of throughput in network pore volumes. It shows that by injecting 8.5 network pore volumes of water, the total areal coverage by the flooding water was about 5.65 times the network area. Also the breakthrough areal sweep efficiency was equal to about 2.5 times the network area.

It was possible to calculate the displacement efficiency for this pattern from Figures 17 and 19. The detailed calculations are given in Appendix VII(b). The average displacement efficiency calculated for the four inverted five-spot case was found to be approximately 58% after a throughput of 8.0 network pore volume of water. Using this calculated value of displacement efficiency, Figures 20 and 21 were prepared relating oil recovery in network displaceable pore volumes and areal sweep efficiency as a function of throughput in network displaceable pore volumes, respectively.





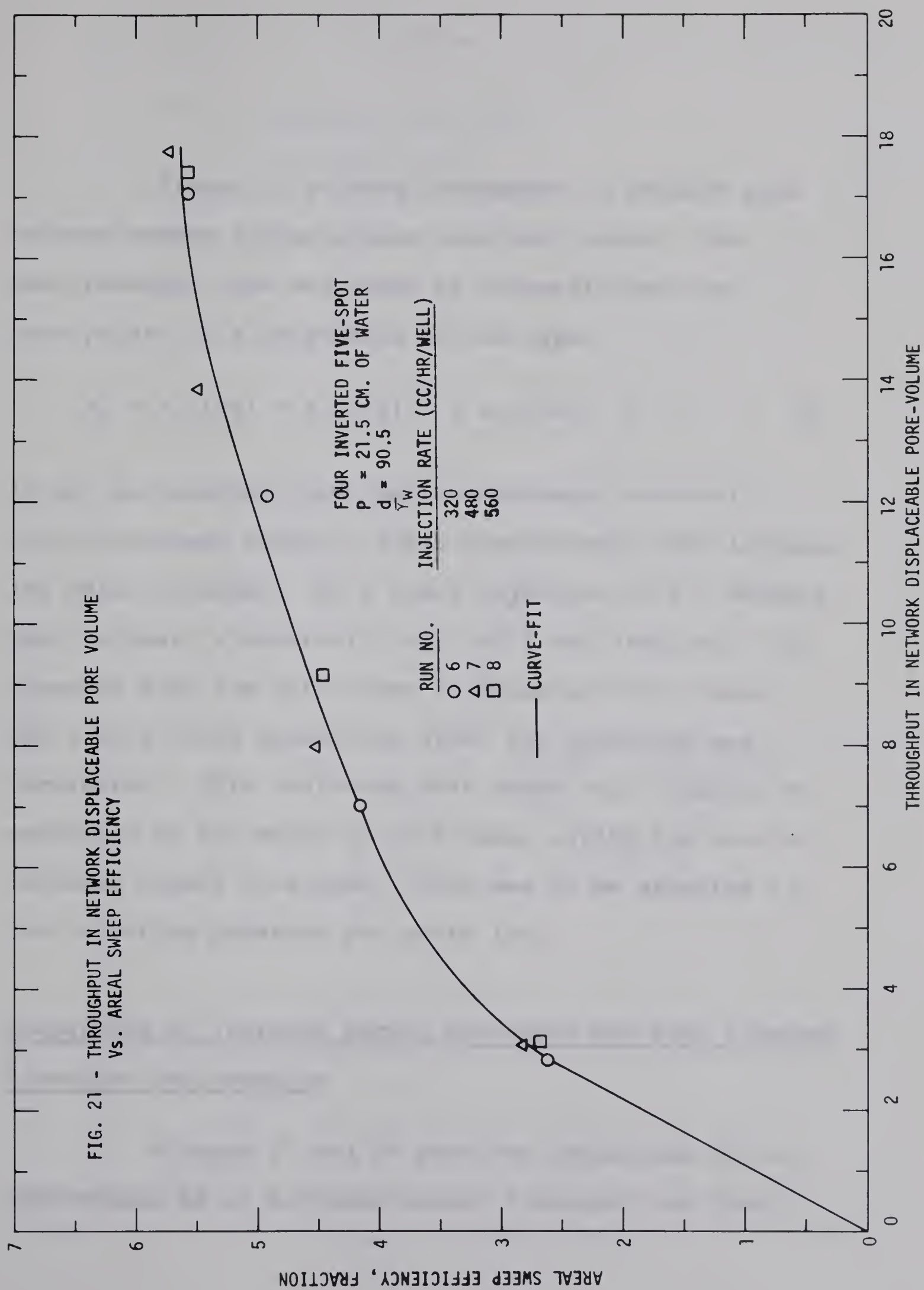


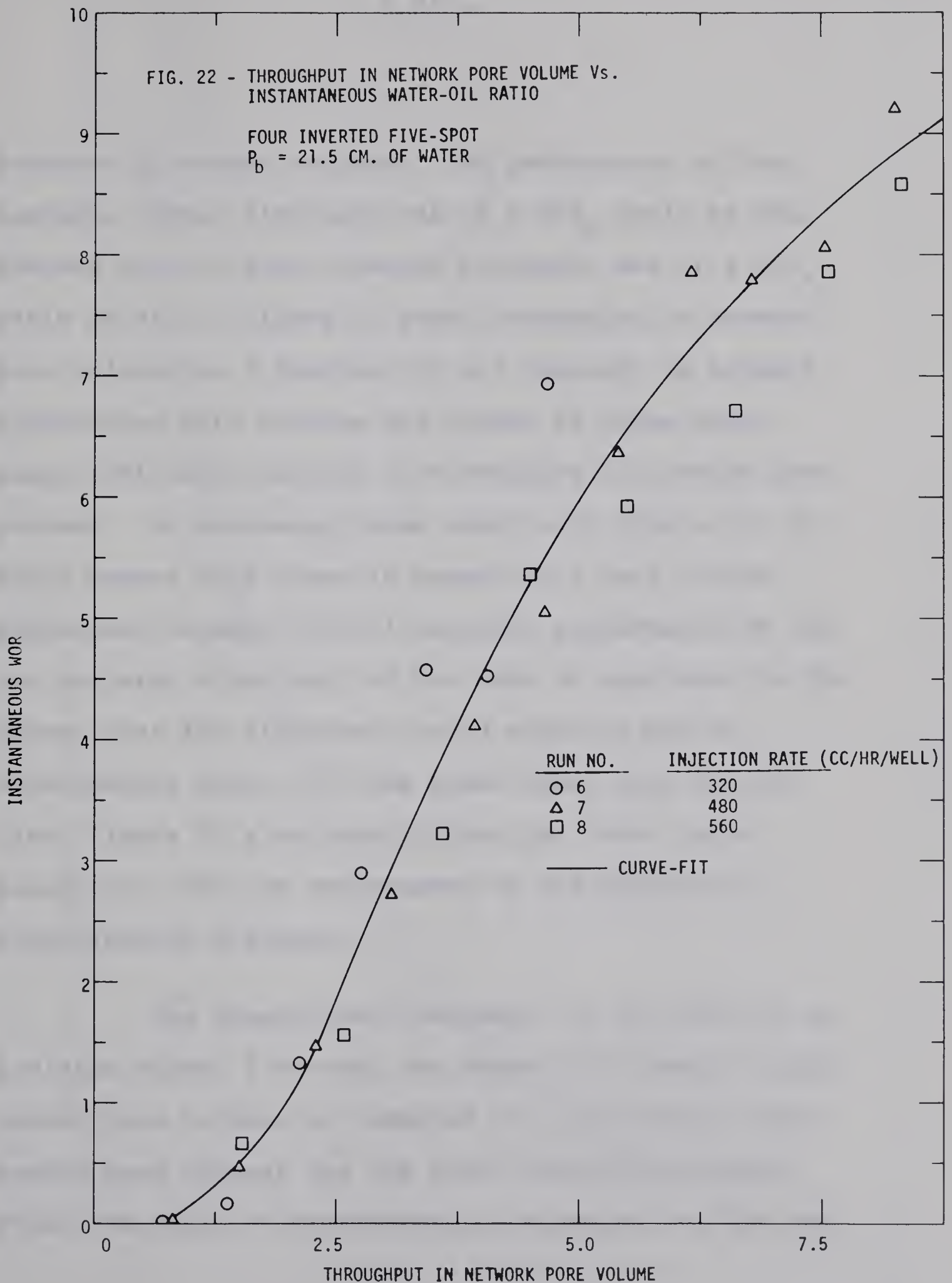
Figure 22 relates throughput in network pore volumes versus instantaneous water-oil ratio. The best possible line was drawn by curve-fitting the data points to a polynomial of the type

$$a_0 + a_1(1/x) + a_2(1/x)^2 + a_3(1/x)^3 + \dots \quad (9)$$

It may be observed that the instantaneous water-oil ratio increased steadily after breakthrough with increasing water injected. At a total injection of 8.5 network pore volumes, a water-oil ratio of 9 was attained. As observed from the data given in Appendix VIII, there was little fluid production after the injection was terminated. This indicates that there was little or no expansion of the model in this case, unlike the case of isolated normal five-spot. This was to be expected as the injection pressure was quite low.

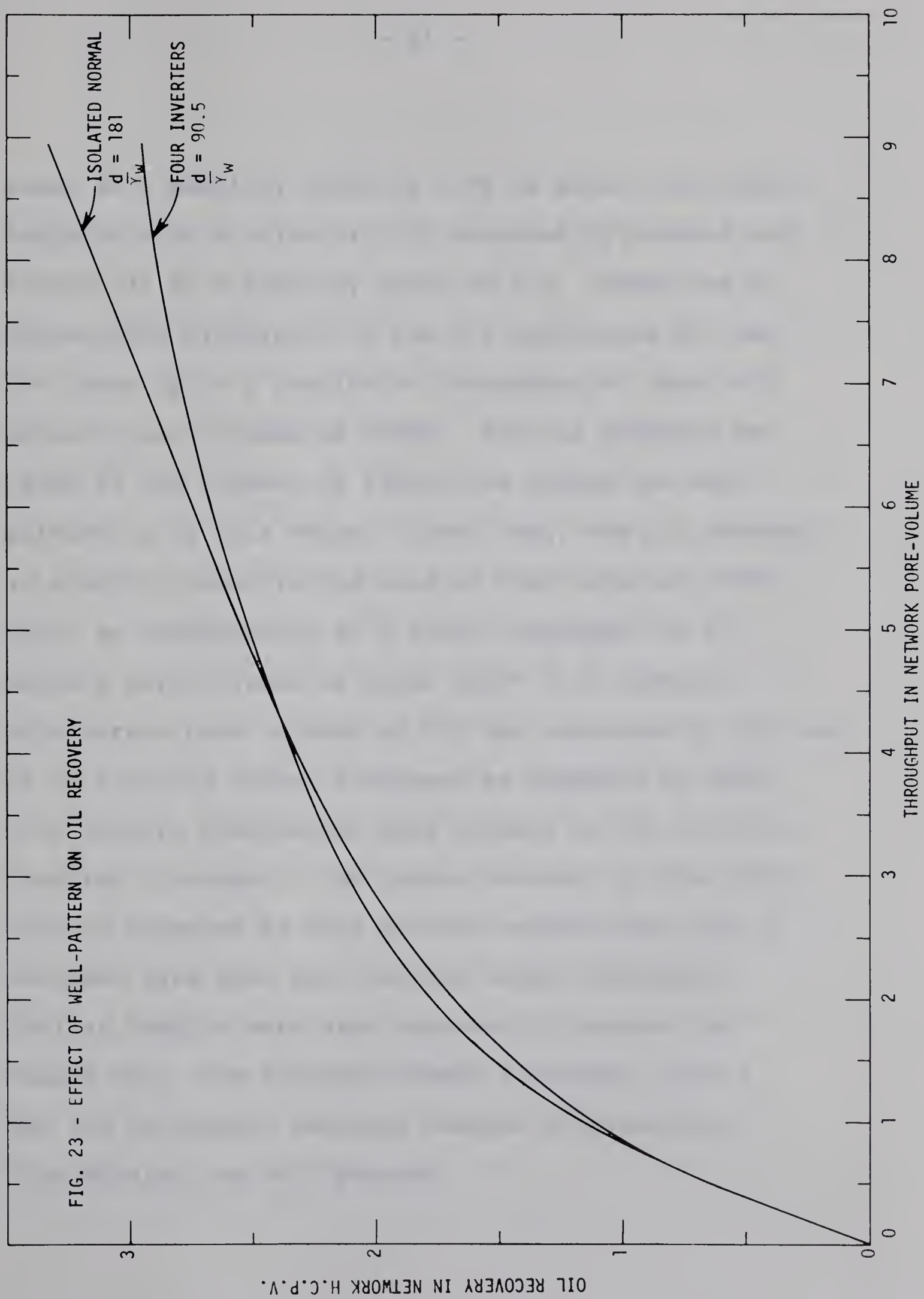
Comparison of Isolated Normal Five-Spot and Four Inverted Five-Spot Performances

Figures 23 and 24 show the comparison of the performance of an isolated normal five-spot and four



inverted five-spot systems. The performance of the isolated normal five-spot was at a d/r_w ratio of 181, whereas that of four inverted five-spot was at a d/r_w ratio of 90.5. Figure 23 shows throughput in network pore volumes as a function of oil recovery in network hydrocarbon pore volumes and Figure 24 shows areal sweep efficiency related to throughput in network pore volumes. On reviewing these results of Figure 23, it would appear that there is essentially very little difference between the oil recovery performance of the two patterns since much of our data is scattered to the extent that the difference noted might be due to experimental error. On the other hand, when one reviews Figure 23 along with Figure 24, there is an indication that the performance of the patterns is significantly different.

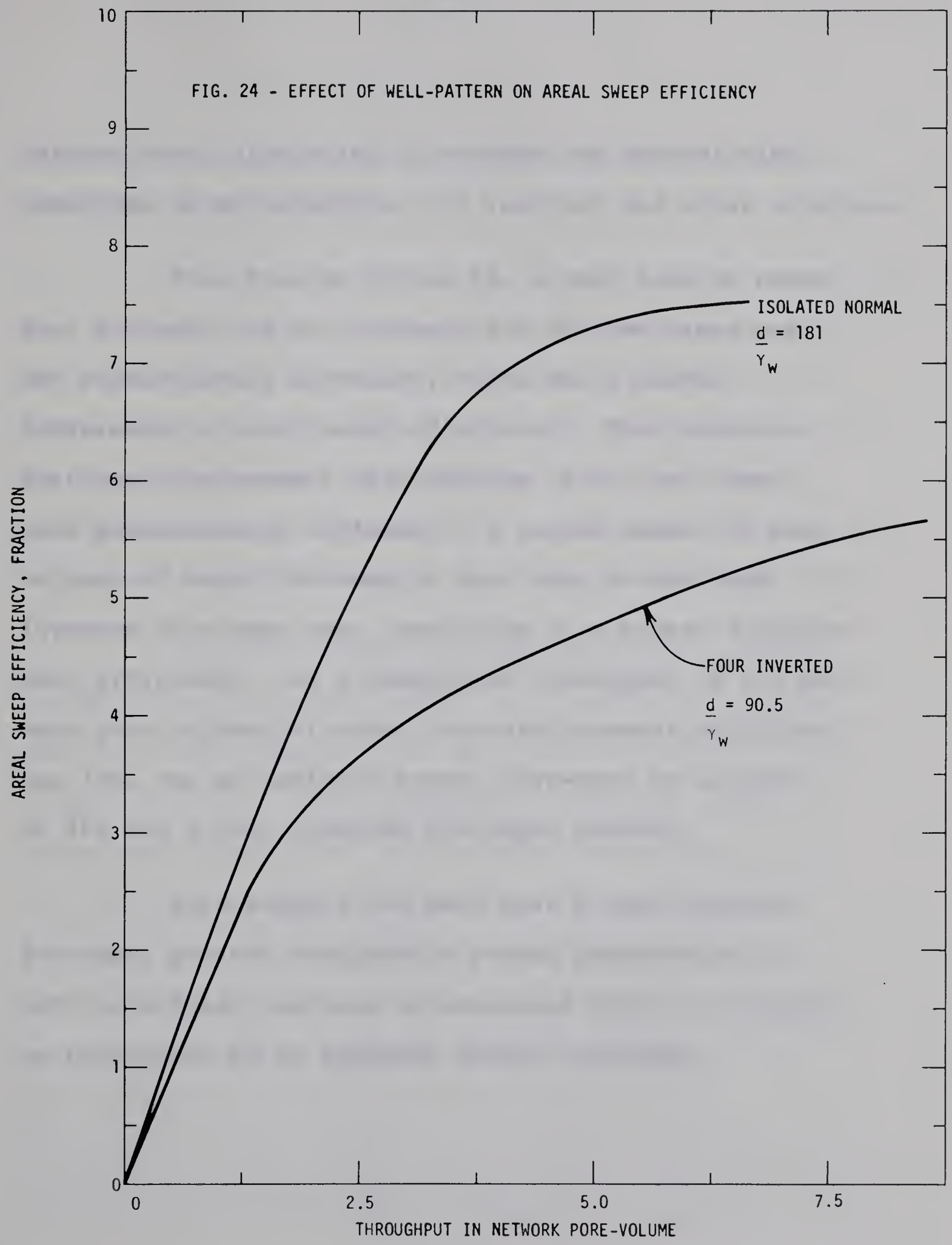
The breakthrough recovery in the case of an isolated normal five-spot was about 0.75 network hydrocarbon pore volumes as compared to 1.10 network hydrocarbon pore volumes for the four inverted five-spot. Thus, the ratio of breakthrough recoveries for the two



cases at a mobility ratio of 0.98 is about 1.46 which compares with a value of 1.25 reported by Bernard and Caudle [4] at a mobility ratio of 1.0. There was no appreciable difference in the oil recoveries for the two cases up to a cumulative throughput of about 4.5 network pore volumes of water. This is probably because of the absence of fluid-flow beyond the well pattern up to this stage. After that, the oil recovery is slightly lower in the case of four inverted five-spot, so consequently at a total throughput of 8.0 network pore volumes of water about 3.15 network hydrocarbon pore volumes of oil was recovered in the case of an isolated normal five-spot as compared to about 2.90 network hydrocarbon pore volumes of oil for four inverted five-spot. The lesser recovery in the latter case is expected as this pattern behaves more like a confined case than the isolated normal five-spot. Similar results were also reported by Bernard and Caudle [4]. The isolated normal five-spot gives a far too optimistic recovery because of significant flow outside the well pattern.

Figure 24 indicates that there was a significant difference in the areal coverage by flooding water for the two cases. From the very start of the injection, the areal coverage by the flooding water was greater for an isolated normal five-spot than for the four inverted five-spot. This difference was not too large up to a throughput of about 1.4 network pore volumes of water but increased later on with increasing throughput. Finally at a cumulative throughput of 6.25 network pore volumes of water, the areal sweep efficiency was approximately 7.5 times the network area for an isolated normal five-spot, whereas it was only about 5.15 times the network area for four inverted five-spot. The lower areal coverage for the four inverted five-spot case was also expected, as the surrounding wells in the network are producers unlike those in the isolated normal five-spot case, where they were injectors. The surrounding producers do not permit a great amount of fluid to be lost outside the network area and the injection water is utilized in sweeping more and more oil from the swept region. In the case with surrounding injectors, a large fraction of injected water is used in sweeping the area outside the

FIG. 24 - EFFECT OF WELL-PATTERN ON AREAL SWEEP EFFICIENCY



network area, displacing it towards the central sink, resulting in an optimistic oil recovery and areal coverage.

From Figures 23 and 24, it may also be noted that although the oil recovery for the two cases was not significantly different, there was a marked difference in areal sweep efficiency. This suggests that the displacement efficiencies in the two cases were substantially different. A larger number of pore volumes of water had swept a unit area in the four inverted five-spot case, resulting in a higher displacement efficiency. At a cumulative throughput of 6.0 network pore volumes of water, the displacement efficiency was 43%, for an isolated normal five-spot as compared to 58% for a four inverted five-spot pattern.

This supports the fact that a four inverted five-spot pattern simulates a closer performance to a unit in a fully confined or developed field as compared to that given by an isolated normal five-spot.

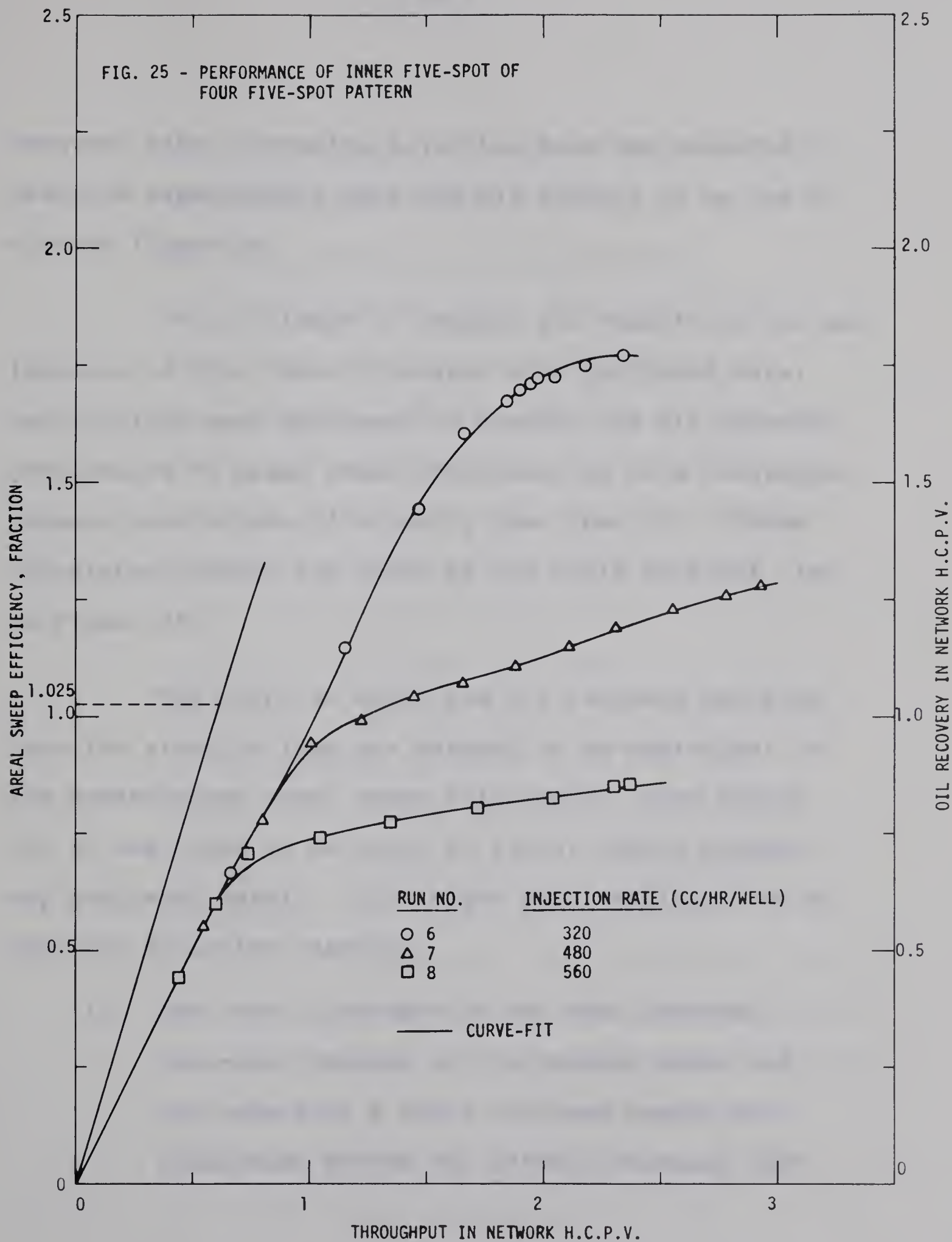
Performance of the Inner Normal Five-Spot of the Four
Inverted Five-Spot Case

In the literature, for a confined five-spot case (no fluid-flow outside the network boundary), the breakthrough sweep efficiency has been reported to be 70-75% for a mobility ratio of 1.0 [44]. To compare the results of the present study at a mobility ratio of 0.98 with published results, the performance of the inner five-spot from the four inverted five-spot case, was studied.

The total amount of fluid produced (oil and water) from the center well in the four inverted five-spot case was assumed to be the total throughput in the inner five-spot. This throughput in network (inner five-spot) hydrocarbon pore volumes was related to the oil recovery in network hydrocarbon pore volumes. Assuming that the displacement efficiency for this inner five-spot was the same as that for the whole four inverted five-spot network, one could calculate the relationship for areal sweep efficiency versus throughput in hydrocarbon pore volumes. This was obtained by dividing the oil recovery in network

hydrocarbon pore volumes by the displacement efficiency.

The relationships have been shown in Figure 25. It was noted that there was a significant difference in the performance of the center well for the three different injection rates. The reason might be explained by one of the shortcomings of the model. As pointed out earlier, the injection pressures in the four inverted five-spot case were very low. As a result even a little friction or a small obstacle in the narrow production tubing might cause the flow of fluids to stop in one well and divert its flow to other wells. This seems to be one of the reasons for this behavior of the center well, because, as observed earlier, the overall performance of the network for the three different runs was essentially the same (Figure 18). It is quite possible that the observed difference in performance (which correlates with injection rate) could be due to the fact that the scaling criterion under which the experimental data in this model was taken were not met in the area of the inner five-spot. Therefore, recovery could decrease with increasing injection rate. A decrease in



recovery with increasing injection rate was observed in previous experimental work and was thought to be due to viscous fingering.

In an attempt to compare the results of the performance of this inner five-spot with published data, calculations were performed to convert the oil recovery performance to areal sweep efficiency up to a throughput network pore volume of slightly less than 1.0. These calculated results are shown by the solid straight line on Figure 25.

The point at which the oil recovery deviates from the straight line was assumed to be equivalent to the breakthrough areal sweep efficiency. From Figure 25, it was found to be equal to 102.5%, which exceeds any published result. This might be a result of one or both the following reasons:

- 1) The inner five-spot of the four inverted five-spot pattern in the present model did not behave as a fully confined system and fluid-flow across the pattern boundary took

place, resulting in a higher breakthrough areal sweep efficiency.

- 2) The assumption that the displacement efficiency for the inner five-spot could be assumed to be that calculated for the four inverted five-spot pattern, may not be valid. As pointed out in the comparison of isolated normal five-spot and four inverted five-spot performances, there would be a higher displacement efficiency if more pore volumes of injection water pass through a unit area. This may result in a higher value of displacement efficiency for the inner five-spot than that for the whole network. The use of a higher value of displacement efficiency will reduce the value for calculated breakthrough areal sweep efficiency and hence this calculated value could approach the figure reported in the literature. Assuming that the inner normal five-spot has a displacement efficiency of 76.3% as shown in the linear tests (Appendix III), the

calculated value of the areal sweep efficiency at breakthrough would be 78%, which compares favorably with the published results.

CONCLUSIONS

Areal sweep efficiency and oil recovery performances for an isolated normal five-spot and four inverted five-spot patterns were studied on a transparent radial lucite model packed with uniform-size glass beads. Kerosene and distilled water were used to simulate non-wetting and wetting phases respectively. Dyed water was used as injection water which permitted the tracing of flood front. The mobility ratio of the system was 0.98. The capillary pressure effects were minimized by using high injection rates.

The results of this study led to the following conclusions:

- 1) Based upon the results of the present study for this model, it was concluded that the oil recovery and areal sweep efficiency in a waterflood are not a function of back pressure. The change in oil recovery and areal sweep efficiency noticed by Serra [43] on the same model for an isolated normal five-spot pattern is believed to be due to a slight expansion in the model at higher back pressures (and hence, higher injection pressures), resulting in by-passing of the fluids. The

trend of higher recovery at higher back pressures in later stages in Serra's work may be due to the formation of a thin film of oil floating on top as a result of expansion in the model. This film may be easily displaced by the injection water resulting in a higher recovery.

2) There was a significant change in oil recovery with a change in mobility ratio from 0.32 to 0.98. At the same time there was not a significant difference in areal sweep efficiency performance for the two cases, up to the stage the present data was taken. Unfortunately it was not possible to compare the change observed with the published data as most of it is for a confined case.

3) The isolated normal five-spot pattern test showed an optimistic recovery and areal sweep efficiency. This was due to the fact that an isolated normal five-spot is completely unconfined and injection water sweeps a large area outside the network.

4) A four inverted five-spot pattern simulated a performance closer to a confined case as compared to an isolated normal five-spot. The surrounding production

wells did not permit as much fluid to migrate outside the network area.

5) The displacement efficiency in case of the four inverted five-spot was higher (58%) than that for an isolated normal five-spot (43%). More pore volumes of injection water had swept through a unit area in the former case, resulting in more subordinate production and hence, a higher displacement efficiency.

6) One of the major difficulties in analyzing the data was a lack of knowledge of displacement efficiency for various sections of the model at different throughputs. It is recommended that in future studies, either a technique for finding the displacement efficiency of any section of the model at any throughput should be developed or miscible fluids should be used.

REFERENCES

1. Amyx, J.W., Bass, D.M., Jr. and Whiting, R.L.: "Petroleum Reservoir Engineering", McGraw-Hill Book Company, Inc. 1960, 136.
2. Aronofsky, J.S.: "Mobility Ratio - Its Influence on Flood Patterns During Water Encroachment", Trans. AIME (1952), 195, 15.
3. Aronofsky, J.S. and Ramey, H.J., Jr.: "Mobility Ratio - Its Influence on Injection or Production Histories in Five-Spot Water Flood", Trans. AIME (1956), 207, 205.
4. Bernard, W.J. and Caudle, B.H.: "Model Studies of Pilot Water Floods", Jour. of Pet.Tech. March 1967, 404.
5. Breston, J.N. and Hughes, R.V.: "Relation Between Pressure and Recovery in Long Core Water Floods", Trans. AIME (1949), 186, 100.
6. Bobek, J.E. and Mattex, C.C.: "Reservoir Rock Wettability - Its Significance and Evaluation", Trans. AIME (1958), 213, 155.
7. Buckley, S.E. and Leverett, M.C.: "Mechanism of Fluid Displacement in Sands", Trans. AIME (1942), 146, 149.
8. Caudle, B.H., Erickson, R.A., and Slobod, R.L.: "The Encroachment of Fluids Beyond the Normal Well Patterns", Trans. AIME (1955), 204, 79.
9. Caudle, B.H. and Witte, M.D.: "Production Potential Changes During Sweepout in a Five-Spot System", Trans. AIME (1959), 216, 446.
10. Caudle, B.H. and Loncaric, I.G.: "Oil Recovery in Five-Spot Pilot Floods", Trans. AIME (1960), 219, 132.
11. Cheek, R.E. and Menzie, D.E.: "Fluid Mapper Model Studies of Mobility Ratio", Trans. AIME (1955), 204, 278.

12. Craig, F.F., Jr., Geffen, T.M. and Morse, R.A.: "Oil Recovery Performance of Pattern Gas or Water Injection Operations from Model Tests", Trans. AIME (1955), 204, 7.
13. Craig, F.F., Jr.: "Laboratory Model Study of Single Five-Spot and Single Injection Well Pilot Water-flooding", Jour.of Pet.Tech. Dec.(1965), 1454.
14. Crawford, P.B. and Burton, M.B.: "Application of the Gelatin Model for Studying Mobility Ratio Effects", Trans. AIME (1956), 207, 333.
15. Dalton, R.L., Jr., Rappoport, L.A. and Carpenter, C.W., Jr.: "Laboratory Studies of Pilot Water Floods", Trans. AIME (1960), 219, 24.
16. Dyes, A.B., Caudle, B.H., and Erickson, R.A.: "Oil Production After Breakthrough as Influenced by Mobility Ratio", Trans. AIME (1954), 201, 240.
17. Dyes, A.B., Kemp, C.E. and Caudle, B.H.: "Effect of Fractures on Sweep-out Patterns", Pet. Trans. Reprint Series No. 2, "Water Flooding", 152.
18. Earlougher, R.C.: "Relationship Between Velocity, Oil Saturation, and Flooding Efficiency", Trans. AIME (1943), 151, 125.
19. Engelberts, W.F. and Klinkenberg, L.J.: "Laboratory Experiments on the Displacement of Oil by Water from Packs of Granular Materials", Proc. Third World Petroleum Congress, The Hague (1951), Part II, 544.
20. Fay, C.H., and Prats, M.: "The Application of Numerical Methods to Cycling and Flooding Problems", Proc. Third World Petroleum Congress, The Hague (1951), Part II, 555.

21. Johnson, E.F., Bossler, D.P., and Naumann, V.O.: "Calculation of Relative Permeability from Displacement Experiments", Trans. AIME (1959), 216, 370.
22. Kelley, D.L. and Caudle, B.H.: "The Effects of Connate Water on the Efficiency of High-Viscosity Water-floods", Jour.of Pet. Tech. Nov.(1966), 1481.
23. Kennedy, H.T. and Guerrero, E.T.: "The Effect of Surface and Interfacial Tension on the Recovery of Oil by Water Flooding", Trans. AIME (1954), 201, 124.
24. Kinney, P.T. and Neilson, R.F.: "Role of Wettability in Oil Recovery", Producers' Monthly, Jan.(1950), 29.
25. Levine, J.S.: "Displacement Experiments in a Consolidated Porous System", Trans. AIME (1954), 201, 57.
26. Moore, T.F. and Slobod, R.L.: "The Effect of Viscosity and Capillarity on the Displacement of Oil by Water", Producers' Monthly, Aug. (1956), 20.
27. Mungan, N.: "Role of Wettability and Interfacial Tension in Waterflooding", Soc.of Petr.Engr.Jour. June (1964), 115.
28. Mungan, N.: "Interfacial Effects in Immiscible Liquid-Liquid Displacement in Porous Media", Soc.of Petr. Engr. Jour., Sept. (1966), 247.
29. Muskat, M. and Wyckoff, R.D.: "A Theoretical Analysis of Waterflooding Networks", Trans.AIME (1934), 107, 62.
30. Muskat, M.: "The Flow of Homogeneous Fluids Through Porous Media", McGraw-Hill Book Co., Inc. 1937, Chapter 9.
31. Muskat, M.: "Physical Principles of Oil Production", McGraw-Hill Book Co. 1949, 659.
32. Muskat, M.: "The Theory of Potentiometric Models", Trans. AIME (1949), 179, 216.

33. Neilson, I.D.R. and Flock, D.L.: "The Effect of a Free Gas Saturation on the Sweep Efficiency of an Isolated Five-Spot," CIM Bull. (1962), 55, 124.
34. Nobles and Janzen: "Application of a Resistance Network for Studying Mobility Ratio Effects", Trans.AIME (1958), 213, 356.
35. Perkins, F.M., Jr.: "An Investigation of the Role of Capillary Forces in Laboratory Water Floods", Trans. AIME (1957), 210, 409.
36. Prats, M. et al: "Effects of Off-Pattern Wells on the Performance of a Five-Spot Water Flood", Jour. of Petr. Tech. Feb. (1962), 173.
37. Pye, D.J.: "Improved Secondary Recovery by Control of Water Mobility", Jour.of Petr.Tech.Aug.(1964), 911.
38. Rappoport, L.A. and Leas, W.J.: "Properties of Linear Waterfloods", Trans.AIME (1953), 198, 139.
39. Rappoport, L.A., Carpenter, C.W., Jr., and Leas, W.J.: "Laboratory Studies of Five-Spot Water Flood Performance", Trans.AIME (1958), 213, 113.
40. Richardson, J.G. and Perkins, F.M., Jr.: "A Laboratory Investigation of the Effect of Rate on Recovery of Oil by Water Flooding", Trans.AIME(1957),210, 115.
41. Sandiford, B.B.: "Laboratory and Field Studies of Water Floods Using Polymer Solutions to Increase Oil Recoveries", Jour.of Petr.Tech., Aug.(1964), 917.
42. Singhal, A.K.: "Simulation of Unconsolidated Porous Media", M.Sc.Thesis, University of Alberta, (1965).
43. Serra, John: "A Model Study of an Isolated Normal Five-Spot", M.Sc. Thesis, University of Alberta (1966).
44. Slobod, R.L. and Caudle, B.H.: "X-ray Shadowgraph Studies of Areal Sweepout Efficiencies", Trans.AIME (1952), 195, 265.

45. Van Meurs, P.: "The Use of Transparent Three-Dimensional Models for Studying the Mechanism of Flow Processes in Oil Reservoirs", Trans.AIME (1957), 210, 295.
46. Wagner, O.R. and Leach, R.O.: "Effect of Interfacial Tension on Displacement Efficiency", Soc. of Petr. Engr. Jour., Dec. (1966), 335.
47. Watson, R.E., Silberberg, I.H., and Caudle, B.H.: "Model Studies of the Inverted Nine-Spot Injection Pattern", Jour. of Petr. Tech., July (1964), 801.
48. Wyckoff, R.D., Botset, H.G., and Muskat, M.: "The Mechanics of Porous Flow Applied to Water Flooding Problems", Trans. AIME (1933), 103, 219.

APPENDIX I

Calculation of the Porosity of the Glass-Bead Pack in the Model

Dimensions of the model (without any expansion) are:

Diameter = 33.6 inches = 85.4 cms.

Thickness = 0.25 inch

Bulk volume (without any expansion)

$$= \pi/4 (85.4)^2 \times 0.25 \times 2.54$$

$$= 3637.5 \text{ cc.}$$

After packing, an expansion in the model was observed. To take it into account for calculating effective bulk volume, the outside thickness at the rim of the model, where it is bolted, and at a distance from the rim was measured. It was assumed that the expansion was gradual from the rim towards the center of the model.

Thickness at the rim (cms)	Thickness at a distance of 17.5 cm. from the rim (cms.)	Expansion (cms.)
10.49	10.766	0.276
10.52	10.766	0.246
10.70	11.036	0.336
10.63	10.92	0.290

Average = 0.287

Average thickness of packing at 17.5 cms. from rim = 0.25 inch + 0.287 cms.

Radius of the model = 42.7 cms.

By extrapolation, thickness at the center

$$= 0.25 \text{ inch} + 0.700 \text{ cms.}$$

$$= 0.25 \text{ inch} + 0.275 \text{ inch}$$

$$= 0.525 \text{ inch}$$

Using the pyramidal rule, and dividing the bulge in large number of small intervals, the volume of the bulge was calculated. Using this method, the extra bulk volume was found to be 1287 cc.

Effective bulk volume of the model

$$= 3637.5 + 1287.0$$

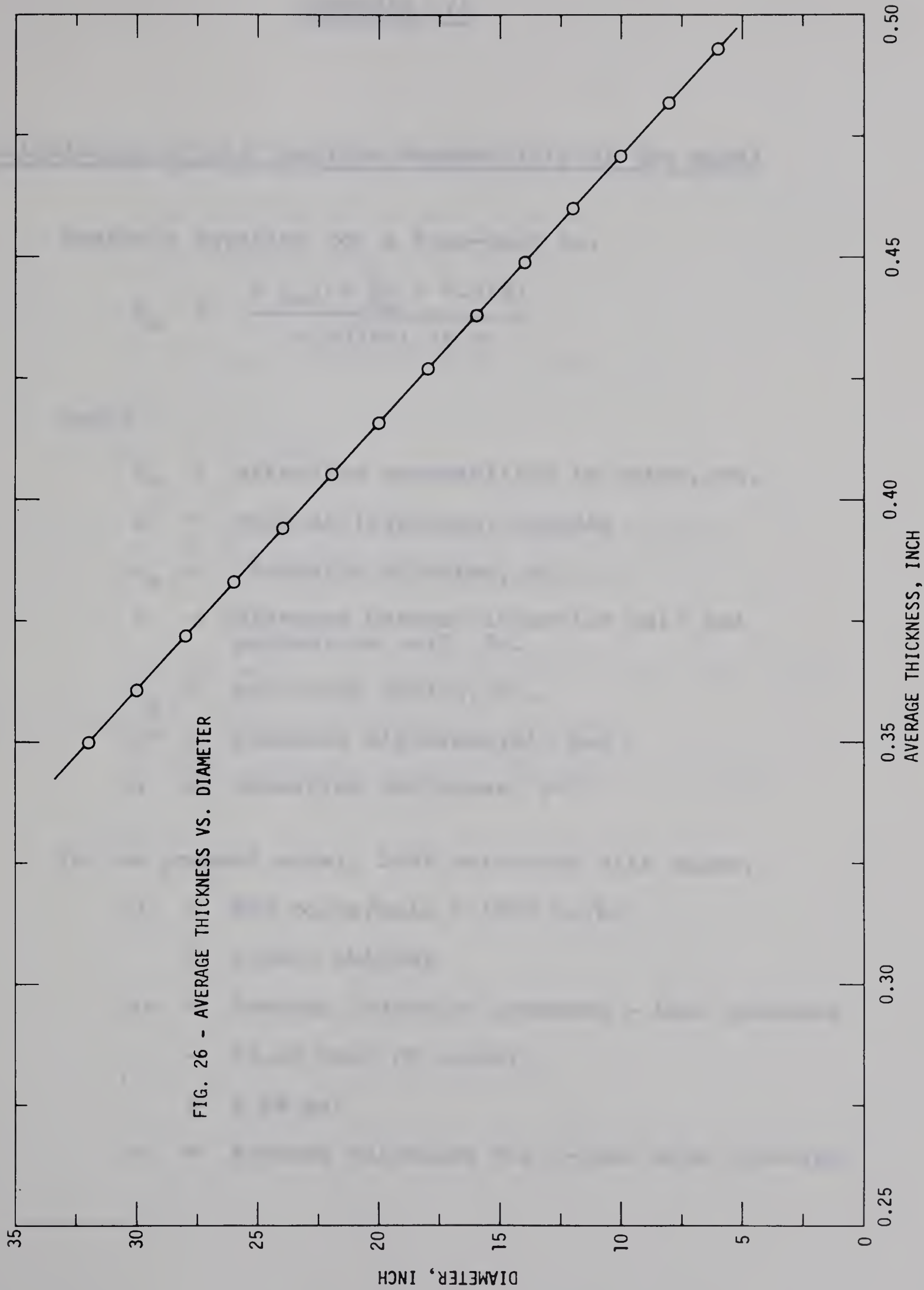
$$= 4924.5 \text{ cc.}$$

After evacuation, water injected to saturate the model completely = 1620 cc.

$$\text{Porosity of the model} = 1620/4924.5 = 32.9\%$$

While calculating the pore volume of the network or displacement efficiency, a volumetric average thickness for the area in question was used. To facilitate the

calculations, a plot (Figure 26) was prepared, giving the volumetric average thickness of the packing against any diameter around the center of the model. This was prepared by calculating the volumes of different areas in small increments (using the pyramidal rule for calculating the extra volume of the bulge), and dividing it by the corresponding area to give the volumetric average thickness.



APPENDIX II

Calculation of the Absolute Permeability of the Model

Muskat's equation for a five-spot is:

$$k_w = \frac{Q \mu_w (\ln \frac{d}{r_w} - 0.619)}{0.003541 \Delta P h}$$

where

k_w = effective permeability to water, md.

Q = rate of injection, bbl/day

μ_w = viscosity of water, cp.

d = distance between injection well and production well, ft.

r_w = well-bore radius, ft.

ΔP = Pressure differential, psi

h = formation thickness, ft.

In the present model, 100% saturated with water,

Q = 400 cc/hr/well = 1600 cc/hr.

= 0.2415 bbl/day

ΔP = Average injection pressure - back pressure

= 25.25 cms. of mercury

= 4.88 psi

h = Average thickness for 8-inch side five-spot

$$\begin{aligned}
 &= 1.17 \text{ cms.} \\
 &= 0.0384 \text{ ft.} \\
 \mu_w &= 0.927 \text{ cp.} \\
 d &= 5.657 \text{ inch} \\
 r_w &= 1/32 \text{ inch} = 0.03125 \text{ inch} \\
 d/r_w &= 181 \\
 \ln d/r_w &= 5.1985 \\
 k_w &= \frac{0.2415 \times 0.927 \times (5.1985 - 0.619)}{0.003541 \times 4.88 \times 0.0384} \\
 &= 1542 \text{ md.}
 \end{aligned}$$

As the model was 100% saturated with water, this is the absolute permeability of the packing.

Absolute permeability of the model = 1542 md.

APPENDIX III

Determination of Relative Permeability Curves

A method for the calculation of relative permeability from displacement experiments performed on a linear porous body, has been described by Johnson, Bossler and Naumann [21]. This method was used to determine the relative permeability curves (Figure 4).

The authors have given the following relations, presented previously by Welge, which were needed for the calculation of individual relative permeabilities:

$$W_i = \frac{1}{f'} = \frac{1}{d_f/d_S} \quad (1)$$

$$\frac{f}{1-f} = \frac{f}{f_o} = \frac{k_{rw} \mu_o}{k_{ro} \mu_w} \quad (2)$$

$$(f_o)_2 = \frac{d S_{av}}{d W_i} \quad (3)$$

$$S_{av} = S_2 + W_i (f_o)_2 \quad (4)$$

$$\frac{d\left(\frac{1}{W_i I_r}\right)}{d\left(\frac{1}{W_i}\right)} = \frac{f_o}{k_{ro}} \quad (5)$$

where,

f = fraction of displacing phase in flowing stream

f_o = fraction of displaced phase in flowing stream

f' = df/ds

S = saturation of displacing phase

W_i = cumulative injection in pore volumes

k_r = relative permeability

μ = viscosity

I_r = relative injectivity, $u/\Delta p \div u/\Delta p$ (at start of injection)

u = average velocity, $= q/A$

q = flow rate

p = pressure differential across the porous body

Subscripts

av = average

w = pertaining to water (displacing phase)

o = pertaining to oil (displaced phase)

2 = pertaining to outlet face of porous body

For any instant in the displacement, i.e., for any value of cumulative injection W_i , the derivative in equation (5) could be evaluated from data collected during the

experiment. For a given value of W_i the fraction of oil in the effluent, f_o , could be evaluated separately by equation (3). The k_{ro} , which was then obtained by dividing f_o by the derivative from the left-hand side of equation (5), is the relative permeability to oil at the outlet face saturation, S_2 . The S_2 for the W_i under consideration was obtained by rearranging equation (4):

$$S_2 = S_{av} - W_i (f_o)_2 \quad (4a)$$

The expression for the relative permeability of the displacing phase at S_2 was obtained by solving equation (2) for k_{rw} :

$$k_{rw} = \frac{(1 - f_o)}{f_o} \cdot \frac{\mu_w}{\mu_o} \cdot k_{ro} \quad (6)$$

For this test, a lucite tube, 28.5 cm. in length was used. Its bulk volume was measured by filling it with water and then measuring the volume of water. It was found to be equal to 235 cc. The tube was packed with glass beads (same as used in the radial model). It was evacuated and then saturated completely with distilled

water (this gave the pore volume and hence porosity). The oil was then injected until no more water was produced in the producing stream. Water was then injected at a constant rate. A record of fluids produced and corresponding injection pressure was kept. From this data, the relative permeability curves were obtained (Figure 4).

Two runs, L-1 and L-2 were taken. The data and the calculations are shown on the following page.

Bulk Volume = 235 cc. Pore Volume = 82.5 cc. Porosity = 35.1%
 Initial water (connate) saturation = $9.5/82.5 = 11.5\%$
 Initial Oil saturation = $73/82.5 = 88.5\%$
 Rate of injection = 400 cc/hr.

RUN NO. L-1

$\frac{\Delta P}{\text{(cm. of } \text{CCl}_4 \text{)}}$	<u>Total Production</u> (cc.)		<u>Water</u> (cc.)		<u>Oil</u> (cc.)	
	<u>Inst.</u>	<u>Cum.</u>	<u>Inst.</u>	<u>Cum.</u>	<u>Inst.</u>	<u>Cum.</u>
22.1	5.6	5.6	-	-	5.6	5.6
22.8	6.7	12.3	-	-	6.7	12.3
22.8	13.2	25.5	-	-	13.2	25.5
23.6	6.5	32.0	-	-	6.5	32.0
24.4	3.9	35.9	0.1	0.1	3.8	35.8
31.2	7.5	43.4	1.2	1.3	6.3	42.1
33.2	5.7	49.1	3.2	4.5	2.5	44.6
22.2	10.9	60.0	8.5	13.0	2.4	47.0
20.2	11.0	71.0	9.5	22.5	1.5	48.5
20.0	14.4	85.4	12.7	35.2	1.7	50.2
19.2	14.4	99.8	13.1	48.3	1.3	51.5
18.6	16.1	115.9	14.6	62.9	1.3	52.8
18.4	17.2	133.1	16.4	79.3	0.6	53.4
18.0	16.4	149.5	15.4	94.7	0.5	53.9
17.8	33.9	183.4	32.2	126.9	0.7	54.6
17.4	49.2	232.6	47.7	174.6	0.5	55.1
17.2	50.3	282.9	49.5	224.1	0.6	55.7
17.0	39.5	322.4	39.0	263.1	0.3	56.0

RUN NO. L-2

17.8	5.5	5.5	-	-	5.5	5.5
18.0	11.9	17.4	-	-	11.9	17.4
18.2	10.1	27.5	-	-	10.1	27.5
18.4	10.9	38.4	0.4	0.4	10.5	38.0
23.8	7.0	45.4	1.5	1.9	5.5	43.5
18.2	9.8	55.2	6.5	8.4	3.3	46.8
16.8	10.5	65.7	8.5	16.9	2.0	48.8
16.0	12.6	78.3	11.0	27.9	1.6	50.4
15.4	12.7	91.0	11.7	39.6	1.0	51.4
15.0	12.2	103.2	11.3	50.9	0.9	52.3
14.6	12.2	115.4	11.5	62.4	0.7	53.0
14.2	13.3	128.7	12.9	75.3	0.4	53.4
15.2	16.2	144.9	15.6	90.9	0.6	54.0
13.8	13.5	158.4	13.1	104.0	0.4	54.4
13.7	14.0	172.4	13.6	117.6	0.4	54.8
13.7	15.2	187.6	14.9	132.5	0.3	55.1
14.0	14.3	201.9	14.1	146.6	0.2	55.3
13.8	14.5	216.4	14.3	160.9	0.2	55.5
13.9	14.1	230.5	14.0	174.9	0.1	55.6
15.2	50.9	281.4	50.6	225.5	0.3	55.9
15.2	24.0	305.4	23.9	249.4	0.1	56.0

Calculations for Run Nos. L-1 and L-2

$u = 48.51 \text{ cm/hr.}$ $(\Delta P)_{\text{initial}} = 21$ $(u/\Delta P)_{\text{initial}} = 2.31$

RUN NO. L-1

<u>W_i</u>	<u>$1/W_i$</u>	<u>$u/\Delta P$</u>	<u>I_r</u>	<u>$1/W_i I_r$</u>	<u>S_{av}</u>
0.068	14.706	2.195	0.950	15.480	0.183
0.309	3.236	2.128	0.921	3.514	0.424
0.388	2.577	2.056	0.890	2.896	0.503
0.435	2.299	1.988	0.861	2.670	0.549
0.526	1.901	1.555	0.673	2.825	0.625
0.595	1.681	1.461	0.632	2.660	0.656
0.727	1.376	2.185	0.946	1.455	0.685
0.861	1.161	2.401	1.039	1.117	0.703
1.035	0.966	2.426	1.050	0.920	0.724
1.210	0.826	2.527	1.094	0.755	0.739
1.405	0.712	2.608	1.129	0.631	0.755
1.613	0.620	2.636	1.141	0.543	0.762
1.812	0.552	2.695	1.167	0.473	0.768
2.223	0.450	2.725	1.180	0.381	0.777
2.819	0.355	2.788	1.207	0.294	0.783
3.429	0.292	2.820	1.221	0.239	0.790
3.908	0.256	2.854	1.235	0.207	0.794

RUN NO. L-2

$u = 48.51 \text{ cm/hr}$ $(\Delta P)_{\text{initial}} = 17.7$ $(u/\Delta P)_{\text{initial}} = 2.741$

0.067	14.925	2.725	0.994	15.015	0.182
0.211	4.739	2.695	0.983	4.821	0.326
0.333	3.000	2.665	0.972	3.086	0.448
0.465	2.151	2.636	0.962	2.236	0.576
0.550	1.818	2.038	0.744	2.444	0.642
0.669	1.495	2.665	0.972	1.538	0.682
0.796	1.256	2.888	1.054	1.192	0.707
0.949	1.054	3.032	1.106	0.953	0.726
1.103	0.907	3.150	1.149	0.789	0.738
1.251	0.799	3.234	1.180	0.677	0.749
1.399	0.715	3.323	1.212	0.590	0.758
1.560	0.641	3.416	1.246	0.514	0.762
1.756	0.569	3.416	1.246	0.457	0.770
1.920	0.521	3.515	1.282	0.406	0.775
2.090	0.478	3.541	1.292	0.370	0.779
2.274	0.440	3.541	1.292	0.341	0.783
2.447	0.409	3.465	1.264	0.324	0.785
2.623	0.381	3.515	1.282	0.297	0.788
2.794	0.358	3.490	1.273	0.281	0.789
3.411	0.293	3.191	1.164	0.252	0.793
3.702	0.270	3.191	1.164	0.232	0.794

Note: All of these columns were calculated from experimental data.

FIG. 27 - CALCULATION OF RELATIVE PERMEABILITY

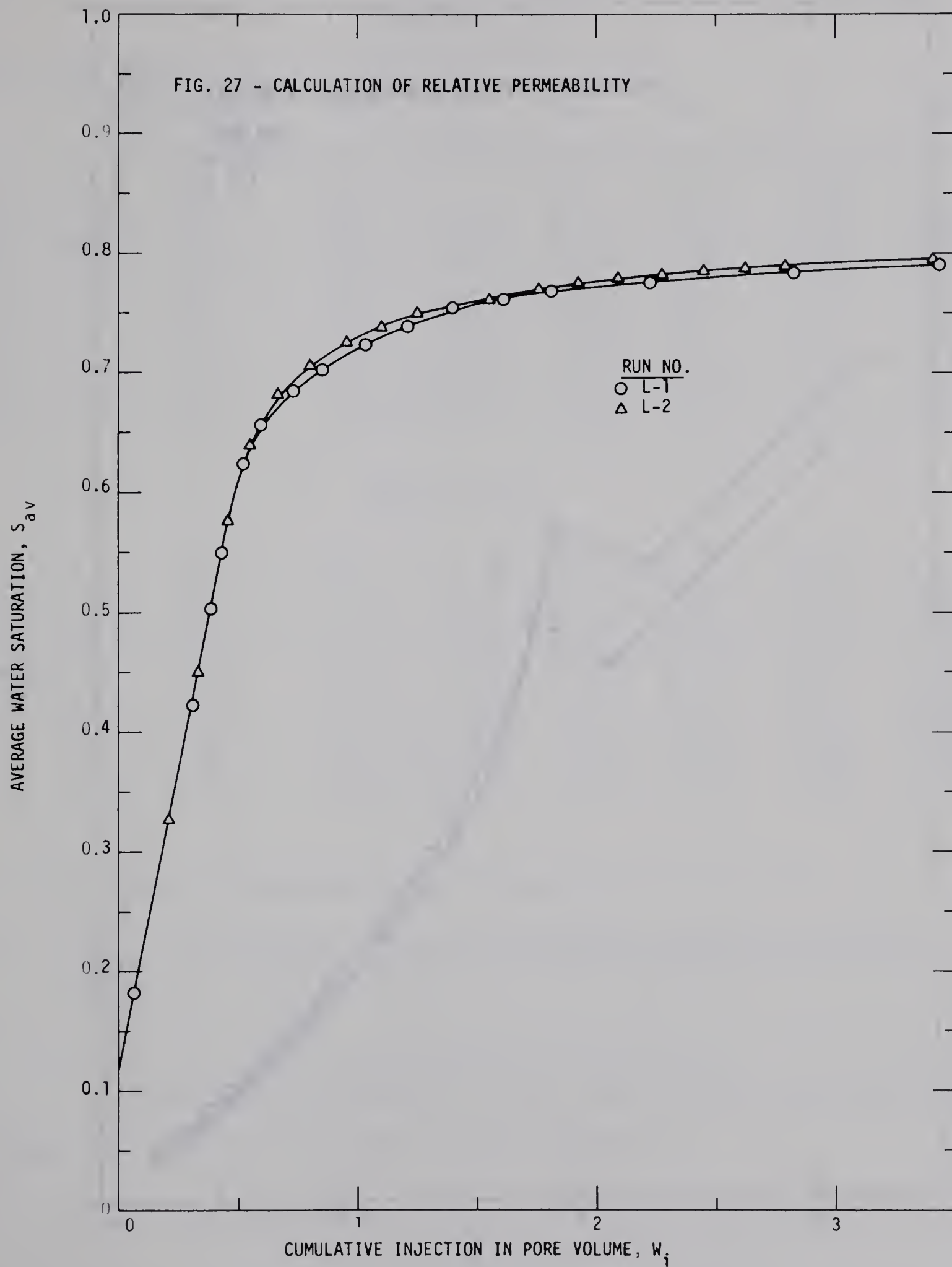
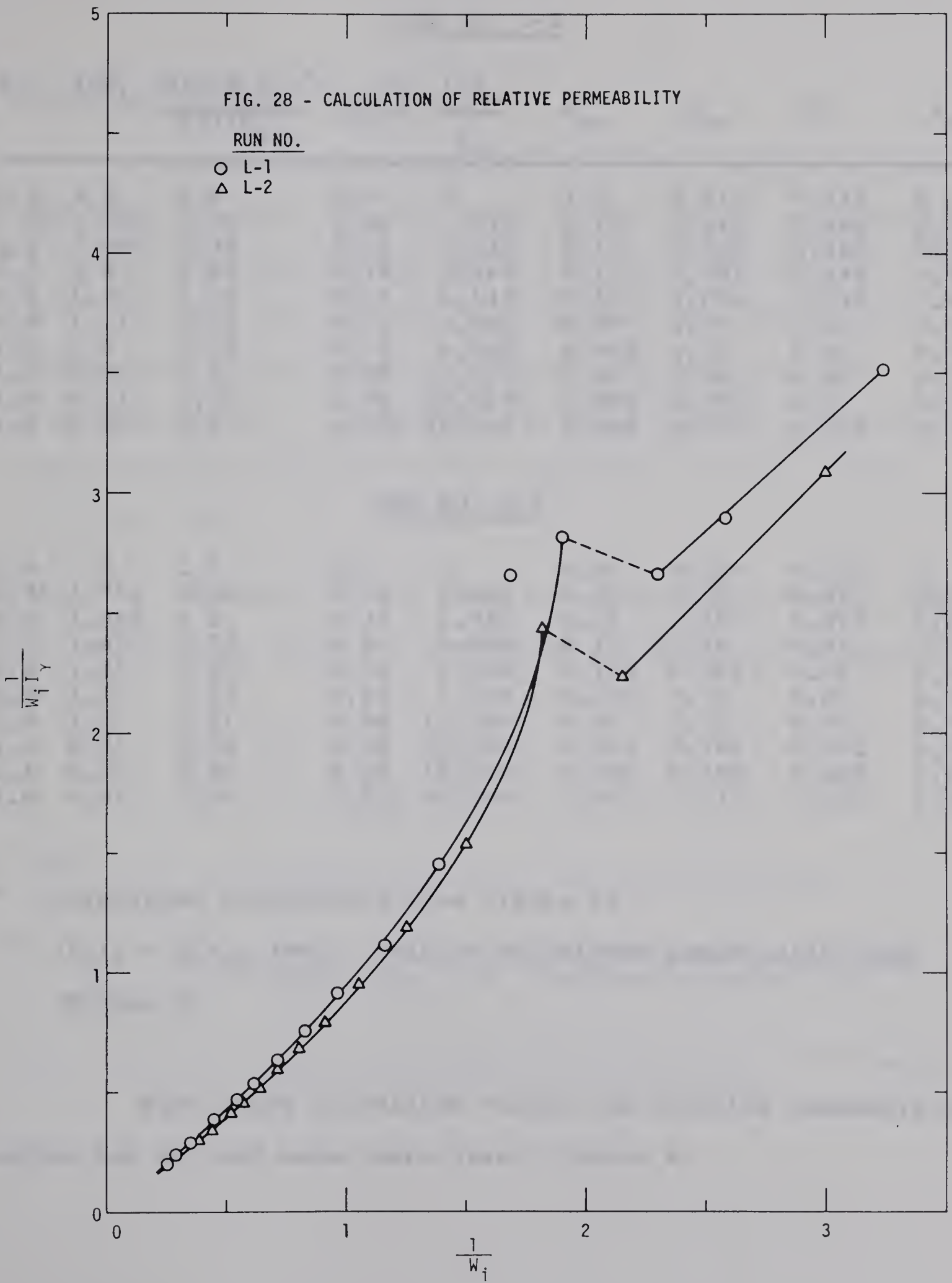


FIG. 28 - CALCULATION OF RELATIVE PERMEABILITY

RUN NO.
○ L-1
△ L-2



Calculations for Run Nos. L-1 and L-2 (cont'd)

RUN NO. L-1

W_i	$1/W_i$	$\frac{d(1/W_i I_r)^*}{d(1/W_i)}$	$(f_o)^{**}_2$	$\frac{1-f_o}{f_o}$	k_{ro}	S_{av}	S_2	k_{rw}
0.4	2.5	1.0	1.0	0	1.0	0.515	0.115	0
0.56	1.786	3.15	0.44	1.273	0.14	0.642	0.396	0.126
0.6	1.667	2.34	0.31	2.226	0.13	0.658	0.469	0.204
0.7	1.43	1.67	0.19	4.263	0.11	0.681	0.548	0.330
0.8	1.25	1.37	0.14	6.143	0.10	0.698	0.576	0.433
0.9	1.11	1.23	0.11	8.091	0.09	0.71	0.61	0.513
1.0	1.0	1.18	0.10	9.000	0.085	0.72	0.62	0.539
1.2	0.83	1.11	0.09	10.111	0.08	0.74	0.63	0.570
1.4	0.71	1.07	0.06	15.667	0.056	0.755	0.67	0.618
1.8	0.56	0.97	0.025	39.000	0.026	0.77	0.725	0.714

RUN NO. L-2

0.4	2.5	1.0	1.0	0	0.99	0.515	0.115	0
0.56	1.786	5.36	0.55	0.818	0.10	0.65	0.34	0.576 (x)
0.6	1.667	2.2	0.34	1.941	0.15	0.667	0.463	0.205
0.7	1.43	1.53	0.2	4.000	0.13	0.69	0.55	0.366
0.8	1.25	1.27	0.16	5.250	0.126	0.708	0.58	0.466
0.9	1.11	1.13	0.12	7.333	0.106	0.72	0.61	0.547
1.0	1.0	1.11	0.08	11.500	0.07	0.73	0.65	0.567
1.2	0.83	1.04	0.07	13.286	0.067	0.746	0.662	0.627
1.4	0.71	0.96	0.05	19.000	0.052	0.758	0.688	0.696
1.8	0.56	0.92	0.025	39.000	0.027	0.772	0.727	0.741

* Calculated graphically from Figure 28.

** $(f_o)_2 = d(S_{av})/dW_i$. This is calculated graphically from Figure 27.

From these calculated values the relative permeability curves for oil and water were drawn (Figure 4)

Calculation of Mobility Ratio

As pointed out earlier, it is not possible to find the exact value of mobility ratio in the case of two immiscible fluids. The range between which the useful value of the mobility ratio will lie may be calculated from the linear tests conducted for relative permeability determination (See Appendix III). The useful value of the mobility ratio was calculated using the method suggested by Craig, Geffen, and Morse [12].

According to the above reference, the useful value of the mobility ratio for immiscible fluids may be defined as,

$$M = \frac{k_w}{\mu_w} \cdot \frac{\mu_o}{k_o}$$

where

μ_o, μ_w = viscosities of oil and flooding water, respectively

k_o = relative permeability to oil at initial oil saturation, i.e., existing ahead of the flood front

k_w = relative permeability to water at the average water saturation at breakthrough.

1. From Linear Test

The data of Run No. L-2 was used.

In this case,

$$S_{oi} = 0.885$$

$$\bar{S}_{obt} = 0.424$$

$$\therefore S_{wi} = 1 - 0.885 = 0.115$$

$$\therefore \bar{S}_{wbt} = 1 - 0.424 = 0.576$$

where \bar{S}_{obt} , \bar{S}_{wbt} = average oil and water saturation at breakthrough, respectively.

From Figure 4,

$$k_o = 1.0$$

$$k_w = 0.433$$

Also

$$\mu_o = 1.265 \text{ cp}$$

$$\mu_w = 0.927$$

$$\begin{aligned} \therefore M &= \frac{0.433 \times 1.265}{0.927 \times 1.0} \\ &= 0.59 \end{aligned}$$

If we take oil saturation behind the flood front as irreducible oil saturation (assuming plug flow), which was equal to 0.206, then from Figure 4,

$$k_w = 0.84$$

$$M = \frac{0.8 \times 1.265}{0.927 \times 1.0}$$

$$= 1.15$$

Therefore, the mobility ratio in the present flow system may be anywhere between 0.59 and 1.15.

2. Craig, Geffen and Morse Method

Knowing the viscosity ratio, $\mu_w/\mu_o = 0.927/1.265 = 0.735$, and the relative permeability curves (Figure 4), the following table was prepared, showing the water saturation and corresponding fractional flow of water in the flow-stream.

S_w	k_o	k_w	$\frac{k_o}{k_w}$	$\frac{k_o/\mu_o}{k_w/\mu_w}$	$1 + \frac{k_o/\mu_o}{k_w/\mu_w}$	$f_w = \frac{1}{1 + \frac{k_o/\mu_o}{k_w/\mu_w}}$
0.15	0.91	0.005	182.0	134.0	135.0	0.007
0.20	0.78	0.02	39.0	28.6	29.6	0.034
0.25	0.66	0.035	18.85	13.85	14.85	0.067
0.30	0.535	0.06	8.92	6.55	7.55	0.133
0.35	0.425	0.09	4.72	3.47	4.47	0.224
0.40	0.33	0.13	2.54	1.87	2.87	0.348
0.45	0.25	0.18	1.39	1.02	2.02	0.495
0.50	0.185	0.245	0.755	0.555	1.555	0.644
0.55	0.135	0.35	0.386	0.284	1.284	0.778
0.60	0.098	0.50	0.196	0.144	1.144	0.874
0.65	0.07	0.605	0.116	0.085	1.085	0.920
0.70	0.045	0.69	0.065	0.048	1.048	0.955

From this, a curve was drawn between f_w and S_w (Figure 29). A tangent was drawn to this curve from $S_w = 0.17$ (connate water saturation in the radial case) and was extended to $f_w = 1.0$. The value of S_w at this point gave the average water saturation at breakthrough.

From Figure 29,

$$\bar{S}_{wbt} = 0.658$$

$$S_{wi} = 0.17$$

From Figure 4,

$$k_o = 0.86$$

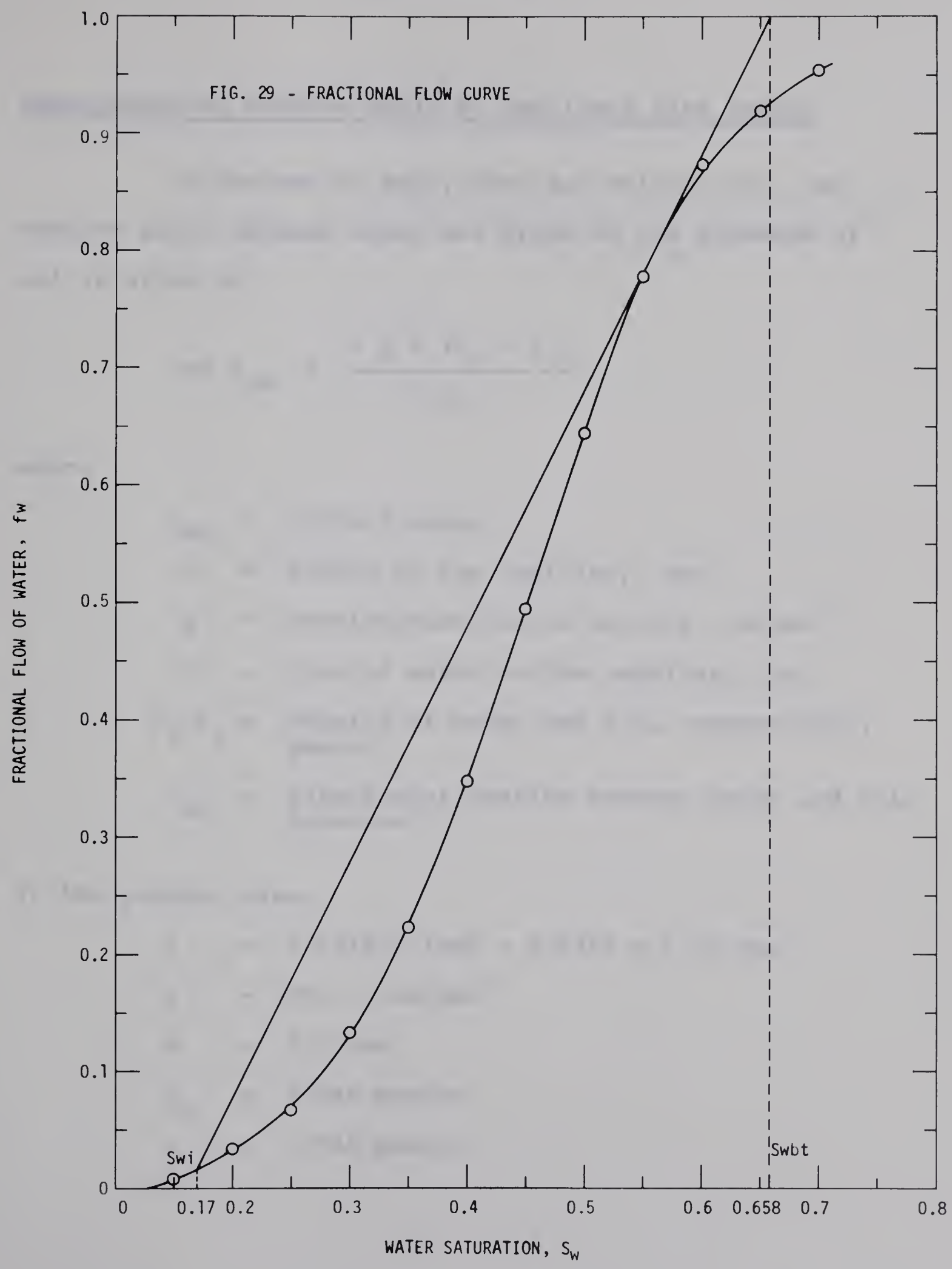
$$k_w = 0.62$$

$$M = \frac{0.62 \times 1.265}{0.927 \times 0.86}$$

$$= 0.98$$

Hence the useful value of the mobility ratio for the present fluid-flow system was equal to 0.98.

FIG. 29 - FRACTIONAL FLOW CURVE



APPENDIX V

Measurement of Contact Angle by Capillary Rise Method

As derived by Amyx, Bass and Whiting [1], the contact angle between water and glass in the presence of oil is given by

$$\cos \theta_{wo} = \frac{r g h (\rho_w - \rho_o)}{2 \sigma_{wo}}$$

where

θ_{wo} = contact angle

r = radius of the capillary, cms.

g = acceleration due to gravity, cm/sec²

h = rise of water in the capillary, cm.

ρ_w, ρ_o = density of water and oil, respectively, gms/cc.

σ_{wo} = interfacial tension between water and oil, dynes/cm.

In the present case,

r = 0.0315/2 inch = 0.0315 x 1.27 cms.

g = 980.7 cms/sec²

h = 7.5 cms.

ρ_w = 0.996 gms/cc.

ρ_o = 0.794 gms/cc.

$$\sigma_{\text{WO}} = 30.73 \text{ dynes/cm.}$$

$$\begin{aligned} \therefore \cos \theta_{\text{WO}} &= \frac{0.0315 \times 1.27 \times 980.7 \times 7.5 \times 0.202}{2 \times 30.73} \\ &= 0.97 \end{aligned}$$

$$\therefore \theta_{\text{WO}} \approx 14^\circ$$

APPENDIX VI

Calculation of Critical Rate of Injection

According to Rappoport, Carpenter and Leas [39], the critical value for dimensionless scaling coefficient, C_2 , for a viscosity ratio of 1, is 3.5×10^{-3} . C_2 is given by,

$$C_2 = \frac{q \mu_w}{\sigma \cos \theta \sqrt{k\phi}}$$

where

q = rate of injection per unit sand thickness, bbl/day/ft.

μ_w = viscosity of water, cp.

σ = water-oil interfacial tension, dyne/cm.

k = absolute permeability, md.

ϕ = porosity, fraction

θ = contact angle

In the present case,

$\mu_w = 0.927$ cp.

$\sigma = 30.73$ dyne/cm

$\cos \theta = \cos 14^\circ = 0.97$

$k = 1542$ md.

$\phi = 0.329$

$$\begin{aligned}
 \therefore q &= \frac{3.5 \times 10^{-3} \times 30.73 \times 0.97 \times (1542 \times 0.329)^{1/2}}{0.927} \\
 &= \frac{3.5 \times 10^{-3} \times 30.73 \times 0.97 \times 22.52}{0.927} \\
 &= 2.53 \text{ bbl/day/ft.} \\
 &= 644 \text{ cc/hr for the average thickness of} \\
 &\quad 1.17 \text{ cm. of the network.}
 \end{aligned}$$

This means that if the injection rate was kept above 644 cc/hr., the floods will be stabilized and will not be rate sensitive. In other words, the effect of capillary forces will be negligible. All the injection rates used were considerably higher than this value.

APPENDIX VII(a)

Calculation of Displacement Efficiency for Isolated Normal Five-Spot

Displacement efficiency, E_d

$$= \frac{\text{Oil recovered at any stage}}{\text{Area contacted by flooding water at this stage} \\ \times \text{average thickness} \times \text{porosity} \times \text{initial oil saturation}}$$

In the case of isolated normal five-spot,

$$\text{Porosity} = 0.329$$

$$\begin{array}{l} \text{Initial Oil} \\ \text{Saturation} \end{array} = 0.826^*$$

From Figures 8 and 10, it is observed that at a total injection of 6.0 network pore volumes of water,

$$\text{Recovery of oil} = 2.75 \text{ HCPV} = 2.75 \times 131.7^{**} = 362.0 \text{ cc.}$$

$$\text{Areal sweep efficiency, } E_{as} = 7.5$$

$$\text{Area contacted by flooding water} - 7.5 \times 64 = 480 \text{ sq.in.}$$

From Figure 26, average thickness for 480 sq. inch in the center of the model (equivalent to about 24.7 inch diameter) = 0.39 inch.

* Initial oil saturation for Run Nos. 1 and 3.

** Network HCPV for Run Nos. 1 and 3.

Displacement efficiency

$$= \frac{362.0}{480 \times 0.39 \times 0.826 \times 0.329 \times 16.387^{***}}$$

$$\approx 43\%$$

*** 1 cu. inch = 16.387 cc.

APPENDIX VII(b)

Calculation of Displacement Efficiency for Four Inverted
Five-Spot

Displacement efficiency, E_d

$$= \frac{\text{Oil recovered at any stage}}{\text{Area contacted by flooding water at this stage} \\ \times \text{average thickness} \times \text{porosity} \times \text{initial oil sat.}}$$

In the case of four inverted five-spot,

$$\text{Porosity} = 0.329$$

$$\begin{array}{l} \text{Initial Oil} \\ \text{Saturation} \end{array} = 0.8475$$

From Figures 17 and 19, at a total injection of 8.0
network pore volumes of water,

$$\text{Recovery of oil} = 2.87 \text{ HCPV} = 2.87 \times 134.75^* = 386.7 \text{ cc.}$$

$$\text{Areal sweep efficiency} = 5.61$$

$$\text{Area contacted by flooding water} = 5.61 \times 64 = 359.04 \text{ sq.in.}$$

From Figure 26, average thickness for 359.04 sq. inch
in the center of the model (equivalent to about 21.4 inch
diameter) = 0.407 inch.

* Network HCPV = 134.75 cc.

Displacement efficiency

$$= \frac{386.7}{359.04 \times 0.407 \times 0.8475 \times 0.329 \times 16.387} **$$

$$\approx 58\%$$

** 1 cu. inch = 16.387 cc.

APPENDIX VIII

APPENDIX VIII

EXPERIMENTAL DATA AND CALCULATIONS

NOMENCLATURE USED IN THE TABLES

N	Initial oil in place in the model, cc.
L	Length of one side of the well-pattern, cm.
d	Distance between injection and production wells, cm.
r_w	Well-bore radius, cm.
h_{av}	Volumetric average thickness of the packing in the well-pattern.
q	Injection rate, cc/hr.
ΔQ_p	Total(oil + water) production during an interval, cc.
Q_p	Cumulative total production, cc.
ΔW_p	Water produced during an interval, cc.
W_p	Cumulative water produced, cc.
ΔN_p	Oil produced during an interval, cc.
N_p	Cumulative oil produced, cc.
F_{wo}	Instantaneous producing water-oil ratio.
Q_{NPV}	Cumulative throughput in network pore volume.
Q_{HPV}	Cumulative throughput in network hydrocarbon pore volume.
Q_{DPV}	Cumulative throughput in network displaceable pore volume
$ONPV$	Cumulative oil produced in network pore volume.
$OHPV$	Cumulative oil produced in network hydrocarbon pore volume.
$ODPV$	Cumulative oil produced in network displaceable pore volume.

TABLE 1-A

RUN NO. 1

ISOLATED NORMAL FIVE-SPOT

$N = 1342 \text{ cc.}$
 $L = 8 \text{ inch} = 20.32 \text{ cm.}$
 $d/r_w = 181$
 $h_{av} = 1.17 \text{ cm}$
 Porosity = 32.9%

$S_{oi} = 0.8284$
 $S_{wc} = 0.1716$
 $q = 400 \text{ cc/hr/well} = 1600 \text{ cc/hr}$
 Network Pore Volume = 159 cc.
 Network HCPV = $159 \times 0.8284 = 131.7 \text{ cc}$
 Back Pressure = 0

ΔQ_p	Q_p	ΔW_p	W_p	ΔN_p	N_p	QNPV
71.0	71.0	0.0	0.0	71.0	71.0	0.45
24.0	95.0	0.0	0.0	24.0	95.0	0.60
10.5	105.5	0.0	0.0	10.5	105.5	0.66
24.4	129.9	4.0	4.0	20.4	125.9	0.82
24.1	154.0	7.2	11.2	16.9	142.8	0.97
25.1	179.1	9.5	20.7	15.6	158.4	1.13
25.0	204.1	10.9	31.6	14.1	172.5	1.28
25.0	229.1	12.5	44.1	12.5	185.0	1.44
8.0	237.1	4.5	48.6	3.5	188.5	1.49
24.5	261.6	13.5	62.1	11.0	199.5	1.65
25.8	287.4	15.4	77.5	10.4	209.9	1.81
23.5	310.9	14.6	92.1	8.9	218.8	1.96
24.5	335.4	15.5	107.6	9.0	227.8	2.11
25.7	361.1	16.8	124.4	8.9	236.7	2.27
25.0	386.1	16.9	141.3	8.1	244.8	2.43
24.0	410.1	16.9	158.2	7.1	251.9	2.58
24.1	434.2	17.0	175.2	7.1	259.0	2.73
9.3	443.5	6.6	181.8	2.7	261.7	2.79
24.5	468.0	18.2	200.0	6.3	268.0	2.94
26.2	494.2	20.8	220.8	5.4	273.4	3.11
24.2	518.4	19.0	239.8	5.2	278.6	3.26
24.3	542.7	19.5	259.3	4.8	283.4	3.41
25.1	567.8	20.0	279.3	5.1	288.5	3.57
24.5	592.3	19.5	298.8	5.0	293.5	3.73
25.0	617.3	20.0	318.8	5.0	298.5	3.88

TABLE 1-A

(cont'd)

ΔQ_p	Q_p	ΔW_p	W_p	ΔN_p	N_p	QNPV
24.9	642.2	20.5	339.3	4.4	302.9	4.04
24.9	667.1	20.5	359.8	4.4	307.3	4.20
25.0	692.1	20.7	380.5	4.3	311.6	4.35
25.5	717.6	21.0	401.5	4.5	316.1	4.51
24.7	742.3	20.5	422.0	4.2	320.3	4.67
25.2	767.5	20.8	442.8	4.4	324.7	4.83
24.4	791.9	20.0	462.8	4.4	329.1	4.98
24.7	816.6	20.5	483.3	4.2	333.3	5.14
23.5	840.1	19.5	502.8	4.0	337.3	5.28
25.5	865.6	21.1	523.9	4.4	341.7	5.44
24.4	890.0	20.2	544.1	4.2	345.9	5.60
24.9	914.9	20.6	564.7	4.3	350.2	5.75
23.6	938.5	19.5	584.2	4.1	354.3	5.90
24.9	963.4	20.7	604.9	4.2	358.5	6.06
26.5	989.9	22.1	627.0	4.4	362.9	6.23
11.5	1001.4	9.5	636.5	2.0	364.9	6.30
24.0	1025.4	20.0	656.5	4.0	368.9	6.45
97.8	1123.2	81.5	738.0	16.3	385.2	7.06
85.0	1208.2	73.0	811.0	12.0	397.2	7.60
*168.0	1376.2	140.0	951.0	28.0	425.2	8.66

* Production after injection ceased.

TABLE 1-B

RUN NO. 1

QNPV	QHPV	QDPV	F _{wo}	ONPV	OHPV	ODPV
0.45	0.54	1.28	0.0	0.45	0.54	1.28
0.60	0.72	1.72	0.0	0.60	0.72	1.72
0.66	0.80	1.91	0.0	0.66	0.80	1.91
0.82	0.99	2.35	0.20	0.79	0.96	2.28
0.97	1.17	2.78	0.43	0.90	1.08	2.58
1.13	1.36	3.24	0.61	1.0	1.20	2.86
1.28	1.55	3.69	0.77	1.09	1.31	3.12
1.44	1.74	4.14	1.00	1.16	1.41	3.35
1.49	1.80	4.29	1.29	1.19	1.43	3.41
1.65	1.99	4.73	1.23	1.26	1.52	3.61
1.81	2.18	5.20	1.48	1.32	1.59	3.80
1.96	2.36	5.62	1.64	1.38	1.66	3.96
2.11	2.55	6.06	1.72	1.43	1.73	4.12
2.27	2.74	6.53	1.89	1.49	1.80	4.28
2.43	2.93	6.98	2.09	1.54	1.86	4.43
2.58	3.11	7.41	2.38	1.58	1.91	4.55
2.73	3.30	7.85	2.39	1.63	1.97	4.68
2.79	3.37	8.02	2.44	1.65	1.99	4.73
2.94	3.55	8.46	2.89	1.69	2.04	4.85
3.11	3.75	8.93	3.85	1.72	2.08	4.94
3.26	3.94	9.37	3.65	1.75	2.12	5.04
3.41	4.12	9.81	4.06	1.78	2.15	5.12
3.57	4.31	10.27	3.92	1.81	2.19	5.22
3.73	4.50	10.71	3.90	1.85	2.23	5.31
3.88	4.69	11.16	4.00	1.88	2.27	5.40
4.04	4.88	11.61	4.66	1.91	2.30	5.48
4.20	5.07	12.06	4.66	1.93	2.33	5.56
4.35	5.26	12.51	4.81	1.96	2.37	5.63
4.51	5.45	12.97	4.67	1.99	2.40	5.72
4.67	5.64	13.42	4.88	2.01	2.43	5.79
4.83	5.83	13.88	4.73	2.04	2.47	5.87
4.98	6.01	14.32	4.55	2.07	2.50	5.95
5.14	6.20	14.76	4.88	2.10	2.53	6.03
5.28	6.38	15.19	4.88	2.12	2.56	6.10
5.44	6.57	15.65	4.80	2.15	2.60	6.18
5.60	6.76	16.09	4.81	2.18	2.63	6.25
5.75	6.95	16.54	4.79	2.20	2.66	6.33

TABLE 1-B

(cont'd)

QNPV	QHPV	QDPV	F _{wo}	ONPV	OHPV	ODPV
5.90	7.13	16.97	4.76	2.23	2.69	6.41
6.06	7.32	17.42	4.93	2.26	2.72	6.48
6.23	7.52	17.90	5.02	2.28	2.76	6.56
6.30	7.60	18.10	4.75	2.30	2.77	6.60
6.45	7.79	18.54	5.00	2.32	2.80	6.67
7.06	8.53	20.31	5.00	2.42	2.93	6.96
7.60	9.17	21.84	6.08	2.50	3.02	7.18
* 8.66	10.45	24.88	5.00	2.67	3.23	7.69

* Production after injection ceased.

TABLE 2-A

RUN NO. 2

ISOLATED NORMAL FIVE-SPOT

$N = 1278.0 \text{ cc}$ $S_{oi} = 0.7889$
 $L = 8 \text{ inch} = 20.32 \text{ cm}$ $S_{wc} = 0.2111$
 $d/r_w = 181$ $q = 400 \text{ cc/hr/well} = 1600 \text{ cc/hr}$
 $h_{av} = 1.17 \text{ cm}$ Network Pore Volume = 159 cc
Porosity = 32.9% Network HCPV = 159 x 0.7880 = 125.4cc
Back Pressure = 15.6 cm of water

ΔQ_p	Q_p	ΔW_p	W_p	ΔN_p	N_p	QNPV
24.0	24.0	0.0	0.0	24.0	24.0	0.15
24.0	48.0	0.0	0.0	24.0	48.0	0.30
23.5	71.5	0.0	0.0	23.5	71.5	0.45
22.0	93.5	0.0	0.0	22.0	93.5	0.59
12.0	105.5	0.0	0.0	12.0	105.5	0.66
4.7	110.2	0.0	0.0	4.7	110.2	0.69
23.3	133.5	5.9	5.9	17.4	127.6	0.84
24.8	158.3	9.1	15.0	15.7	143.3	1.00
5.5	163.8	2.4	17.4	3.1	146.4	1.03
24.0	187.8	10.1	27.5	13.9	160.3	1.18
25.1	212.9	11.5	39.0	13.6	173.9	1.34
25.0	237.9	12.0	51.0	13.0	186.9	1.50
5.0	242.9	2.5	53.5	2.5	189.4	1.53
24.0	266.9	13.0	66.5	11.0	200.4	1.68
24.6	291.5	14.3	80.8	10.3	210.7	1.83
24.1	315.6	14.7	95.5	9.4	220.1	1.99
25.5	341.1	16.0	111.5	9.5	229.6	2.15
24.5	365.6	16.9	128.4	7.6	237.2	2.30
25.0	390.6	17.9	146.3	7.1	244.3	2.46
24.9	415.5	18.0	164.3	6.9	251.2	2.61
6.0	421.5	4.6	168.9	1.4	252.6	2.65
25.0	446.5	19.0	187.9	6.0	258.6	2.81
26.0	472.5	19.7	207.6	6.3	264.9	2.97
25.5	498.0	19.5	227.1	6.0	270.9	3.13
24.5	522.5	19.0	246.1	5.5	276.4	3.29
27.4	549.9	21.2	267.3	6.2	282.6	3.46
26.9	576.8	21.4	288.7	5.5	288.1	3.63

TABLE 2-A

(cont'd)

ΔQ_p	Q_p	ΔW_p	W_p	ΔN_p	N_p	QNPV
23.5	600.3	18.9	307.6	4.6	292.7	3.78
24.5	624.8	19.7	327.3	4.8	297.5	3.93
26.0	650.8	21.0	348.3	5.0	302.5	4.09
24.9	675.7	20.0	368.3	4.9	307.4	4.25
24.5	700.2	19.9	388.2	4.6	312.0	4.40
25.0	725.2	20.4	408.6	4.6	316.6	4.56
24.3	749.5	21.3	429.9	3.0	319.6	4.71
102.7	852.2	90.2	520.1	12.5	332.1	5.36
102.8	955.0	90.0	610.1	12.8	344.9	6.01
25.6	980.6	22.5	632.6	3.1	348.0	6.17
25.0	1005.6	22.0	654.6	3.0	351.0	6.33
10.5	1016.1	9.2	663.8	1.3	352.3	6.39
28.9	1045.0	25.6	689.4	3.3	355.6	6.57
26.0	1071.0	23.2	712.6	2.8	358.4	6.74
*269.2	1340.2	222.0	934.6	47.2	405.6	8.43

* Production after injection ceased.

TABLE 2-B

RUN NO. 2

QNPV	QHPV	QDPV	F _{wo}	ONPV	OHPV	ODPV
0.15	0.19	0.46	0.0	0.15	0.19	0.46
0.30	0.38	0.91	0.0	0.30	0.38	0.91
0.45	0.57	1.36	0.0	0.45	0.57	1.36
0.59	0.75	1.78	0.0	0.59	0.75	1.78
0.66	0.84	2.00	0.0	0.66	0.84	2.00
0.69	0.88	2.09	0.0	0.69	0.88	2.09
0.84	1.07	2.54	0.34	0.80	1.02	2.42
1.00	1.26	3.01	0.58	0.90	1.14	2.72
1.03	1.31	3.11	0.77	0.92	1.17	2.78
1.18	1.50	3.57	0.73	1.01	1.28	3.04
1.34	1.70	4.04	0.85	1.09	1.39	3.30
1.50	1.90	4.52	0.92	1.18	1.49	3.55
1.53	1.94	4.61	1.00	1.19	1.51	3.60
1.68	2.13	5.07	1.18	1.26	1.60	3.81
1.83	2.33	5.54	1.39	1.33	1.68	4.00
1.99	2.52	5.99	1.56	1.38	1.76	4.18
2.15	2.72	6.48	1.68	1.44	1.83	4.36
2.30	2.92	6.94	2.22	1.49	1.89	4.50
2.46	3.12	7.42	2.52	1.54	1.95	4.64
2.61	3.31	7.89	2.61	1.58	2.00	4.77
2.65	3.36	8.00	3.29	1.59	2.01	4.80
2.81	3.56	8.48	3.17	1.63	2.06	4.91
2.97	3.77	8.97	3.13	1.67	2.11	5.03
3.13	3.97	9.46	3.25	1.70	2.16	5.14
3.29	4.17	9.92	3.46	1.74	2.20	5.25
3.46	4.39	10.44	3.42	1.78	2.25	5.37
3.63	4.60	10.95	3.89	1.81	2.30	5.47
3.78	4.79	11.40	4.11	1.84	2.33	5.56
3.93	4.98	11.86	4.10	1.87	2.37	5.65
4.09	5.19	12.36	4.20	1.90	2.41	5.74
4.25	5.39	12.83	4.08	1.93	2.45	5.84
4.40	5.58	13.30	4.33	1.96	2.49	5.92
4.56	5.78	13.77	4.44	1.99	2.53	6.01
4.71	5.98	14.23	7.10	2.01	2.55	6.07
5.36	6.80	16.18	7.22	2.09	2.65	6.31
6.01	7.62	18.13	7.03	2.17	2.75	6.55
6.17	7.82	18.62	7.26	2.19	2.78	6.61
6.33	8.02	19.09	7.33	2.21	2.80	6.66
6.39	8.10	19.29	7.08	2.22	2.81	6.69
6.57	8.33	19.84	7.76	2.24	2.84	6.75
6.74	8.54	20.34	8.29	2.25	2.86	6.81
* 8.43	10.69	25.45	4.70	2.55	3.23	7.70

TABLE 3-A

RUN NO. 3

ISOLATED NORMAL FIVE-SPOT

$N = 1342 \text{ cc.}$ $S_{oi} = 0.8284$
 $L = 8 \text{ inch} = 20.32 \text{ cm}$ $S_{wc} = 0.1716$
 $d/r_w = 181$ $q = 400 \text{ cc/hr/well} = 1600 \text{ cc/hr}$
 $h_{av} = 1.17 \text{ cm}$ Network Pore Volume = 159 cc
Porosity = 32.9% Network HCPV = $159 \times 0.8284 = 131.7 \text{ cc}$
Back Pressure = 67.7 cm of water

ΔQ_p	Q_p	ΔW_p	W_p	ΔN_p	N_p	QNPV
70.0	70.0	0.0	0.0	70.0	70.0	0.44
25.0	95.0	0.0	0.0	25.0	95.0	0.60
9.0	104.0	0.5	0.5	8.5	103.5	0.65
23.6	127.6	5.7	6.2	17.9	121.4	0.80
24.5	152.1	9.5	15.7	15.0	136.4	0.96
24.0	176.1	10.4	26.1	13.6	150.0	1.11
24.5	200.6	12.0	38.1	12.5	162.5	1.26
24.1	224.7	12.7	50.8	11.4	173.9	1.41
24.5	249.2	13.8	64.6	10.7	184.6	1.57
24.5	273.7	14.9	79.5	9.6	194.2	1.72
23.5	297.2	15.0	94.5	8.5	202.7	1.87
8.0	305.2	5.4	99.9	2.6	205.3	1.92
24.5	329.7	16.0	115.9	8.5	213.8	2.07
25.0	354.7	16.7	132.6	8.3	222.1	2.23
24.4	379.1	16.4	149.0	8.0	230.1	2.38
24.1	403.2	16.5	165.5	7.6	237.7	2.54
24.5	427.7	16.9	182.4	7.6	245.3	2.69
24.6	452.3	17.3	199.7	7.3	252.6	2.85
24.4	476.7	17.1	216.8	7.3	259.9	3.00
24.2	500.9	17.0	233.8	7.2	267.1	3.15
26.4	527.3	18.5	252.3	7.9	275.0	3.32
10.2	537.5	7.5	259.8	2.7	277.7	3.38
24.5	562.0	18.5	278.3	6.0	283.7	3.54
24.0	586.0	18.1	296.4	5.9	289.6	3.69
24.3	610.3	18.5	314.9	5.8	295.4	3.84
24.5	634.8	18.5	333.4	6.0	301.4	3.99
24.5	659.3	18.9	352.3	5.6	307.0	4.15
24.1	683.4	18.7	371.0	5.4	312.4	4.30

TABLE 3-A

(cont'd)

ΔQ_p	Q_p	ΔW_p	W_p	ΔN_p	N_p	QNPV
24.1	707.5	19.0	390.0	5.1	317.5	4.45
24.5	732.0	19.5	409.5	5.0	322.5	4.60
24.5	756.5	19.5	429.0	5.0	327.5	4.76
24.5	781.0	19.5	448.5	5.0	332.5	4.91
24.5	805.5	19.5	468.0	5.0	337.5	5.07
24.5	830.0	19.5	487.5	5.0	342.5	5.22
25.0	855.0	20.0	507.5	5.0	347.5	5.38
25.3	880.3	20.4	527.9	4.9	352.4	5.54
23.8	904.1	19.1	547.0	4.7	357.1	5.69
24.4	928.5	19.8	566.8	4.6	361.7	5.84
24.4	952.9	19.9	586.7	4.5	366.2	5.99
22.8	975.7	18.5	605.2	4.3	370.5	6.14
10.8	986.5	8.9	614.1	1.9	372.4	6.20
24.0	1010.5	19.5	633.6	4.5	376.9	6.36
25.0	1035.5	20.4	654.0	4.6	381.5	6.51
25.7	1061.2	21.0	675.0	4.7	386.2	6.67
24.9	1086.1	19.5	694.5	5.4	391.6	6.83
24.5	1110.6	20.0	714.5	4.5	396.1	6.99
*272.6	1383.2	219.0	933.5	53.6	449.7	8.70

* Production after injection ceased.

TABLE 3-B

RUN NO. 3

QNPV	QHPV	QDPV	F _{wo}	ONPV	OHPV	ODPV
0.44	0.53	1.27	0.0	0.44	0.53	1.27
0.60	0.72	1.72	0.0	0.60	0.72	1.72
0.65	0.79	1.88	0.06	0.65	0.79	1.87
0.80	0.97	2.31	0.32	0.76	0.92	2.20
0.96	1.16	2.75	0.63	0.86	1.04	2.47
1.11	1.34	3.18	0.77	0.94	1.14	2.71
1.26	1.52	3.63	0.96	1.02	1.23	2.94
1.41	1.71	4.06	1.11	1.09	1.32	3.14
1.57	1.89	4.51	1.29	1.16	1.40	3.34
1.72	2.08	4.95	1.55	1.22	1.48	3.51
1.87	2.26	5.37	1.77	1.28	1.54	3.67
1.92	2.32	5.52	2.08	1.29	1.56	3.71
2.07	2.50	5.96	1.88	1.35	1.62	3.87
2.23	2.69	6.41	2.01	1.40	1.69	4.02
2.38	2.88	6.85	2.05	1.45	1.75	4.16
2.54	3.06	7.29	2.17	1.50	1.81	4.30
2.69	3.25	7.73	2.22	1.54	1.86	4.44
2.85	3.43	8.18	2.37	1.59	1.92	4.57
3.00	3.62	8.62	2.34	1.64	1.97	4.70
3.15	3.80	9.06	2.36	1.68	2.03	4.83
3.32	4.00	9.53	2.34	1.73	2.09	4.97
3.38	4.08	9.72	2.78	1.75	2.11	5.02
3.54	4.27	10.16	3.08	1.78	2.15	5.13
3.69	4.45	10.59	3.07	1.82	2.20	5.24
3.84	4.63	11.03	3.19	1.86	2.24	5.34
3.99	4.82	11.48	3.08	1.90	2.29	5.45
4.15	5.01	11.92	3.38	1.93	2.33	5.55
4.30	5.19	12.36	3.46	1.97	2.37	5.65
4.45	5.37	12.79	3.73	2.00	2.41	5.74
4.60	5.56	13.23	3.90	2.03	2.45	5.83
4.76	5.74	13.68	3.90	2.06	2.49	5.92
4.91	5.93	14.12	3.90	2.09	2.53	6.01
5.07	6.12	14.56	3.90	2.12	2.56	6.10
5.22	6.30	15.01	3.90	2.15	2.60	6.19
5.38	6.49	15.46	4.00	2.19	2.64	6.28
5.54	6.68	15.92	4.16	2.22	2.68	6.37
5.69	6.87	16.35	4.06	2.25	2.71	6.46
5.84	7.05	16.79	4.30	2.28	2.75	6.54
5.99	7.24	17.23	4.42	2.30	2.78	6.62

TABLE 3-B

(cont'd)

QNPV	QHPV	QDPV	F_{wo}	ONPV	OHPV	ODPV
6.14	7.41	17.64	4.30	2.33	2.81	6.70
6.20	7.49	17.84	4.68	2.34	2.83	6.73
6.36	7.67	18.27	4.33	2.37	2.86	6.81
6.51	7.86	18.72	4.44	2.40	2.90	6.90
6.67	8.06	19.19	4.47	2.43	2.93	6.98
6.83	8.25	19.64	3.61	2.46	2.97	7.08
6.99	8.43	20.08	4.44	2.49	3.01	7.16
*8.70	10.50	25.01	4.09	2.83	3.42	8.13

* Production after injection ceased

TABLE 4-A

RUN NO. 4

ISOLATED NORMAL FIVE-SPOT

$N = 1278 \text{ cc}$ $S_{oi} = 0.7889$
 $L = 8 \text{ inch} = 20.32 \text{ cm}$ $S_{wc} = 0.2111$
 $d/r_w = 181$ $q = 400 \text{ cc/hr/well} = 1600 \text{ cc/hr}$
 $h_{av} = 1.17 \text{ cm}$ Network Pore Volume = 159 cc.
Porosity = 32.9% Network HCPV = $159 \times 0.7889 = 125.4 \text{ cc}$
Back Pressure = 104.4 cm of water

ΔQ_p	Q_p	ΔW_p	W_p	ΔN_p	N_p	QNPV
74.0	74.0	0.0	0.0	74.0	74.0	0.47
21.0	95.0	0.0	0.0	21.0	95.0	0.60
15.4	110.4	2.2	2.2	13.2	108.2	0.69
6.5	116.9	2.0	4.2	4.5	112.7	0.74
23.4	140.3	8.5	12.7	14.9	127.6	0.88
24.0	164.3	11.1	23.8	12.9	140.5	1.03
24.5	188.8	12.7	36.5	11.8	152.3	1.19
27.0	215.8	15.5	52.0	11.5	163.8	1.36
5.6	221.4	3.5	55.5	2.1	165.9	1.39
24.0	245.4	15.3	70.8	8.7	174.6	1.54
24.6	270.0	16.0	86.8	8.6	183.2	1.70
24.4	294.4	16.5	103.3	7.9	191.1	1.85
24.3	318.7	16.7	120.0	7.6	198.7	2.00
24.2	342.9	16.9	136.9	7.3	206.0	2.16
24.3	367.2	17.5	154.4	6.8	212.8	2.31
25.1	392.3	19.0	173.4	6.1	218.9	2.47
24.5	416.8	18.8	192.2	5.7	224.6	2.62
8.5	425.3	6.8	199.0	1.7	226.3	2.68
24.1	449.4	18.9	217.9	5.2	231.5	2.83
24.4	473.8	19.6	237.5	4.8	236.3	2.98
24.5	498.3	19.8	257.3	4.7	241.0	3.13
24.0	522.3	19.5	276.8	4.5	245.5	3.29
24.3	546.6	19.8	296.6	4.5	250.0	3.44
26.6	573.2	21.8	318.4	4.8	254.8	3.61
24.0	597.2	19.7	338.1	4.3	259.1	3.76
24.9	622.1	20.5	358.6	4.4	263.5	3.91
25.4	647.5	21.0	379.6	4.4	267.9	4.07
24.7	672.2	20.3	399.9	4.4	272.3	4.23

TABLE 4-A
(cont'd)

ΔQ_p	Q_p	ΔW_p	W_p	ΔN_p	N_p	QNPV
26.6	698.8	22.5	422.4	4.1	276.4	4.40
24.9	723.7	20.7	443.1	4.2	280.6	4.55
12.0	735.7	10.0	453.1	2.0	282.6	4.63
24.0	759.7	20.0	473.1	4.0	286.6	4.78
24.5	784.2	20.7	493.8	3.8	290.4	4.93
24.5	808.7	20.7	514.5	3.8	294.2	5.09
24.5	833.2	21.0	535.5	3.5	297.7	5.24
24.0	857.2	20.5	556.0	3.5	301.2	5.39
24.0	881.2	20.5	576.5	3.5	304.7	5.54
24.0	905.2	20.3	596.8	3.7	308.4	5.69
24.3	929.5	20.5	617.3	3.8	312.2	5.85
24.5	954.0	21.0	638.3	3.5	315.7	6.00
25.8	979.8	22.0	660.3	3.8	319.5	6.16
*363.6	1343.4	309.2	969.5	54.4	373.9	8.45

* Production after injection ceased.

TABLE 4-B

RUN NO. 4

QNPV	QHPV	QDPV	F _{wo}	ONPV	OHPV	ODPV
0.47	0.59	1.41	0.0	0.47	0.59	1.41
0.60	0.76	1.80	0.0	0.60	0.76	1.80
0.69	0.88	2.10	0.17	0.68	0.86	2.05
0.74	0.93	2.22	0.44	0.71	0.90	2.14
0.88	1.12	2.66	0.57	0.80	1.02	2.42
1.03	1.31	3.12	0.86	0.88	1.12	2.67
1.19	1.51	3.59	1.08	0.96	1.22	2.89
1.36	1.72	4.10	1.35	1.03	1.31	3.11
1.39	1.77	4.20	1.67	1.04	1.32	3.15
1.54	1.96	4.66	1.76	1.10	1.39	3.32
1.70	2.15	5.13	1.86	1.15	1.46	3.48
1.85	2.35	5.59	2.09	1.20	1.52	3.63
2.00	2.54	6.05	2.20	1.25	1.59	3.77
2.16	2.73	6.51	2.32	1.30	1.64	3.91
2.31	2.93	6.97	2.57	1.34	1.70	4.04
2.47	3.13	7.45	3.12	1.38	1.75	4.16
2.62	3.32	7.91	3.30	1.41	1.79	4.26
2.68	3.39	8.08	4.00	1.42	1.81	4.30
2.83	3.58	8.53	3.64	1.46	1.85	4.40
2.98	3.78	9.00	4.08	1.49	1.88	4.49
3.13	3.97	9.46	4.21	1.52	1.92	4.58
3.29	4.17	9.92	4.33	1.54	1.96	4.66
3.44	4.36	10.38	4.40	1.57	1.99	4.75
3.61	4.57	10.88	4.54	1.60	2.03	4.84
3.76	4.76	11.34	4.58	1.63	2.07	4.92
3.91	4.96	11.81	4.66	1.66	2.10	5.00
4.07	5.16	12.29	4.77	1.69	2.14	5.09
4.23	5.36	12.76	4.61	1.71	2.17	5.17
4.40	5.57	13.27	5.49	1.74	2.20	5.25
4.55	5.77	13.74	4.93	1.77	2.24	5.33
4.63	5.87	13.97	5.00	1.78	2.25	5.37
4.78	6.06	14.42	5.00	1.80	2.29	5.44
4.93	6.25	14.89	5.45	1.83	2.32	5.51
5.09	6.45	15.36	5.45	1.85	2.35	5.59
5.24	6.64	15.82	6.00	1.87	2.37	5.65
5.39	6.84	16.28	5.86	1.89	2.40	5.72
5.54	7.03	16.73	5.86	1.92	2.43	5.79
5.69	7.22	17.19	5.49	1.94	2.46	5.86
5.85	7.41	17.65	5.40	1.96	2.49	5.93
6.00	7.61	18.11	6.00	1.99	2.52	5.99
6.16	7.81	18.60	5.79	2.01	2.55	6.07
*8.45	10.71	25.51	5.68	2.35	2.98	7.10

TABLE 5-A

RUN NO. 5

ISOLATED NORMAL FIVE-SPOT

$N = 1342 \text{ cc}$ $S_{oi} = 0.8284$
 $L = 8 \text{ inch} = 20.32 \text{ cm}$ $S_{wc} = 0.1716$
 $d/r_w = 181$ $q = 400 \text{ cc/hr/well} = 1600 \text{ cc/hr}$
 $h_{av} = 1.17 \text{ cm}$ Network Pore Volume = 159 cc
Porosity = 32.9% Network HCPV = $159 \times 0.8284 = 131.7 \text{ cc}$
Back Pressure = 104.4 cm of water

ΔQ_p	Q_p	ΔW_p	W_p	ΔN_p	N_p	Q_{NPV}
78.0	78.0	0.0	0.0	78.0	78.0	0.49
24.5	102.5	1.4	1.4	23.1	101.1	0.65
18.6	121.1	3.6	5.0	15.0	116.1	0.76
24.1	145.2	7.7	12.7	16.4	132.5	0.91
24.3	169.5	9.8	22.5	14.5	147.0	1.07
24.0	193.5	11.5	34.0	12.5	159.5	1.22
29.0	222.5	16.4	50.4	12.6	172.1	1.40
24.5	247.0	14.8	65.2	9.7	181.8	1.55
27.9	274.9	17.5	82.7	10.4	192.2	1.73
23.5	298.4	16.1	98.8	7.4	199.6	1.88
24.0	322.4	16.9	115.7	7.1	206.7	2.03
26.9	349.3	19.3	135.0	7.6	214.3	2.20
24.3	373.6	17.9	152.9	6.4	220.7	2.35
25.0	398.6	18.5	171.4	6.5	227.2	2.51
24.6	423.2	18.7	190.1	5.9	233.1	2.66
25.0	448.2	19.5	209.6	5.5	238.6	2.82
24.4	472.6	18.7	228.3	5.7	244.3	2.97
25.1	497.7	19.5	247.8	5.6	249.9	3.13
24.5	522.2	19.0	266.8	5.5	255.4	3.28
24.4	546.6	19.0	285.8	5.4	260.8	3.44
9.5	556.1	7.5	293.3	2.0	262.8	3.50
25.1	581.2	20.0	313.3	5.1	267.9	3.66
24.4	605.6	19.5	332.8	4.9	272.8	3.81
24.6	630.2	19.9	352.7	4.7	277.5	3.96
24.0	654.2	19.5	372.2	4.5	282.0	4.11
24.8	679.0	20.0	392.2	4.8	286.8	4.27
24.5	703.5	20.0	412.2	4.5	291.3	4.43
23.2	726.7	18.8	431.0	4.4	295.7	4.57

TABLE 5-A

(cont'd)

ΔQ_p	Q_p	ΔW_p	W_p	ΔN_p	N_p	QNPV
24.5	751.2	19.9	450.9	4.6	300.3	4.73
24.5	775.7	20.0	470.9	4.5	304.8	4.88
24.7	800.4	20.4	491.3	4.3	309.1	5.03
24.0	824.4	19.6	510.9	4.4	313.5	5.19
24.0	848.4	19.6	530.5	4.4	317.9	5.34
24.1	872.5	20.0	550.5	4.1	322.0	5.49
23.5	896.0	19.5	570.0	4.0	326.0	5.64
26.1	922.1	21.5	591.5	4.6	330.6	5.80
24.5	946.6	20.5	612.0	4.0	334.6	5.95
22.0	968.6	18.5	630.5	3.5	338.1	6.09
101.0	1069.6	84.0	714.5	17.0	355.1	6.73
86.4	1156.0	72.1	786.6	14.3	369.4	7.27
*209.0	1365.0	167.5	954.1	41.5	410.9	8.59

* Production after injection ceased.

TABLE 5-B

RUN NO. 5

QNPV	QHPV	QDPV	F _{WO}	ONPV	OHPV	ODPV
0.49	0.59	1.41	0.0	0.49	0.59	1.41
0.65	0.78	1.85	0.06	0.64	0.77	1.83
0.76	0.92	2.19	0.24	0.73	0.88	2.10
0.91	1.10	2.63	0.47	0.83	1.01	2.40
1.07	1.29	3.06	0.68	0.93	1.12	2.66
1.22	1.47	3.50	0.92	1.00	1.21	2.88
1.40	1.69	4.02	1.30	1.08	1.31	3.11
1.55	1.88	4.47	1.53	1.14	1.38	3.29
1.73	2.09	4.97	1.68	1.21	1.46	3.48
1.88	2.27	5.40	2.18	1.26	1.52	3.61
2.03	2.45	5.83	2.38	1.30	1.57	3.74
2.20	2.65	6.32	2.54	1.35	1.63	3.87
2.35	2.84	6.75	2.80	1.39	1.68	3.99
2.51	3.03	7.21	2.85	1.43	1.73	4.11
2.66	3.21	7.65	3.17	1.47	1.77	4.21
2.82	3.40	8.10	3.55	1.50	1.81	4.31
2.97	3.59	8.54	3.28	1.54	1.86	4.42
3.13	3.78	9.00	3.48	1.57	1.90	4.52
3.28	3.97	9.44	3.46	1.61	1.94	4.62
3.44	4.15	9.88	3.52	1.64	1.98	4.72
3.50	4.22	10.05	3.75	1.65	2.00	4.75
3.66	4.41	10.51	3.92	1.69	2.03	4.84
3.81	4.60	10.95	3.98	1.72	2.07	4.93
3.96	4.79	11.39	4.23	1.75	2.11	5.02
4.11	4.97	11.83	4.33	1.77	2.14	5.10
4.27	5.16	12.28	4.17	1.80	2.18	5.19
4.43	5.34	12.72	4.44	1.83	2.21	5.27
4.57	5.52	13.14	4.27	1.86	2.25	5.35
4.73	5.70	13.58	4.33	1.89	2.28	5.43
4.88	5.89	14.02	4.44	1.92	2.31	5.51
5.03	6.08	14.47	4.74	1.94	2.35	5.59
5.19	6.26	14.90	4.46	1.97	2.38	5.67
5.34	6.44	15.34	4.46	2.00	2.41	5.75
5.49	6.63	15.77	4.88	2.03	2.45	5.82
5.64	6.80	16.20	4.88	2.05	2.48	5.89
5.80	7.00	16.67	4.67	2.08	2.51	5.98
5.95	7.19	17.11	5.13	2.10	2.54	6.05
6.09	7.36	17.51	5.29	2.13	2.57	6.11
6.73	8.12	19.34	4.94	2.23	2.70	6.42
7.27	8.78	20.90	5.04	2.32	2.81	6.68
*8.59	10.36	24.68	4.04	2.58	3.12	7.43

TABLE 6

ISOLATED NORMAL FIVE-SPOT

Injection Rate = 400 cc/hr/well

1.0 Planimeter Sq. inch = 83.88 Sq. inches on the model

Run No.	Back Pressure (cm of water)	QNPV	Planimeter Area (sq. inch)	Area Swept (sq.inch)	E _{as} (fraction)
1	0	0.66	1.010	84.7	1.32
		1.49	2.580	216.4	3.38
		2.78	4.279	358.9	5.61
		6.29	5.666	475.3	7.43
2	15.6	0.69	1.215	101.9	1.59
		1.03	1.817	152.4	2.38
		1.52	2.591	217.3	3.40
		2.65	4.053	340.0	5.31
		6.39	5.602	469.9	7.34
3	67.7	0.65	1.118	93.8	1.47
		1.91	3.290	276.0	4.31
		3.38	4.892	410.3	6.41
		6.20	5.849	490.6	7.67
4	104.4	0.73	1.354	113.6	1.78
		1.39	3.064	257.0	4.02
		2.67	5.010	420.2	6.57
		4.62	6.268	525.8	8.22
5	104.4	0.76	1.376	115.4	1.80
		1.88	3.581	300.4	4.69
		3.49	4.710	395.1	6.17
		6.09	5.817	487.9	7.62

TABLE 7-A

RUN NO. 6

FOUR INVERTED FIVE-SPOT

$N = 1373 \text{ cc}$ $S_{oi} = 0.8475$
 $L = 4 \text{ inch} = 10.16 \text{ cm}$ $S_{wc} = 0.1525$
 $d/r_w = 90.5$ $q = 320 \text{ cc/hr/well} = 1280 \text{ cc/hr}$
 $h_{av} = 1.17 \text{ cm}$ Network Pore Volume = 159 cc
Porosity = 32.9% Network HCPV = $159 \times 0.8475 = 134.75 \text{ cc}$
Back Pressure = 21.5 cm of water

ΔQ_p	Q_p	ΔW_p	W_p	ΔN_p	N_p	QNPV
110.7	110.7	1.5	1.5	109.2	109.2	0.70
108.7	219.4	14.6	16.1	94.1	203.3	1.38
118.4	337.8	67.5	83.6	50.9	254.2	2.13
105.2	443.0	78.2	161.8	27.0	281.2	2.79
104.4	547.4	85.7	247.5	18.7	299.9	3.44
98.4	645.8	80.6	328.1	17.8	317.7	4.06
99.2	745.0	86.7	414.8	12.5	330.2	4.69
112.0	857.0	85.1	499.9	26.9	357.1	5.39
88.7	945.7	82.5	582.4	6.2	363.3	5.95
97.4	1043.1	91.4	673.8	6.0	369.3	6.56
98.0	1141.1	92.6	766.4	5.4	374.7	7.18
99.8	1240.9	93.6	860.0	6.2	380.9	7.80
93.6	1334.5	86.1	946.1	7.5	388.4	8.39
58.4	1392.9	54.8	1000.9	3.6	392.0	8.76

TABLE 7-B

RUN NO. 6

QNPV	QHPV	QDPV	F _{wo}	ONPV	OHPV	ODPV
0.70	0.82	1.42	0.01	0.69	0.81	1.40
1.38	1.63	2.81	0.16	1.28	1.51	2.60
2.13	2.51	4.32	1.33	1.60	1.89	3.25
2.79	3.29	5.67	2.90	1.77	2.09	3.60
3.44	4.06	7.00	4.58	1.89	2.23	3.84
4.06	4.79	8.26	4.53	2.00	2.36	4.07
4.69	5.53	9.53	6.94	2.08	2.45	4.23
5.39	6.36	10.97	3.16	2.25	2.65	4.57
5.95	7.02	12.10	13.31	2.29	2.70	4.65
6.56	7.74	13.35	15.23	2.32	2.74	4.73
7.18	8.47	14.60	17.15	2.36	2.78	4.79
7.80	9.21	15.88	15.10	2.40	2.83	4.87
8.39	9.90	17.08	11.48	2.44	2.88	4.97
8.76	10.34	17.82	15.22	2.47	2.91	5.02

TABLE 8-A

RUN NO. 7

FOUR INVERTED FIVE-SPOT

N = 1373 cc S_{oi} = 0.8475
L = 4 inch = 10.16 cm S_{wc} = 0.1525
d/r_w = 90.5 q = 480 cc/hr/well = 1920 cc/hr
h_{av} = 1.17 cm Network Pore Volume = 159 cc
Porosity = 32.9% Network HCPV = 159 x 0.8475 = 134.75 cc
Back Pressure = 21.5 cm of water

ΔQ_p	Q_p	ΔW_p	W_p	ΔN_p	N_p	QNPV
129.5	129.5	2.6	2.6	126.9	126.9	0.81
111.5	241.0	35.6	38.2	75.9	202.8	1.52
125.6	366.6	74.8	113.0	50.8	253.6	2.31
121.0	487.6	88.6	201.6	32.4	286.0	3.07
136.9	624.5	110.2	311.8	26.7	312.7	3.93
115.1	739.6	96.1	407.9	19.0	331.7	4.65
120.9	860.5	104.5	512.4	16.4	348.1	5.41
117.8	978.3	104.5	616.9	13.3	361.4	6.15
102.0	1080.3	90.4	707.3	11.6	373.0	6.79
119.7	1200.0	106.5	813.8	13.2	386.2	7.55
112.3	1312.3	101.3	915.1	11.0	397.2	8.25
76.0	1388.3	69.3	984.4	6.7	403.9	8.73
19.6	1407.9	16.3	1000.7	3.3	407.2	8.86

TABLE 8-B

RUN NO. 7

QNPV	QHPV	QDPV	F_{WO}	ONPV	OHPV	ODPV
0.81	0.96	1.66	0.02	0.80	0.94	1.62
1.52	1.79	3.08	0.47	1.28	1.51	2.60
2.31	2.72	4.69	1.47	1.60	1.88	3.25
3.07	3.62	6.24	2.74	1.80	2.12	3.66
3.93	4.64	7.99	4.13	1.97	2.32	4.00
4.65	5.49	9.46	5.06	2.09	2.46	4.24
5.41	6.39	11.01	6.37	2.19	2.58	4.45
6.15	7.26	12.52	7.86	2.27	2.68	4.62
6.79	8.02	13.82	7.79	2.35	2.77	4.77
7.55	8.91	15.35	8.07	2.43	2.87	4.94
8.25	9.74	16.79	9.21	2.50	2.95	5.08
8.73	10.30	17.76	10.34	2.54	3.00	5.17
8.86	10.45	18.01	4.94	2.56	3.02	5.21

TABLE 9-A

RUN NO. 8

FOUR INVERTED FIVE-SPOT

$N = 1373 \text{ cc}$ $S_{oi} = 0.8475$
 $L = 4 \text{ inch} = 10.16 \text{ cm}$ $S_{wc} = 0.1525$
 $d/r_w = 90.5$ $q = 560 \text{ cc/hr/well} = 2240 \text{ cc/hr}$
 $h_{av} = 1.17 \text{ cm}$ Network Pore Volume = 159 cc
Porosity = 32.9% Network HCPV = $159 \times 0.8475 = 134.75 \text{ cc}$
Back Pressure = 21.5 cm of water

ΔQ_p	Q_p	ΔW_p	W_p	ΔN_p	N_p	QNPV
126.8	126.8	2.5	2.5	124.3	124.3	0.80
117.0	243.8	46.8	49.3	70.2	194.5	1.53
166.2	410.0	101.3	150.6	64.9	259.4	3.04
162.0	572.0	123.6	274.2	38.4	297.8	3.60
143.3	715.3	120.8	395.0	22.5	320.3	4.50
160.0	875.3	136.9	531.9	23.1	343.4	5.51
176.7	1052.0	153.8	685.7	22.9	366.3	6.62
152.4	1204.4	135.2	820.9	17.2	383.5	7.58
156.3	1360.7	140.0	960.9	16.3	399.8	8.56
26.3	1387.0	21.0	981.9	5.3	405.1	8.72

TABLE 9-B

RUN NO. 8

QNPV	QHPV	QDPV	F_{WO}	ONPV	OHPV	ODPV
0.80	0.94	1.62	0.02	0.78	0.92	1.59
1.53	1.81	3.12	0.67	1.22	1.44	2.49
2.58	3.04	5.25	1.56	1.63	1.93	3.32
3.60	4.25	7.32	3.22	1.87	2.21	3.81
4.50	5.31	9.15	5.37	2.01	2.38	4.10
5.51	6.50	11.20	5.93	2.16	2.55	4.39
6.62	7.81	13.46	6.72	2.30	2.72	4.69
7.58	8.94	15.41	7.86	2.41	2.85	4.91
8.56	10.10	17.41	8.59	2.51	2.97	5.12
8.72	10.29	17.75	3.96	2.55	3.01	5.18

TABLE 10

FOUR INVERTED FIVE-SPOT

Back Pressure = 21.5 cm of water

1.0 Planimeter Sq. inch = 83.88 Sq. inches on the model

Run No.	Injection Rate (cc/hour)	QNPV	Planimeter Area (sq.inch)	Area Swept (sq.inch)	E _{as} (fraction)
6	1280	1.38	2.010	168.60	2.63
		3.44	3.172	266.07	4.16
		5.95	3.763	315.64	4.93
		8.39	4.258	357.16	5.58
7	1920	1.52	2.150	180.34	2.82
		3.93	3.440	288.55	4.51
		6.79	4.182	350.79	5.48
		8.73	4.376	367.06	5.735
8	2240	1.53	2.053	172.21	2.69
		4.50	3.462	290.39	4.47
		8.56	4.247	356.24	5.57

TABLE 11

INNER NORMAL FIVE-SPOT OF FOUR INVERTED FIVE-SPOT

$$H_{av} = 1.25 \text{ cm}$$

$$\text{Network Pore Volume} = 10.16 \times 10.16 \times 1.25 \times 0.329 = 42.45 \text{ cc}$$

$$\text{Network HCPV} = 42.45 \times 0.8475 = 35.98 \approx 36.0 \text{ cc}$$

ΔQ_p	Q_p	ΔW_p	W_p	ΔN_p	N_p	QHPV	OHPV
<u>Run No. 6</u>							
24.0	24.0	0.0	0.0	24.0	24.0	0.67	0.67
17.4	41.4	0.0	0.0	17.4	41.4	1.15	1.15
11.6	53.0	1.0	1.0	10.6	52.0	1.47	1.44
6.7	59.7	0.8	1.8	5.9	57.9	1.66	1.61
7.0	66.7	4.6	6.4	2.4	60.3	1.85	1.68
0.9	67.6	0.1	6.5	0.8	61.1	1.88	1.70
2.2	69.8	1.7	8.2	0.5	61.6	1.94	1.71
1.3	71.1	1.0	9.2	0.3	61.9	1.98	1.72
2.8	73.9	2.5	11.7	0.3	62.2	2.05	1.73
0.7	74.6	0.5	12.2	0.2	62.4	2.07	1.73
4.0	78.6	3.5	15.7	0.5	62.9	2.18	1.75
2.8	81.4	2.5	18.2	0.3	63.2	2.26	1.76
3.0	84.4	2.5	20.7	0.5	63.7	2.34	1.77
<u>Run No. 7</u>							
19.7	19.7	0.0	0.0	19.7	19.7	0.55	0.55
9.1	28.8	0.6	0.6	8.5	28.2	0.80	0.78
7.5	36.3	1.9	2.5	5.6	33.8	1.01	0.94
7.6	43.9	5.8	8.3	1.8	35.6	1.22	0.99
8.3	52.2	6.6	14.9	1.7	37.3	1.45	1.04
7.6	59.8	6.4	21.3	1.2	38.5	1.66	1.07
7.9	67.7	6.4	27.7	1.5	40.0	1.88	1.11
8.4	76.1	7.0	34.7	1.4	41.4	2.11	1.15
6.9	83.0	5.5	40.2	1.4	42.8	2.31	1.19
8.9	91.9	7.5	47.7	1.4	44.2	2.55	1.23
8.2	100.1	7.0	54.7	1.2	45.4	2.78	1.26
5.5	105.6	4.7	59.4	0.8	46.2	2.93	1.28

TABLE 11
(cont'd)

ΔQ_p	Q_p	ΔW_p	W_p	ΔN_p	N_p	QHPV	OHPV
<u>Run No. 8</u>							
15.9	15.9	0.0	0.0	15.9	15.9	0.44	0.44
5.6	21.5	0.0	0.0	5.6	21.5	0.60	0.60
2.5	24.0	0.0	0.0	2.5	24.0	0.67	0.67
2.5	26.5	1.0	1.0	1.5	25.5	0.74	0.71
10.2	26.7	9.0	10.0	1.2	26.7	1.02	0.74
11.9	48.6	10.7	20.7	1.2	27.9	1.35	0.78
13.2	61.8	12.0	32.7	1.2	29.1	1.72	0.81
10.8	72.6	10.0	42.7	0.8	29.9	2.02	0.83
10.1	82.7	9.4	52.1	0.7	30.6	2.30	0.85
2.7	85.4	2.4	54.5	0.3	30.9	2.37	0.86

B29869